Nano Today 26 (2019) 16–56

Contents lists available at ScienceDirect

Nano Today

journal homepage: www.elsevier.com/locate/nanotoday

Review

# Tumour microenvironment responsive nanoconstructs for cancer theranostic

Arif Gulzar[a,1], Jiating Xu[a,1], Chen Wang[a], Fei He[a,*], Dan Yang[a], Shili Gai[a], Piaoping Yang[a,*], Jun Lin[b,*], Dayong Jin[c], Bengang Xing[d]

[a] Key Laboratory of Superlight Materials and Surface Technology, Ministry of Education, Harbin Engineering University, Harbin 150001, PR China
[b] State Key Laboratory of Rare Earth Resource Utilization, Changchun Institute of Applied Chemistry, Chinese Academy of Sciences, Changchun 130022, PR China
[c] Institute for Biomedical Materials and Devices, Faculty of Science, University of Technology, Sydney, NSW 2007, Australia
[d] School of Physical & Mathematical Sciences, Nanyang Technological University, Singapore

ARTICLE INFO

*Article history:*
Received 17 October 2018
Received in revised form 12 March 2019
Accepted 25 March 2019
Available online 19 April 2019

*Keywords:*
Tumour microenvironment
Hypoxia
Imaging
Theranostic

ABSTRACT

The tumour mass is made up of not only of a heterogeneous population of cancer cells nonetheless also a mixture of resident as well as the infiltrating host cells, secreted factors besides extracellular matrix proteins, together recognized as the tumour microenvironment (TME). Tumour development is overwhelmingly affected through the dealings of cancer cells with their environment which eventually conclude whether the primary tumour is eliminated, metastasizes or creates dormant micro metastases. The TME may perhaps shape therapeutic responses as well as resistance. Some inimitable features of TME, for example vascular abnormalities, hypoxia, acidic pH and glutathione (GSH) are comparative to normal tissue. Several types of cells, together with tumour cells, macrophages, immune and fibroblast cells are nourished by flawed blood vessels in the solid tumour. To dispense anticancer agents to tumour sites nanovehicles can be competent carts. For augmented therapeutic efficacy, TME is the key for designing of nanoparticles (NPs). In this review, we will discuss the TME and summarize the current advancement in several nano-formulations for cancer therapy, with an extraordinary stress on TME-responsive ones. Scheme 1 highlights several TME modulation tactics with positive cancer therapeutic competence. The design of nanoconstructs and future challenges, consideration and opportunities are also discussed in detail. We have confidence in that these modulation approaches of TME tender a reliable opportunity for the practical translation of nanoparticle formulas into clinic.



**Contents**



*Abbreviations:* 2D, two-dimensional; APCs, antigen presenting cells; BNCT, boron neutron capture therapy; CAF's, cancer associated fibroblast; CT, computed tomography; DCs, dendritic cells; DCFH, dichlorodihydrofluorescein diacetate; DOC, doxorubicin; ECM, extracellular matrix; EPCs, endothelial progenitor cells; EPR, endoplasmic retention; EMT, mesenchymal cell transition; FGF, fibroblast growth facto; FRET, Förster resonance energy transfer; Grb2, growth factor receptor-bound protein 2; GOD, glucose oxidase; GSH, glutathione; HIF-1, hypoxia-inducible factor-1; HGF, hepatocyte growth factor; LCP, lipid-calcium-phosphate; LOX, lysyl oxidase; LOXL, lysyl oxidase like; mAb, monoclonal antibody; MRI, magnetic resonance imaging; MMPs, metalloproteinases; MONs, mesoporous organosilica nanoparticles; MSN, mesoporous silica NPs; NIFR, near-infrared fluorescence; NPs, nanoparticles; NTR, nitroreductase; PDT, photodynamic therapy; PDGF, platelet derived growth factor; PET, positron emission tomography imaging; PHF, perfluorohexane; QD's, quantum dots; rHuPH20, recombinant human hyaluronidase PH20; ROS, reactive oxygen species; SMA, smooth muscle actin alpha; TGF-b, transform growth factor-b; TME, tumor microenvironment; VEGF, vascular endothelial growth factor; VHL, von Hippel-Lindau.

* Corresponding authors.
*E-mail addresses:* hefei@hrbeu.edu.cn (F. He), yangpiaoping@hrbeu.edu.cn (P. Yang), jlin@ciac.ac.cn (J. Lin).
[1] These authors contributed equally to this work.

https://doi.org/10.1016/j.nantod.2019.03.007
1748-0132/

## Introduction

The cancer cells malignant characters cannot be demonstrated devoid of a vital interchange amongst cancer cells and their indigenous environment. Immune cells, angiogenic vascular cells, lymphatic endothelial cells, and cancer-associated fibroblastic cells are the tumour intrudes which aid vigorously to cancer advancement. The power of alteration in these environs is an imperative asset through which tumour cells are capable to attain some of the trademark tasks indispensable for tumour growth and metastatic propagation. Consequently, aiming at the TME to encapsulate or destroy cancer cells in their indigenous environment has become compulsory in the clinical setups. Some mammoth tasks for therapies aiming the TME are the diversity of stromal cells, the intricacy of the molecular constituents of the tumour stroma, and the resemblance with normal tissue. Cancers are complicated diseases comprising of various pathways and complex microenvironment [1]. The advance of multitasking theranostic nanoplatforms to fulfil tumour-specific imaging and improved cancer therapy through countering or moderating the TME has lately engrossed remarkable attentions in the arena of nanomedicine. Various categories of solid tumours are agreed to possess certain distinctive physiognomies for example hypoxia, elevated interstitial pressure, and squat extracellular pH in their TME [2–5]. For improved cancer diagnosis and prediction TME-responsive nanomaterials, spotting the microenvironment features of tumours have grasped considerable courtesy for personalized medicine [6–9]. To examine TME imaging functionalities for instance optical [10,11], magnetic resonance (MR) [12,13], and positron emission tomography imaging [14] have been extensively used. Several TME sensitive imaging probes which are responsive to pH [15,16], GSH [17], $H_2O_2$ [18], and hypoxia [19,20] have been created for tumour explicit imaging, which would deliver valuable data for superior analysis and forecast of tumours, in addition to better-quality cancer therapy projection. Instead, some usual TME characters for example acidic pH and hypoxia might encourage the therapeutic resistance for cancer treatment, the advance of smart therapeutic nanoagents to control TME for superior therapeutic results has also been projected to be an appealing approach for the next generation cancer therapy [21,22]. A unique class of 2D nanomaterials, transition metals have emerged into a favourable class of nanostructures with massive potential in varied areas including biomedicine in recent years [23,24]. Various researchers have lately advanced the usage of transition metal dichalcogenides (TMDCs) such as molybdenum disulfide ($MoS_2$) [25–27], tungsten disulfide ($WS_2$) [28,29], bismuth selenide ($Bi_2Se_3$) [30,31], and titanium disulfide ($TiS_2$)

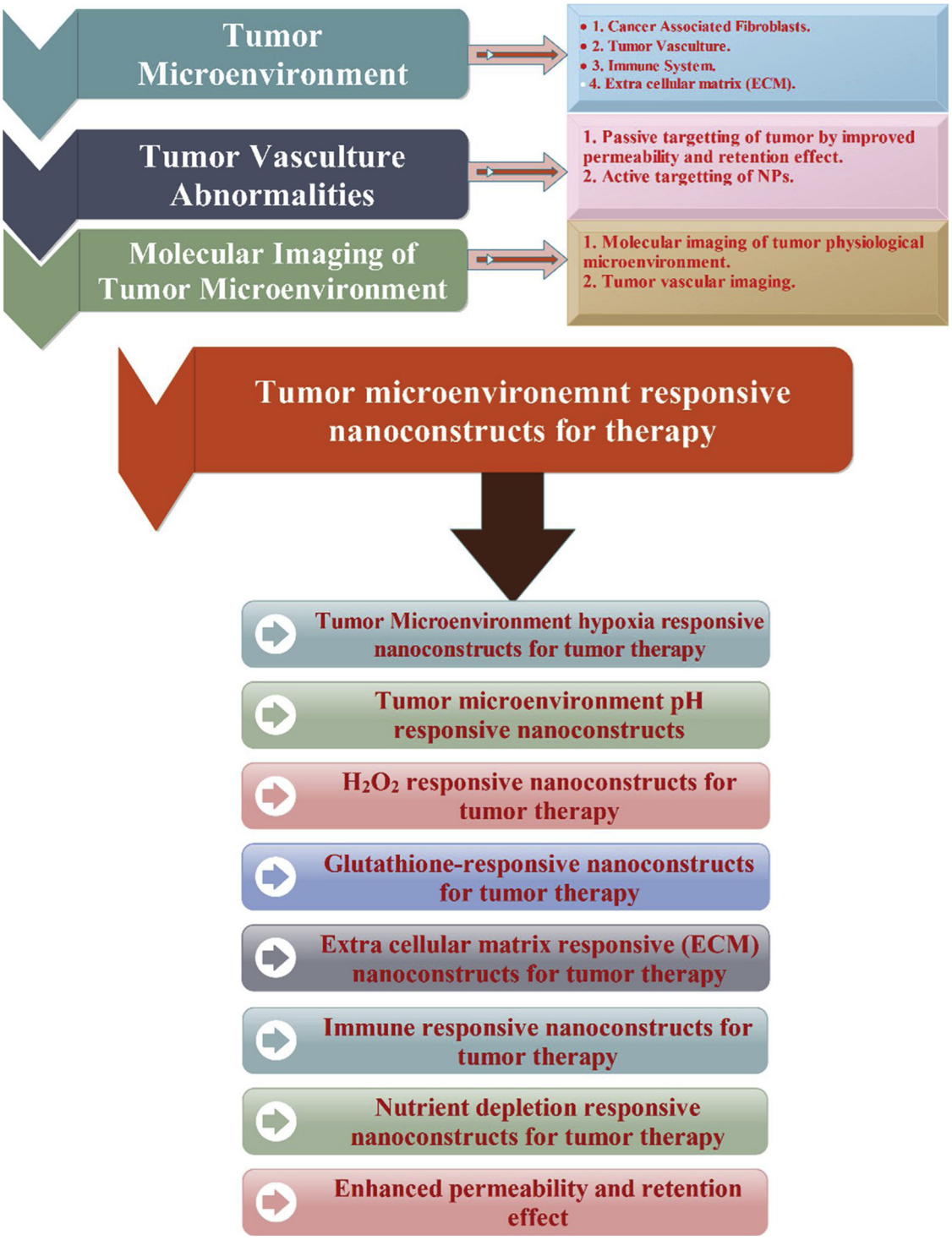


**Scheme 1.** Tumour microenvironment modulation strategies.

nanosheet [24] for multimodal imaging, drug delivery, and cancer therapy owing to their high surface area, absorbance in the near-infrared (NIR) region, and other unique physical-chemical properties. Herein the review paper, we will elucidate the TME and investigate the anomalous characters as therapeutic prospects for the advance of TME responsive nanoconstructs for cancer theranostic (Scheme 1).

## Tumour microenvironment (TME)

Tumorigenesis is a multifaceted and vibrant progression comprising of diverse physiognomies blamable for propagation and tumour growth as depicted in Scheme 2. Tumour intricacy are due to these unique qualities comprised of: amplified proliferative signals, dodging of growth suppressor, counterattacking

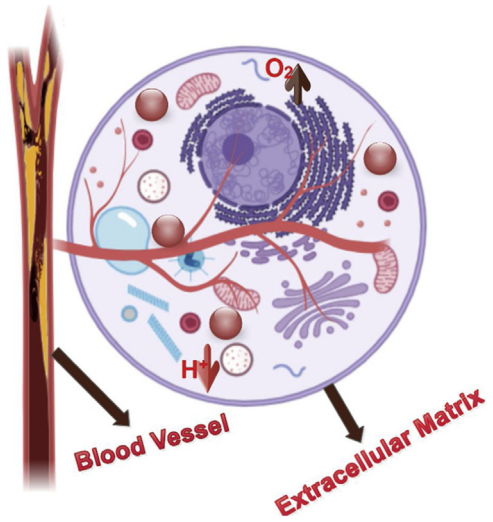


**Scheme 2.** The key constituents of the TME, which comprise malignant cells, non-malignant cells (*e.g.* T cells, tumour associated fibroblasts and dendritic cells), tumour extracellular matrix and blood vessels.

apoptosis, unobstructed reproduction, stimulating angiogenesis, boosting invasion and metastasis, controlling cells metabolism and dodging immune annihilation [32]. Such characteristics are assimilated *via* collaboration amongst diverse cellular and non-cellular components of tumours characterizing TME. Non-malignant cells of the tumour for example cancer associated fibroblasts (CAFs), endothelial cells and pericytes constituting tumour vasculature, immune and inflammatory cells, bone marrow derived cells, and the extracellular matrix (ECM) creating a multifaceted cross-talk with tumour include the TME [33]. Certain stromal cells, recruited and stimulated by the budding neoplastic cells, which sequentially stimulate biological signals that authorize cancer cells to conquer adjoining ordinary tissue and to metastasize in remote organ. Tumour cells metastasizing in a tissue different from that of an original tissue can tolerate and progress in ordinary microenvironment or encounter a sympathetic microenvironment (pre-metastatic niches), positively pre-conditioned prior to the influx of tumoral cells from numerous environments for instance circulating factors emitted by primary tumours [34,35].

*Cancer associated fibroblasts in cancer therapy*

Constituents of stromal tissue which take part in wound healing procedure are fibroblasts [36]. Such cells develop into skilled category of fibroblasts through this approach labelled as myofibroblasts. Such type of cells enters the abrasions and breed ECM functioning like a scaffold for tissue rejuvenation through breeding a range of collagen and fibronectin. Cells like resident fibroblasts and myofibroblasts are two differing sub-categories of fibroblasts indicated by the term CAFs. Growth factors, conventional cell–cell communication, adhesion molecules, communicating with leukocytes, reactive oxygen species and microRNA are several milieus involved in the stimulation of the fibroblasts [37]. CAFs are considered as fibroblasts after the activation, contrarily to ordinary fibroblast, CAFs are recurrently stimulated, they do not return to an ordinary phenotype, they do not undergo apoptosis, and provoke cancer progress.

In the tumour growth CAFs play a vibrant role as they provoke cell proliferation, invasion, angiogenesis, and motility *via* liberation of growth factors and cytokines, *via* deregulating Notch and p53 signalling pathways, and through the breeding of metalloproteinases (MMPs) [37–39]. ECM stiffness at primary tumours might be distressed by CAFs, supplementing cancer cell incursion supporting metastatic spread by bringing epithelial to mesenchymal cell change (EMT) [40]. Due to the expression of intercellular adhesion molecule 1 (ICAM1) they also regulate the immune response and automated cell death protein 1 ligand 1 (PDL1) and PDL2, which enable immunosuppressive roles [41,42]. A biological progression known as EMT characterized by ample discrepancies through which epithelial cells lose their biological distinctiveness of gaining a mesenchymal phenotype. Contrary to epithelial cells, mesenchymal cells do not generate an organized layer and they lack intercellular adhesion complex responsible for their itinerant capability. Several identified soluble factors breed by CAF which are involved in the EMT progression are vascular endothelial growth factor (VEGF), fibroblast growth factor (FGF), platelet derived growth factor (PDGF), transforming growth factor b (TGFb), epithelial growth factors (EGF) and hepatocyte growth factor (HGF) [43]. A signalling cascade triggered by the partnership amongst these growth factors with their associated receptors which supports the EMT progression. For the growth factor receptor-bound protein 2 (Grb2), phosphoinositide-3-kinase (PI3K), and Src, functions as landing site of these receptors owing to autophosphorylation of tyrosine residue. Grb2 activation of prompts a cascade of a downstream protein including RAS/RAF/MEK1/ERK with ensuing nuclear localization of mitogen-activated protein kinase (MAPK) governing the expression of genes say activating protein 1 (Ap-1) and erythroblast transformation specific (Ets) protein [43]. The primary one encourages Smad expression approving spindle tumour cell incursion. MMP-2 expression is accelerated by the expression of the second enzyme know to be authorized to be extraordinarily express in invasive cancer cells. EMT is stimulated by the MMPs not only by means of supporting the cell migration due to ECM dilapidation, even so by releasing growth factors and cytokines correspondingly. Ets Supplementary role includes the phosphorylating of transcription factors, for instance Slug Repressing E-cadherin levels, exasperating the expression of mesenchymal markers, and cell cycle development with succeeding proliferation. b-catenin instigates the EMT by overriding of E-cadherin expression while as PI3K/AKT pathway phosphorylates and deactivates GSK3b inhibiting proteosomal degradation of Snail.

TGF-b is regarded as manager of EMT through binding with type II receptor which then phosphorylates the type I receptor and turns the phosphorylates cytoplasmic Small mother counter to decapentaplegic 2/3 (Smad2/3) protein establishing a complex with Smad4 and consequently controlling the expression of genes tangled in the cell proliferation, differentiation, migration, and ECM breeding [44]. Expression of N-cadherin, fibronectin and smooth muscle actin alpha (αSMA), cytoskeletal markers expressed in advanced stages of EMT and related with the cancer advancement is provoked by this growth factor. Yet EMT is activated by TGF-b *via* Smad-independent method by means of activation of MAPK, PI3K, integrin related kinases and Rho GTPases as portrayed directly above for other growth factors [45].

*Tumour vasculture in cancer therapy*

Two unlike biological routes through which tumour vasculature pops up are: a creation of fresh blood vessel over the pre-existent vessels known as angiogenesis and development of fresh blood vessels *via* staffing and mingling endothelial progenitor cells called as vasculogenesis [46]. Several molecules regulate the angiogenetic development, signalling pathways as well as related receptors, for instance, VEGFs, VEGF receptors (VEGFRs), FGFs including their receptors (FGFRs), PDGF-β and PDGF-β receptor (PDGFRb), Notch ligand, semaphorine, neuropilin, angiopoietin, robo proteins, Ephrin-A and B. A significant signals governing angiogenesis procedure known as the hypoxia-inducible factor (HIF) as it prompt transcription of genes which promotes the angiogenesis stimu-

lation. Oxygen-controlled HIF1a as well as HIF2a subunit are the components of HIFs which are constitutively expressed HIF1b subunit [47]. Prolyl hydroxylation which is reliant on the oxygen hydrolyzes α subunits through binding with the von Hippel-Lindau (VHL) tumour suppressor protein responsible for their ubiquitylation besides proteasomal degradation in physiological condition. Such a hydroxylation reaction dangles over existence of certain cofactors, for example, oxygen as well as a-ketoglutarate. In such circumstance of hypoxia, such kinds of reaction remain subdued and subsequently HIF1α besides HIF2α dimerize alongside HIF1β subunit then afterwards binds with the hypoxia responsive elements in affected gene promoters [48]. To counter the hypoxia, HIF normalizes the angiogenic factors expression which is blamed for vascular permeability, proliferation of endothelial cell, sprouting, migration, adhesion besides development of the tube [49].

Growth factors, oncogenic activation and damage or inactivation of VHL genes are accountable for HIF genes stimulation besides oxygen tension [50,51]. Oxygen tension also stimulates EMT by mounting the expression of Smad3, stimulating the release of TGF-b2 activating TGF-b signalling in addition blocking HIF-1a transcription [52]. Snail transcription factors also regulate cell cycle progression and survival during EMT [53]. Wnt signal is augmented due to hypoxia hence responsible for the b-catenin stabilization, encouraging gene expression, coupled alongside EMT responsible for the polarity loss besides adherence junctions through epithelial cells with upregulation of mesenchymal markers, mounting cell spreading movement as well as invasiveness [53]. Vasculogenesis development, consist of bone marrow-derived endothelial progenitor cells (EPCs) in addition to the progenitors pericytes engaged to tumour vasculature location in order to distinguish into endothelial cells and pericytes supporting the vessels formation [54,55]. A dual function is played by the EPC's since not only do they produce fresh blood vessels nonetheless they additionally discharge growth factors preserving inflammatory status blamable for the tumour growth as well as metastatisation [32]. Throughout the tumour advancement EPCs instigate the secretion of VEGF as well as SDF-1 which attracts the tumour and endothelial cells, expressing CXCR4 upon their surface, atop hypoxic tissue generating a pre-metastatic function prior to metastatic cells arrival [56]. Numerous studies have revealed that circulating EPCs remain greater among the cancer patients equated to that of a healthy donor and compare by means of prognosis [57]. The disarrayed landscape of the tumour vasculature ensuing from these advances minimize the entrance of chemotherapeutic agents towards tumour and creates a blockade contrary to the entry of cytotoxic T cells (Tc), shielding tumour from immune response [58]. Additional cells closely allied towards endothelial cells are the endothelial cells of lymphatic vessels since these cells breakdown owing to upsurge in the interstitial fluid pressure (IFP) generating several hindrances towards drug delivery [59]. Higher IFP is instigated in portion through the variations in ECM conformation, fibroblast-arbitrated shrinkage of the interstitial space, as well as a malfunctioning lymphatic system inside the tumour.

*Role of immune system in cancer therapy*

Meddling of the tumour through immune in addition by the inflammatory cells may perhaps assist tumour development in contrary with the main philosophy concerning the role of immune system in detecting in addition eradicating a hefty portion of nascent tumour cells was concluded by an abundance of renewed evidences [60]. All types of immune cell might perhaps be located in TME, such as macrophages, dendritic cells, mast cells, natural killer (NK), naïve and memory lymphocytes B cells, effector T helper (Th) cells including: Th1 cells, Th2 cells and Th17 cells, regulatory T (Treg) cells, T follicular helper (TFH) cells and Tc cells [61]. Immune and inflammatory cells secrete growth factors for example epidermal growth factor (EGF), VEGF-A/C, FGF2, numerous cytokines intensifying inflammatory situation, as well as enzymes degrading extracellular matrix, for example, MMPs, cathepsin, and heparinises. Such dynamics might encourage tumour angiogenesis, tumour cells proliferation, as well as cancer metastatisation. Besides, such cells by discharging TGF-b as well as IL-10 remain guilty towards the immunosuppression through the stimulation of Treg drafted inside tumour [62,63]. Firstly, TGF-b1 pushes Th1 as well as Th2 balance in the direction of the Th2 phenotypes devoid of cytotoxic activity against tumour, prohibits the Th1 response besides M1-type macrophages activity, suppress lymphocytes CD8, natural killer, as well as the dendritic cells function, breeds Treg alongside immunosuppressive function, thus promoting M2 type macrophages having a pro-tumoral activity. TGF-b1 intensifies IL-10 expression as well as the chemo-attractant protein (MCP-1) augmenting tumour penetration besides immune suppression [63]. Alternative trait marked among the immune cells showed inside tumour is the T-cell "exhaustion phenomena" principally diagnosed in enduring infection besides suggesting a vibrant procedure backing the weakened T-cell attack counter to tumours or pathogens [64]. Augmented expression of the multiple immune checkpoints is considered as a key symbol of T-cell exhaustion, for example programmed cell death receptor-1 (PD-1), cytotoxic T-lymphocyte protein 4 (CTLA-4) as well as a new-fangled immune checkpoint molecules, for example, lymphocyte activation gene-3 (LAG-3), T-cell immunoglobulin, ITIM domain (TIGIT), besides T- cell immunoglobulin-3 (TIM-3). As, CTLA-4, LAG-3, TIM-3, and TIGIT predominantly interrelate among their concerned ligands restraining T-cell stimulation [65]. Instead, PD-1 expression stays upregulated upon stimulated T cells besides ligation of PD-1 with PD-L1 or PD-L2 principally befalls in the margin resulting in the suppression of stimulated T cells at the effector phase [66]. The vital constituent in mouse and human tumours is immune cell. Immune cells might emit an inflammatory agent so as to affect TME. Tumour-intruding lymphocytes (TILs), comprising of T cells, B cells besides NK cells, remain primarily receptive for indigenous activation. Functioning of immune response in tumours remains to be contentious, either hindering or else vigorously stimulating tumour growth [67].

*Role of T cells in cancer therapy*

In cell-supported immunity T cells enjoy a stimulating role. T cells of diverse categories, counting cytotoxic T cells, alpha beta T cells in addition gamma delta T cells, characteristic responsibilities allied with each of them [68]. Since as we know that cytotoxic $CD8^+$ T cells may terminate tumour cells besides getting rid of substantial solid tumours. Such immune cells are categorized by means of a CD8 protein on their cell surface which permits them to identify, bind and slaughter cells infested by intracellular bacteria, intracellular viruses besides cancer cells [69,70]. An important role of shielding the body from infections as well as controlling immune responses to tumour cells is being played by CD4+ T cells [70]. CD4+ T helper cells are a type of blood cells which form an indispensable component of the human immune system. They are frequently mentioned as CD4 cells, T-helper cells or T4 cells. Yet, cancer cells also the tumour stromal cells in the TME might manufacture monocyte chemo-attractant protein-1 (MCP-1), that deters the T cells from responsibilities. Consequently, for operational cancer therapy stimulating the immune system is imperative [70]. CD4+ regulatory T cells (T regs) are extremely immune suppressive and has a vital function in the self-tolerance upkeep and immune homeostasis *via* expressing the transcription factor FoxP3, hitherto in malignant tumours they encourage tumour development through overpowering operative antitumor immunity. Undeniably, elevated level of intrusion by T regs is detected in tumour tissues

hence their diminution supplements antitumor immune retorts in animal models. Furthermore, in several categories of human cancers augmented figures of T regs and diminished proportions of CD8+ T cells to T regs amongst tumour-infiltrating lymphocytes are interrelated with inadequate diagnosis. Immune checkpoint blockade made available a novel understanding in cancer treatment due to up-to-date achievements of cancer immunotherapy [71].

*Role of tumour associated macrophages in cancer therapy*

Tumour-associated macrophages are habitually profuse in addition of being present, at every phase of maximum human and experimental murine tumours [72,73]. In the stromal section of solid tumours macrophages are situated which can contribute both in the tumour development (*e.g.* cell proliferation, metastasis and incursion) or in the anti-tumour progresses, contradictory to the macrophage subtypes [74]. Chief immuno-regulatory cells to the immune reaction are the tumour-associated macrophages interrelated by means of a comprehensive variety of growth factors, cytokines and chemokines [75]. A vital role of linking inflammation with cancer is being played by TAMs. TAMs might perhaps encourage propagation, incursion, and metastasis of tumour cells, inspire tumour angiogenesis, besides impeding the antitumor immune response facilitated by T cells, shadowed by means of the advancement of tumour development [75]. In diverse cancer representations there remains solid indications of tumour preferment by TAMs, in addition to an amplified TAM occurrence associates thru short survival rates in numerous human cancers. TAMs are here and now being acknowledged as possible therapeutic targets intended for cancer owing to the disentanglement of the association amongst TAMs and malignant tumours. An innovative approach aimed at treatment of cancers is the targeting TAMs.

*Role of dendritic cells in cancer therapy*

Distinctive immune cells present in the tumour are known as dendritic cells (DCs). In addition, of being involved in cancer immunotherapy, DCs can stimulate, sustain and trigger the antitumor immunity [76]. Certain DCs might stimulate B cells, natural killer (NK) cells in addition natural killer T (NKT) cells [77–79]. T cell responses in tumour tissues have been discovered to be subdued by certain DCs, in addition the DCs maybe engaged in place of the sensor by seizing attacking microbes and diffusing ensuing data headed for lymphocytes. Moreover, in tumour-specific effector T cell generation DCs correspondingly have an important role [80]. There are indications that the immune system is involved in the scrutiny and rejection of initial tumours, and in manipulating the advance of clinically evident disease [78]. Henceforth, an extraordinary amount of research has been directed on the breeding of DC and other cellular cancer vaccines for tumour immunotherapy, although clinical success has been limited to date. One promising exception is adoptive cell therapy (ACT), which involves extracting infiltrating lymphocytes from a patient's tumour, expanding them *in vitro* and reintroducing them into the patient. This is a difficult procedure, and sufficient numbers of high-affinity tumour-specific T cells are not always achieved; however, it has resulted in some remarkable tumour regressions [78]. Although ACT patients are pre-conditioned by lymphodepletion and the number of transferred T cells is very high, ACT does at least indicate that given the right conditions, the immune system can indeed be a powerful tool in cancer therapy.

*Role of B cells in cancer therapy*

B cells situated inside draining lymph nodes additionally in the lymphoid assemblies adjoining tumour microenvironment are a class of lymphocytes [81]. B cells carrying distinct functionalities in the tumour possess a wide-ranging populace [82]. Autoimmune stimulates related B cell are every so often placed in contrasting tumours. Cytokines discharged by the B cells might impact the roles of additional cells in cancer development [83]. Perhaps, to realize immuno-suppression or accelerate tumour development B cells can discharge IL10 and Ig G to increase antigen IgG antibody complexes [84]. Furthermore, B cells might identify an antigen, control antigen release besides moderate immune responses of the T cell. Antibodies formed by B cells, may perhaps amend the functions of their corresponding antigenic marks on cancer cells, opsonize tumour cells to demonstrate and cross-demonstrate the tumour antigens by means of dendritic cells *via* stimulating the counterpart cascade, otherwise contribute to natural killer (NK) cell arbitrated tumour assassination by means of antibody-reliant on cell-facilitated cytotoxicity. Even though antibodies contrary to tumour antigens recurrently located in cancer patient's serum [84], the functioning of the humoral immune responses counter to cancer continues to be contentious. Additionally, several antibodies present in the cancer patients are focused counter to autoantigens-molecules which are existing in all the tumour cells along with unmutated host cells.

*Role of myeloid-derived suppressor cells (MDSCs) in cancer therapy*

Immune cells nurtured up from bone marrow precursor cells are known as MDSCs [85]. Monocytic MDSCs together with polymorphonuclear MDSCs are regarded as the two critical categories of MDSCs. Preceding one is analogous to monocytes, while as the latter ones are equivalent to neutrophils [86]. In tumour tissues and peripheral lymphoid organs MDSCs primarily amass in addition may subdue tumour evolution through obstructing the purposes of T cells besides NK cells [87]. Consequently, a major encouraging cancer therapeutic tactic is through the extension of MDSCs. Additionally, MDSCs might perhaps be cast-off ways to aim augmentation of the accretion of chemotherapeutic agents besides immunotherapeutic agents. The function of MDSCs in tumour development has been well-recognized. Only under certain pathological circumstances for instance chronic inflammation besides cancer these cells were discovered to be formed. Recognized tumours might perhaps yield numerous factors which can harm the myelopoiesis preferring formation of the MDSC, transferring to the tumour site besides their stimulation. MDSCs encourage tumour development through impeding of the anti-tumour roles of T and NK cells, as being one amongst the utmost effective immunosuppressive cells [87].

*Role of tumour endothelial cells (TECs) in cancer therapy*

Angiogenesis is the course of development of fresh blood vessels upon which tumour development depends. Fresh blood vessels formed because of angiogenesis stream oxygen in addition nutrients to the tumour, supporting its development besides offering an entry intended for tumour metastasis. An equilibrium amongst angiogenic activators in addition inhibitors inside the TME controls the tumour angiogenesis process. Since these newly made tumour blood vessels begin after former ordinary vessels, tumour blood vessels, besides tumour endothelial cells (TECs) have factually stayed the similar as the normal blood vessels and endothelial cells. However, sign of TECs' differentiating asymmetrical phenotypes has amplified [88]. Furthermore, it was discovered that TECs comprises of a varied population. Accordingly, the targets in cancer therapy are TECs lining tumour blood vessels. Paralleled with ordinary endothelial cells, TECs possess heterogeneity in addition they can react to growth factors besides many other diverse drug molecules. Numerous aspects counting the VEGF together with FGF in tumour can arouse TECs for cancer development. Tumour blood vessels possessing uneven morphologies besides having a leaky assembly plays serious a part in tumour development and metastasis has been well acknowledged. Roughly amongst all the

cancers TECs are phenotypically comparable, hence are a confident of targeting the most cancer groups [88]. Numerous testified TEC targeting arrangements such, arginine-glycine- aspartic acid (RGD) peptides were employed towards identifying the integrin $a_vb_3$, which is overexpressed in TECs [89].

*Role of natural killer (NK) and natural Killer T (NKTs) cells in cancer therapy*

At the boundary amongst the innate and the adaptive immune system natural killer T (NKT) cells are a subsection of CD1d-restricted T cells. NKT cells might perhaps be divided into efficient subcategories which can reply swiftly towards an extensive range of the glycolipids in addition stress-related proteins by means of T or natural killer (NK) cell-like effector procedure. They have a leading controlling outcome on immune stimulus by releasing cytokines, in the tumour immune surveillance NKT cells are also well thought-out as vital competitors. Throughout the initial tumour progression, T helper (TH)1-like NKT cell subsets possess the capacity towards speedily activating the tumour-specific T cells in addition to the effector NK cells which could eradicate tumour cells. In the event of tumour development, NKT cells possibly will turn out to be over-activated besides anergic steering towards the removal of a portion of the NKT cell populace in patients by means of activation-induced cell death. Moreover, residual NKT cells turn out to be hypo reactive, or else shift in the direction of immunosuppressive TH2-/T controlling-corresponding NKT cell subsets, in that way enabling tumour development besides immune escape [90]. NK as well as NKT cells are vital participants for controlling anti-tumor immunity, allocating analogous phenotypes in addition to the roles. NK cells which are in the lymphocytic penetrates besides the surroundings of tumour tissue are not in a straight interaction by means of tumour cells nonetheless can instigate a fast-immune response inside tumour stroma. A mixed assembly of T cells which enjoy the physiognomies of both T cells and NK cells are NKT cells. αβ T-cell receptors in addition to a collection of molecular indicators which are typically attached by means of NK cells are expressed by the NKT cells. NKT cells may dynamically provoke NK cells through making IFNg, which then participates in shaping the adaptive immune reaction [90]. NKT cell bluntly provoke immune reaction, for example, identifying glycolipid antigen as well as manufacturing pro-inflammatory T helper1(TH1) cytokines and anti-inflammatory TH2 cytokines [91].

*Role of pericytes in cancer therapy*

Cells capable of producing contraction and cloak near the endothelial cells of blood capillaries throughout the body are known as Pericytes [92]. Pericytes afford an encouragement assembly for blood vessel in tumour vasculature [93]. Pericytes are vital controllers which control the angiogenesis as well as vascular stability [94], besides can be engaged in place of stromal target intended for cancer therapy. Twofold attack of endothelial cells as well as pericytes *via* anti-VEGF therapy besides the PDGF-b aptamer is additionally effective compared to the monotherapy in human ovarian carcinoma models as documented by Sood's group [95]. Nonetheless, the pericytes handling of tumour vasculature is squat because of the elevated degree of pro-angiogenic factors, that correspondingly associates through meagre prognosis besides abnormal metastases [96]. Therefore, increasing the pericyte coverage could be anticipated as a means of inspiring approach for cancer therapy. With the sufficient coverage of pericytes and the normal contacts amongst ECs and pericytes, the stable and mature vessel structure/function can be moulded. Because the pericytes coverage and pericytes-ECs interactions are every so often abnormal in cancer-related vasculatures, targeting pericytes would be a vital approach for anticancer treatment [95]. The restoration of normal pericytes coverage and function may augment cancers responses to chemo and radiation therapies by means of upholding the normalization of cancer vasculature, together with increasing the perfusion and oxygenation of located cancer [96].

*Role of tumour associated neutrophils (TANs) in cancer therapy*

Through secretion of the cytokines and chemokines TANs play a crucial function in augmenting angiogenesis as well as immunosuppression at the tumour site. Numerous findings established TANs might secrete a matrix metalloprotease 9 (MMP9) in addition VEGF, then exert an extraordinary effect on tumour motility, migration as well as invasion [97]. Alternative key role of TANs is to manufacture reactive oxygen species (ROS), the degree reactive oxygen species (ROS) interconnected to carcinogenesis. Neutrophils could encourage mutation in Chinese hamster ovary (CHO) cells was recognized by the Stossel's group [98]. TANs rapidly endure apoptosis besides carrying a minuscule blood circulation half-life of around 6–8 h under physiological conditions [99].

*Extra-cellular matrix (ECM) in cancer therapy*

An intricate association amongst collagen, proteoglycans plus additional molecules is known as extra cellular matrix (ECM) is a vital component of ordinary tissues plus bids indispensable signals aimed at cell development, migration, adhesion, proliferation, survival, besides further metabolic roles [100,101]. Some important proteins present in the ECM comprise of fibrous proteins (collagen, elastin, fibronectin, laminin) plus proteoglycans (chondroitin sulphate, heparin sulphate, keratin sulphate and hyaluronic acid) aiding tissue rigorousness besides organization of basement membrane, which functions as a blockade amongst tumour cells and stroma [101]. While as we signify ECM, thus not only do we deliberate upon proteins as significant component nonetheless likewise integrate cytokines, growth factor, hormones secreted by stromal and tumour cells, physical as well as chemical parameters, for example, pH, oxygen tension, interstitial pressure, and fluid flux regulating cancer progression and metastatic dissemination [101]. Intratumoral hypoxia, loss-of-function for VHL gene, gain-of-function for oncogenes, viral transforming genes, besides surge in hypoxia-inducible factors (HIFs) action simultaneous amid tumour growth, vascularization, plus metastasis in animal models besides in clinical studies [50]. HIF-1 activates transcription of genes encoding proteases that degrade (CTSC, MMP2, MMP9, MMP14, PLAUR) or remodel (LOX, LOXL2, LOXL4) the extracellular matrix inside the primary tissue and at distant sites of metastasis [50]. Moreover, activation of the motility factors (AMF, MET), permeability factors (VEGF, ANGPT2) promoting the intravasation of cancer cells into blood vessels, cell surface (L1CAM), and secreted (ANGPTL4) proteins responsible for extravasation of cancer cells into the parenchyma at metastatic sites [50]. HIFs correspondingly control cell proliferation as well as endurance through connexion of hypoxia receptive constituent in the genes encoding for VEGF, stromal cell-derived factor 1 (SDF-1 also known as CXCL12), TGF-α, angiopoietin, PDGFb, placental growth factor (PGF), FGF2, besides connective tissue growth factor (CTGF) [50]. Integrin's exist as cell surface receptors controlling communications among cells with the ECM proteins subsequently to adjudicate linkage to the extracellular matrix. Subsequently due to these communication, proteins stimulate several molecular signalling, such as, focal adhesion kinases (FAKs), Src family kinases (SFKs), as well as the scaffolding molecules, for example, p130 CRK-associated substrate (p130CAS; additionally, well-known as BCAR1) indorsing the focal cellular adhesion [102]. Furthermore, they employee proteins, for example, talin, paxillin, α-actinin, tensin besides vinculin coupling the ECM to the actin cytoskeleton [102]. A mounting attention is dedicated over association among integrin and cancer as numerous analyses narrated that integrin's are considerably up-regulated

in a variety of solid tumours engaged in tumorigenesis as well as tumour progression [103].

## Tumour vasculture abnormalities

In the cancer nanotechnology research, efficacious carriage of nanomedicine into the solid tumour is of grave importance [104]. For the distribution of nanomedicine an efficient vascular network is an essential perquisite to facilitate consistent transport of these mediators through convection as well as diffusion-based approach [105]. Although similar to regular blood vessels, tumour blood vessels are made up of endothelial cells, mural cells besides basement membranes, the blood vessels of cancerous tumours have innumerable physical as well as functional distortions [106,107]. These vessels exist as leaky, feebly systematized, haphazardly moulded besides being twisted. The physical as well as the operational irregularities among these vascular links happens due to the disparity amongst proangiogenic plus antiangiogenic signals inside the TME, pushed *via* an unchallenged activity of the features, for example, vascular endothelial growth factor (VEGF). If appropriately implemented, angiogenesis inhibition may perhaps reasonably refurbish the physical reliability of tumour vessels as well as expedite the intratumoral transfer of minute molecules [108]. The missing tumour choosiness is the challenge encountered by the chemotherapeutic mediators. Aiming at the competent tumour delivery nanosized vehicles are admirable entrants [109]. Manipulating the TME might help to fashion nanoparticles possessing elevated tumour buildup through passive or active targeting, besides consequently, augment their cancer therapy effectiveness [107,110].

### *Role of passive targeting to tumour by improved permeability and retention effect in cancer therapy*

Macromolecules along with NPs amass especially in the neoplastic tissues in passive targeting because of the enhanced permeability and retention (EPR) effect. The nanometres size as well as range of the nanoparticles are two important physiognomies of the neoplastic tissues on which EPR is founded, explicitly the leaky vasculature as well as the spoilt lymphatic drainage. The EPR effect regarded as a feature *via* which nanoparticles with appropriate dimensions manage to amass inside tumour tissues considerably compared to normal tissues besides lengthening the retention time of nanoparticles in the tumour region [111,112].

The abnormal tumour blood vessels stimulate vascular permeability is the main reason for such purpose [113]. Nanoparticles within the size range of 20–200 nm incline towards penetration of the inner section of interstitial space because of inadequately allied flawed endothelial cells [107,114]. Furthermore, authorization of the nanoparticles present in the interstitial area of tumour tissue are sluggish because of the scarcity of lymphatic drainage in tumour tissue [114]. Through dodging of the immune scrutiny besides boosting circulation of NPs the EPR effect could be enhanced [109]. The properties of NPs strongly influence the EPR effect (Scheme 3).

In most of the cancer nanomedicines, EPR effect has become an important mainstay. Although in case of small animal models carrying a transplanted tumour it has been well-established, however it's relevancy towards human tumours continues to be contentious [114]. Latest models emphasizing on this disagreement contain declarations, for example, the "EPR effect flops in the clinic" besides it "functions in rodents except not in humans", whereas some emphasize on this fact that "EPR effect continues to be the key mechanism for additional emphasize concerning the complications plus heterogeneities related with clinically pertinent tumours [113,114]. Key idea of passive targeting NPs is the tumour microvasculature. Mediators controlling blood pressure besides vascular calibre perhaps controlled towards swinging the balance to an additional appealing tumour environment aimed at NPs. Cynics opinion towards a fact that passive targeting simplicities effective build-up of the NPs in the tumour interstitium nonetheless cannot advance their uptake by cancer cells. Such uptake possibly will be realized *via* actively targeting NPs towards receptors overexpressed upon objective cancer cells.

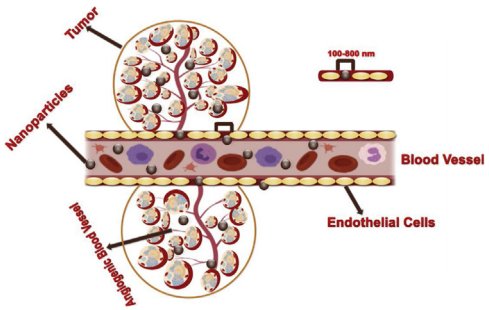


**Scheme 3.** A graphic illustration of the enhanced permeability and retention (EPR) effect. Angiogenic vessels in the tumour site are abnormal in form with large vascular fenestrae.

### *Effect of size on the retention of nanoparticles in cancer therapy*

Transporting the nanomedicine towards solid tumours are subject to abnormal TME besides physicochemical features possessed by the nanoparticle. EPR effect symbolizes a large part the TME but it is not satisfactory to cause effective delivery of nanoparticle formulations. The effect of the nanoparticle properties and particularly its size must be considered to optimize drug delivery and therapeutic outcome. The dimensions of NPs might meaningfully influence their bio-distribution as well as build-up inside tumour tissue [115–117]. In order to evade filtration by the kidney to achieve a lengthened blood circulation the size must stand greater than 4–5 nm. Also, these NPs should be below 200 nm thus to extravasate the leaky vasculature [118]. A 50 nm MSNs coated with the PEI-PEG copolymer realized improved passive tumour build-up compared to 100 nm ones in the KB-31 tumour model was validated Meng et al. [116]. For cancer therapy MSNs continue evolve as promising drug carriers. The distribution, absorption, excretion as well as the toxicity of 110 nm MSNs was reported by Tang's group [119]. After hypodermic and intramuscular administration MSNs were challenging to absorb was established by them. Moreover, Kim et al. methodically examined particle size-dependent tumour stockpile by means of PEGylated MSNs in a U87MG tumour model. A 100–150 nm-sized particles suffered a 4–6.5-fold higher tumour uptake compared to the one possessing a diameter of 30 or 4300 nm was reported by them [120]. MDA-MB-231 breast tumour uptake of spherical silica beads varying in size from 700 nm to 3 mm were scrutinized by Decuzzi et al. [117]. Their group established that number of beads amassed inside tumour location amplified monotonically whilst diameter dwindled from 3 mm to 700 nm. Though all the overhead researches engaged in spherical silica as way for prototype towards assess EPR effect, EPR effect correspondingly reliant over the category of tumour type as well as tumour size because of the variances in tumour vascularization and angiogenesis [2]. Arrangement of nanoparticles biodistribution is exceedingly reliant on their structure plus stiffness [121–123]. Non-spherical nanoparticles and spherical one's parade distinctive activities *in vivo* [124]. As in case of spherical particles having diameter higher than 200 nm could not pass across the spleen, nevertheless concave-shaped red blood cells (B10 mm in diameter) may permeate across splenic tissue somewhat effortlessly [121]. Short-rod shaped MSNs (an aspect ratio of

1.5) ensured extra prompt clearance rate compared to the long-rod MSNs (an aspect ratio of 5) as established by Huang et al. [122]. NPs prompt clearance from blood is a core concern regarding their clinical applications. Possession of nanoparticles in the blood may profit them to arrive at the tumour tissue through EPR effect. The long-rod MSNs may perhaps recuperate blood habitation of NPs besides augmenting the EPR effect. Compared to spherical micelles, micelles with wormlike morphology incline to endure a circulation time due to leisurelier clearance *via* the mononuclear phagocyte system was established Alexis et al. [125]. Here it is worth mentioning that regarding the shape effect on *in vivo* functioning is yet inadequate due to nonexistence of suitable synthetic procedure to formulate homogeneous NPs having subtly tuned morphology.

*Effect of the surface properties in cancer therapy*

Modification of superficial features stands greatly employed towards advancing the blood circulation as well as tumour build-up of NPs. Negatively charged surface of the blood vessels, besides the positively charged NPs may perhaps attach to the luminal surface of vascular walls and being exonerated promptly from the blood circulation [126]. Because of charge-selective filtration negatively charged particles, instead, display a superior build-up inside liver [127]. Masking NPs with antibiofouling synthetic polymers or cell membranes is an encouraging tactic to avert NPs from clearance [128]. As stated that neutral synthetic polymers might lessen detrimental adhesion of protein [129]. A FDA permitted polymer poly (ethylene glycol) (PEG) celebrated due to its knack to augment NPs surface hydrophilicity besides lessening the protein association [130]. PEG has been mostly viewed as a safe (GRAS). Abuchowsky et al. initially reported and established that due the modification of albumin as well as catalase *via* PEGylation might perhaps augment blood circulation in mice [131,132]. Moreover, the PEGylation tactic stands magnificently applied in numerous agents comprising nanovehicles. Lately, Chan's group narrated that surface density as well as molecular weight of PEG significantly impact the capability of NPs to defy protein adsorption with longer PEG chains besides superior PEG surface density being superior [133,134]. Zwitterionic materials enclosing together the positively as well as negatively charged groups preserve an inclusive neutral charge exist as assuring an replacements which could successfully defy generic protein adsorption [135,136]. Zwitterionic polymers for example poly(phosphoryl-choline) [137,138], poly(sulfobetaine) [139] and poly(carboxybetaine) revealed analogous functioning along PEG towards opposing the protein adsorption from plasma [139,140]. The zwitterionic poly(carboxybetaine) (PCB)-coated gold NPs (PCB- GNPs) unveiled a much lengthier circulation half-life ($t_{1/2}$ = 55.8 h) than PEG-coated GNPs (8.7 h) as validated by Yang et al. Additionally, second dosage of PEG-G NPs underwent an intense reduction in $t_{1/2}$ to 5.2 h, the PCB-G NPs preserved a comparable blood circulation half-life ($t_{1/2}$ = 55.6 h for the second dose) [140]. To employ cell-membranes to mask NPs is an alternative functional tactic [141–143]. NPs stand entangled in several types of cell membranes, for example red blood cells, human platelets, leukocytes and cancer cells. NPs with membrane-cloaked might impersonate cells so as to avoid uptake by the macrophage. Formulation of polymeric NPs enfolded in the plasma membranes of human platelets was reported by Hu et al. Such NPs demonstrated platelet-mimicking features besides a decline in macrophage uptake through macrophage-like cells in autologous human plasma [141]. For gold NPs such as (RBC-Au NPs) red blood cells were also employed as a masquerade [143]. Subsequent RBC-AuNPs might circumvent macrophage uptake *via* conferring immuno-suppressive characteristics as well as protect the particles from cooperating through thiolated compounds on the AuNPs. Leucocyte as well as cancer-cell membranes where reported to augment the blood circulation and tumour buildup [144,145].

*Role of active targeting of NPs in cancer therapy*

An ideal delivery approach founded on receptor-based active targeting of nanoparticles possess great potential. Aimed at premature tumour identification, therapy as well as post-therapeutic continuation tumour-targeted nanovehicles are being engaged. Moreover, active targeting permitted disabling numerous hindrances, for example, side-stepping blood-brain barricade as well as multi-drug resistance in tumours. Though NPs anticipate hoarding inside tumour tissue because of EPR effect, passive tumour targeting is reliant over tumour vascularization, angiogenesis hence consequently scarcities specificity as well as equilibrium. Together with tumour model category as well as tumour circumstances could extremely disturb the passive targeting efficiency [2,146]. Ligands that might singularly attach with analogous receptors overexpressed around tumour area (either the tumour cells or the TME) have been enclosed to the NPs for active targeting [147–149].

*Role of vascular endothelial growth factor (VEGF) in cancer therapy*

Angiogenesis is very vital for the growth of tumour as well as metastasis. An imperative signalling protein is the VEGF receptor (VEFR) provoking tumour angiogenesis which is overexpressed inside endothelium of the maximum solid tumours [150].

In 1983, Senger et al. initially acknowledged vascular permeability factor (VPF), which is a protein provoking vascular leakage in guinea, hamsters, pigs as well as mice [151]. Henceforth, anti-VEGF mono-clonal antibodies as well as other VEGF blockers were testified to have to have been able to efficaciously impede tumour development. Intended for VEGFR explicit targeting the usage of MSNs was postulated by Goel et al. Non-targeted NPs, in comparison to the targeted NPs displayed an augmentation of approximately three times that of tumour buildup in a U87MG human glioblastoma xenograft model. Macrocyclic chelator 1,4,7-triazacyclononane-triacetic acid (NOTA) was employed to alter the MSNs besides labelling it with $^{64}$Cu intended for positron emission tomography (PET) imaging also laden with an anti-VEGFR drug (sunitinib) aimed at therapy (Fig. 1) [152]. Intended for achieving the active targeting VEGF has been used over a range of NPs. For instance, conjugated VEGF was conjugated with 1,4,7,10-tetraazacyclododecane-1,4,7,10-tetraacetic acid (DOTA, $^{64}$Cu chelator) on top of quantum dots (QDs) designed for VEGFR-targeted PET/near-infrared fluorescence (NIRF) imaging by Chen et al. [153]. A magnetic coordination containing monoclonal antibodies counter to the vascular endothelial growth factor (mAb-VEGF) stayed linked to the BSA coated magnetic NPs ($Fe_3O_4$) were synthesized by Chekhonin group [154]. VEGF was also linked to organic NPs such as boronated polyamidoamine dendrimers. Sharp buildup of the dendrimer by the side of the periphery of 4T1 breast carcinoma tumour was established by the fluorescence imaging. Such dendrimers stood accompanying and intended for boron neutron capture therapy (BNCT) [155].

*Role of $\alpha_v\beta_3$ integrin in cancer therapy*

An endothelial cell receptor expressed in tumour-associated endothelial cells of numerous rapidly-increasing tumours is known as $\alpha_v\beta_3$ integrin [156]. Intended for arbitrating cell-to-cell as well as cell-to-matrix exchanges the $\alpha_v\beta_3$ integrin is very vital [156,157]. Investigators have spent ample time and efforts to advance $\alpha_v\beta_3$-targeted NPs designed for cancer diagnosis besides therapy. The advance of a cyclic RGD peptide-labelled QDs designed for tumour vasculature targeted NIR fluorescence imaging was

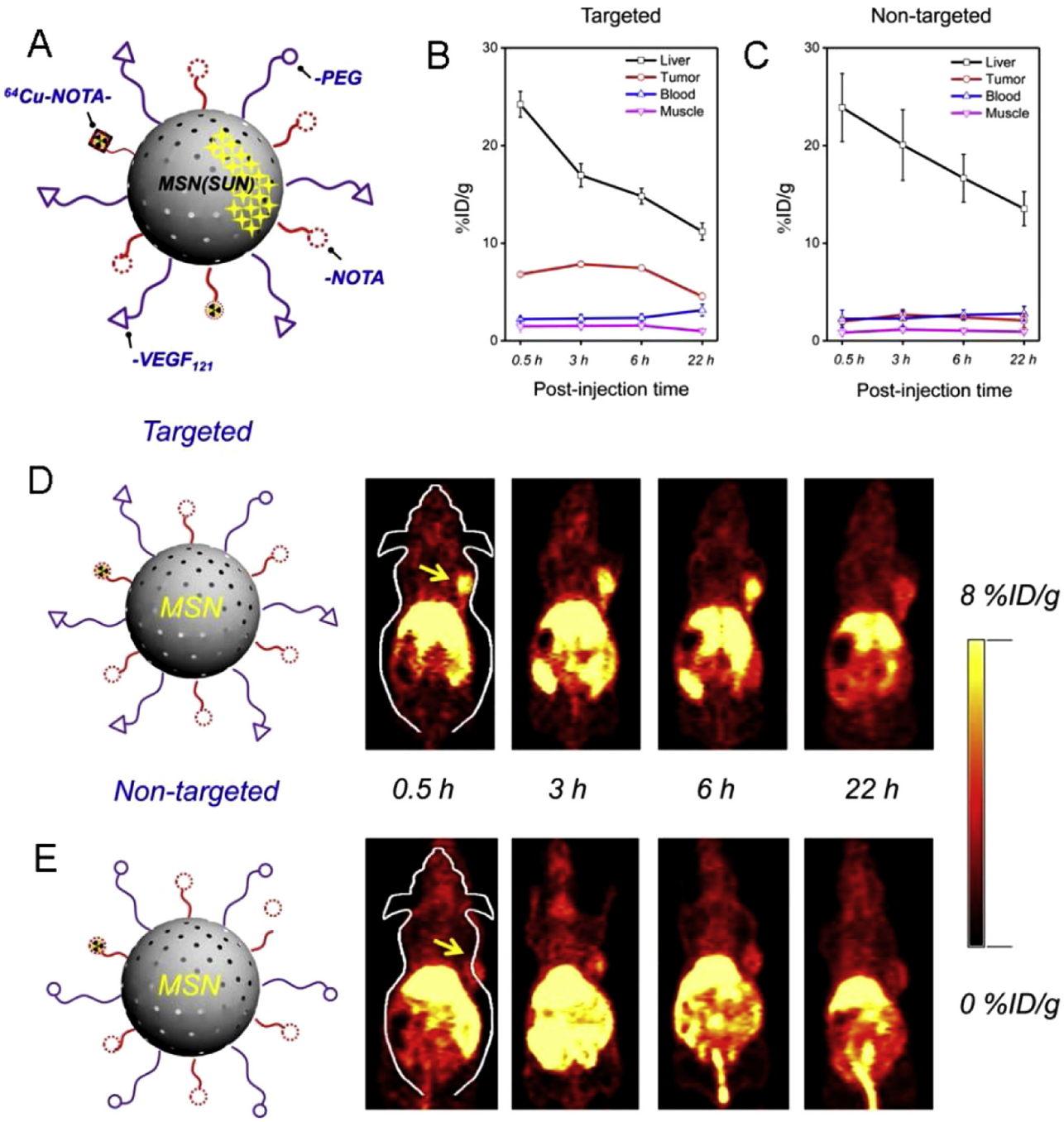


**Fig. 1.** (A) Graphic sketch of radioisotope $^{64}$Cu-labelled VEGF121 conjugated mesoporous silica NPs ($^{64}$Cu-NOTA-MSN-VEGF$_{121}$). (B and C) Region-of-interest (ROI) quantification of liver, U87MG tumour, blood, and muscle upon intravenous injection of (B) $^{64}$Cu-NOTA-MSN-PEG-VEGF$_{121}$ (targeted group), and (C) $^{64}$Cu-NOTA-MSN-PEG (non-targeted group) after various time points. (D and E) VEGFR targeted PET imaging in U87MG tumour-bearing mice. Coronal PET images of $^{64}$Cu-NOTA-MSN-PEGVEGF$_{121}$ (D) and 64Cu-NOTA-MSN-PEG (E) injected intravenously in U87MG tumour mice at various time points. The location of the tumour is indicated by the yellow arrows. (Reprinted with permission from Ref. [164]. Copyright 2014, American Chemical Society).

reported by Cai et al. [158]. Graf et al. explained that the cyclic pentapeptide c(RGDyK) tailored poly (D, L-lactic-co-glycolic acid)-block-polyethylene glycol (PLGA-PEG) NPs intended for platinum prodrug delivery [159]. In view of its non-toxicity, good bioavailability and biocompatibility polymer knows as PLGA stands permitted by the FDA [160]. PLGA may experience the hydrolysis inside body while manufacturing the novel monomers, lactic acid and glycolic acid. To achieve the selectively delivery of zinc hexadecafluorophthalocyanine ($ZnF_{16}Pc$, a photosensitizer) into the tumour endothelium, Zhen et al. employed an RGD tailored ferritin (RFRT) as a carrier. RFRT possess a robust linking empathy for integrin $\alpha_v\beta_3$. $^1O_2$ fashioned by $ZnF_{16}Pc$ increases tumour vascular permeability as well as steers towards a progressive tumour uptake of therapeutic NPs in the second dose (Fig. 2A-C). Several other NPs such as nonetheless not restricted to only copolymer NPs, magnetic NPs dendrimers, and upconversion NPs were customized by means of RGD aimed at augmenting tumour amassing [161–163].

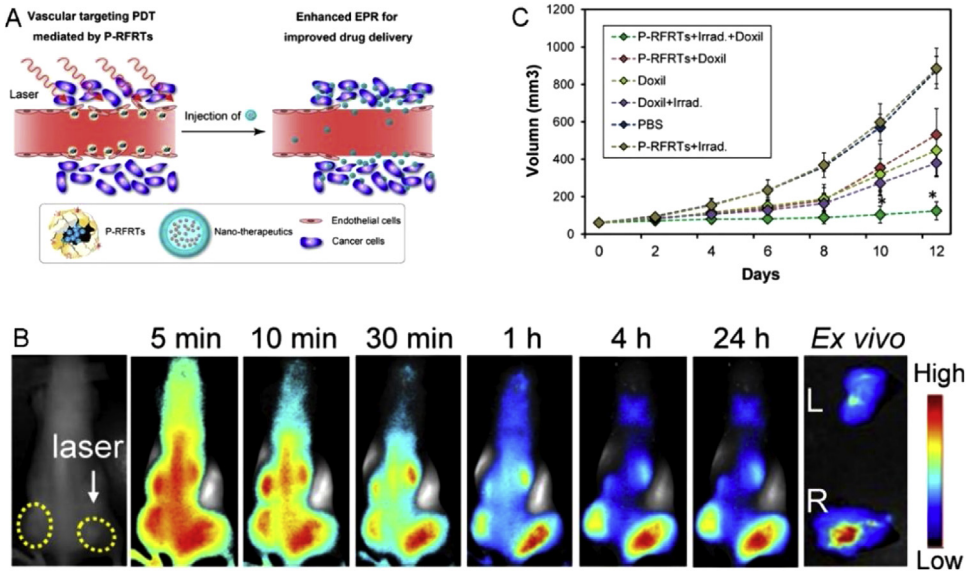


**Fig. 2.** (A) Functioning procedure of $ZnF_{16}Pc$-loaded RGD peptide modified ferritin (P-RFRTs) facilitated photodynamic therapy (PDT) achieved through buildup of P-RFRTs in the tumour after the intravenous injection besides irradiation with a 671-nm laser. (B) EPR improvement by PDT-induced P-RFRTs. At 24 h post-injection of P-RFRT, the right 4T1 tumour was irradiated by a 671 nm laser for 5 min followed by IRDye800-HSA injection. The right tumour has the enhanced EPR effect showing significantly higher albumin accumulation. (C) EPR enhancement led to improved tumour therapy outcome. Doxil was injected 5 min after the end of P-RFRT- mediated PDT. Control groups include animals receiving P-RFRTs and Doxil but no irradiation, Doxil only, irradiation only, P-RFRTs and irradiation but no Doxil, and PBS only. Compared to the control groups, animals receiving the PDT and Doxil combination showed much more significant tumour growth suppression.
(Reprinted with permission from ref. [165]. Copyright 2014, American Chemical Society).

*Role of vascular cell adhesion molecule-1 (VCAM-1) in cancer therapy*

Throughout inflammation and cancer VCAM-1 stays expressed upon equally in the luminal as well as lateral sides of endothelium, arbitrating cell adhesion in addition to spreading [166,167]. Molecules which link exclusively with VCAM-1 are favourable ligands intended for NPs in the direction of advancing the tumour build-up. PEG customized immunoliposomes (ILs) focused in contrast to VCAM-1 besides exploring its targeting ability towards tumour vessels was synthesized by Gosk et al. [168]. Meanwhile VCAM-1 stays rebelliously over-expressed upon the breast cancer cells, though testified as an impending therapeutic target counter to lung metastasis of breast cancer [169]. Cao et al. condensed a water-insoluble VCAM-1 inhibitor, succinobucol (SCB), inside a triblock polymer NPs [170]. Such SCB laden NPs considerably abridged VCAM-1 expression upon 4T1 cells. After the oral administration, such NPs might competently impede the lung metastasis of breast cancer. Same research groups additionally advanced SCB-loaded pH-responsive wormlike micelles aimed at lung metastasis treatment [171].

## Molecular imaging of TME

Molecular imaging permits the uncovering as well as imagining of cancer-associated biomarkers around tumour [172,173]. Molecular imaging may perhaps facilitate the prompt besides precise discovery of cancer, expediting use of molecular signatures to customize efficient in addition to the adapted therapies for better-quality patient persistence. Furthermore, molecular imaging carries prospective towards providing the noninvasive appraisal about TME all through tumour expansion as well as spread. Despite the fact that TME continuously changes in its topography, biomolecules inside the TME stay normally constant in dissimilar tumour categories, consequently crafting them as appropriate molecular imaging targets intended for a comprehensive extent of tumours [1]. Targeted cancer therapy as well as the imaging are currently typically aimed upon the biomarkers of cancer cells. Nonetheless, targeting in addition to the re-modulating the TME has been slowly utilized in aiming innovative therapies [174]. TME molecular imaging continues to play an indispensable function about identifying the reactions, procedures, besides efficiency of such innovative therapies [105]. Hence it may perhaps also assist in the finding of the “premetastatic niche”, accelerating the probability of cancer metastatic sites just before influx of cancer cells [175]. Such a methodology remains strategic since it consents designed for the defined diagnosis of cancer by spotting factors (*e.g.*, hypoxia) which brings heterogeneity in TME, local recurrence, and metastasis. TME molecular imaging offers for the timely, distinction cancer diagnosis, besides it may assist in the invention as well as advancement of novel efficient cancer therapies [176,177]. Two significant gears of cancer molecular imaging are: (1) imaging modalities for example magnetic resonance imaging (MRI), computed tomography (CT), positron emission tomography imaging (PET), ultra-sonography, as well as the optical imaging [178]; and (2) imaging probes or contrast agents, that remain manipulated towards focusing, discovering, besides picturing the cancer biomarkers [179,180]. Such as pitch for the development of imaging agents having amazing sensitivity, specificity, besides little toxicity apart from a comprehensive function are direly intended at precise molecular imaging.

*Molecular imaging of tumour physiological microenvironment*

TME physiology is different in comparison to some of its adjoining ordinary tissues. Deficient and flawed vascular assemblies in tumour are frequently incompetent for delivering nourishment required for the tumour development. Thus, bringing about scarcity of oxygen as well as other essential nutrients, diminished pH, hypoxia, besides augmented interstitial fluid pressure. Such exclusive TME physiognomies pungently narrate to tumour development, metastasis, besides recurrence in addition to therapy resistance. Aimed at better-quality cancer treatment therapeutic stratagems were advanced to normalize the TME [181]. TME molecular imaging due to physiological physiognomies consents

well-timed recognition, accuracy in diagnosis, besides evaluation of the therapeutic response. Decisively, contrasting cancer-specific molecular biomarkers which fluctuate in diverse cancer categories, phases, as well as the sites of origin, such fluctuations in TME physiological physiognomies are further coherent through a variety of cancer categories, that consents the institution of a unanimous stratagem aimed at comprehensive tumour imaging.

*pH fluctuations responsive molecular imaging of TME*

Typically TME is more acidic in comparison to that of an ordinary tissues having a less pH value, which is primarily credited to the creation of lactic acid due to aerobic environments supplemented through protons breed from the hydrolysis throughout synthesis of ATP [182]. Extracellular pH of ordinary tissues is sustained at a pH of 7.4, conversely pH of the TME stands in the scale of 6.2–6.9 [183]. It is postulated that such an acidic pH might support tumour metastasis through breeding invasive atmosphere aimed at ripping off the ECM besides for remodelling of the tissue [184,185].

Consequently, TME acidic pH might perhaps be a valuable target aimed at tumour imaging, investigating tumour metabolism, examining TME distresses, as well as measuring treatment outcomes. pH-stimulated signal "off-on" imaging agents for example fluorescence probes [186,187] as welll as the MRI contrast agents [188,189] were advanced in lieu of molecular imaging of acidic TME. An intresting sequence of ultra pH-sensitive (UPS) nanoprobes were advanced by Gao's group, that happen to be sensitive to pH (4–7.4) fluctuations as delicate as ±0.25. such nanoprobes furthermore endure a fluorescence activation ratio as high as 50-fold [190–192]. Such nanoprobes were grounded over the idea of the supramolecular self-assembly of the ionizable block copolymers (PEG-b-PR) besides PR is an ionizable block supplying a tertiary amine (Fig. 3A) [190]. Ionizable block were used to conjugate the fluorophores. Ionizable block breeds hydrophobic cores of the nanoprobes as well as the conjugated fluorophores compactly amass inside inner core ensuing in fluorescence self-quenching at an elevated pH. At low pH, the ionizable block turn out to be protonated and hydrophilic; prompting the nanoprobes to strip and the fluorophores to disaggregate. Such a consequences in a vivid upsurge in the fluorescence signal (Fig. 3A). Grounded over this idea, Ma et al. instituted a UPS library of nanoprobes with tailored pH transitions (4–7.4) besides broad fluorescent emissions (400–820 nm) through superiority of the hydrophobicity of the ionizable hydrophobic block and manipulating a extensive variety of exclusive fluorophores (Fig. 3B and C) [190].

pH-responsive MRI contrast mediators were devised and aimed at clear-cut jurisdiction of "off-on" distinction at pathological pH intended for TME imaging. A nanosized MR contrast mediator with capability to magnify MR signal in acidic situation were advanced by Mi et al. [193]. Such NPs, named as EGMnCap, and are constituted by a PEG shell besides a degradable calcium phosphate inner core with trapped $Mn^{2+}$ (Fig. 4A). In an acidic environment PEGMnCap NPs were briskly hydrolyzed towards expediting prompt release transported $Mn^{2+}$ (Fig. 4B). $Mn^{2+}$ discharged might further bind with proteins, thus significantly upsurges relaxivity, as well as outcomes into a higher MR signal [194]. Upon introduction to human serum albumin at a pH 6.5, and assessed at 0.59 T plus 37 °C, the longitudinal $r_1$ relaxivity of PEGMnCap amplified from 4.73 $mM^{-1}$ $s^{-1}$ to 19.96 $mM^{-1}$ $s^{-1}$ PEGMnCap improved the tumour contrast augmentation in mice carrying the subcutaneous C26 colon cancer copies upon comparsion with both PEGylated $Mn_2O_3$ nanoparticles, as well as clinically engaged contrast mediator Gd-DTPA. Fascinatingly, PEGMnCap efficiently identified metastatic tumours as irrelevant as 1 mm in the livers of mice bearing C26 colon tumour models (Fig. 4C, D). The connexion of NPs spreading as well as metastatic region was investigated through μ-SR-XRF (micro-synchrotron radiation X-ray fluorescence). Elevated quantities of $Mn^{2+}$ as well as $Ca^{2+}$ from PEGMnCap were located adjoining metastatic area were differentiated through H&E staining plus *via* squat concentrations of iron (Fig. 4E). An inadequacy towards the clinical bid of PEGMnCap might perhaps dut to its toxicity ascending from free $Mn^{2+}$ ions, though PEGMnCap carries six-fold upper average fatal dose comapreed to $MnCl_2$. Higer disclosure to free $Mn^{2+}$ ions could outcome into a neurodegenerative ailment distinguished as "manganism" having signs approximating to those of Parkinson's disease [195].

*Hypoxia responsive molecular imaging of TME*

Hypoxia is renowned trademark of TME, and renders a crucial function in cell propagation, endurance, delineation, in association with tumour angiogenesis, incursion, reappearance, as well as metastasis [196]. TME hypoxia is a consequence of oxygen ingesting through hastily multiplying tumour cells besides the inadequate allocation of oxygen obtainable from the incompetent tumour vasculature [197]. Elevated intensities of hypoxia inside TME remain concurrent alongside higher phases of malignancy [198], besides they are also related through resistance towards chemotherapy as well as radiation [199,200]. Hence, degree hypoxia remains a striking extrapolative aspect. Besides, tumour hypoxia brings about up-regulation of hypoxia-inducible factor-1 (HIF-1), which is regarded as an essential target for anticancer drug development [201]. Accordingly, hypoxia molecular imaging in the TME carries prodigious significance aimed at timely tumour finding besides understanding the pathological physiognomies of the tumour. Thus, it is going to aid in the advance of therapeutic approaches as well as appropriate supervising over treatment response [202]. The tactic of oxygen-responsive optical imaging probes is predominantly grounded over this opinion that the phosphorescence or fluorescence of a numerous dyes is quenchable with smattering quantities of oxygen [203,204].

Zhang et al. testified that boron films and NPs breed over dual-emissive iodide-substituted difluoroboron dibenzoymethane-poly (lactic acid) (BF2dbm(I)PLA) aimed at imaging hypoxia (Fig. 5A) [205]. Such materials flaunted momentous oxygen-insensitive blue fluorescence besides a robust oxygen-quenchable green phosphorescence. BF2dbm(I)PLA, with dissimilar molecular weights of PLA, were synthesized (P1 = 2700 Da, P2 = 7300 Da, and P3 = 17,600 Da). The fluorescence to phosphorescence ratio was tunable by fluctuating the chain length of the PLA (Fig. 5B). NPs prepared from high-molecular-weight BF2dbm(I)PLA (*e.g.*, P2) revealed composed as well as a detectible fluorescence besides phosphorescence intensities, and worked as a ratiometric tumour hypoxia imaging agents. Films made-up from low-molecular-weight BF2dbm(I)PLA (*e.g.*, P1) paraded trivial fluorescence as well as robust phosphorescence, and hence exhibited talent intended to be used as "turn on" sensors in order to discover hypoxic environments. Boron NPs prepared alongside P2 were deliberated and analyzed for optical imaging of tumour hypoxia in mice bearing 4T1 breast tumour models. Such NPs offered extraordinary dissimilarity amongst the microvascular region (red) as well as the tumour region as revealed in oxygen maps by fluorescence/phosphorescence ratios, unfettered by the gas inhaled (Fig. 5C). Nevertheless, the impending purpose of such NPs might get hampered through their ultraviolet-visible emission, which possesses meagre tissue penetration besides extraordinarily elevated background noise. Substantial volume of advancement was achieved to mature optical imaging probes through superior tissue penetration depths as well as shortened tissue autofluorescence [206,207]. Furthermore, besides oxygen-sensitive fluorophores, hypoxia biomarkers for example nitroreductase (NTR) as well as HIF-1 were employed towards advancing the probes intended for imaging tumour hypoxia [208]. In hypoxic tumours, reductive enzyme NTR is over-

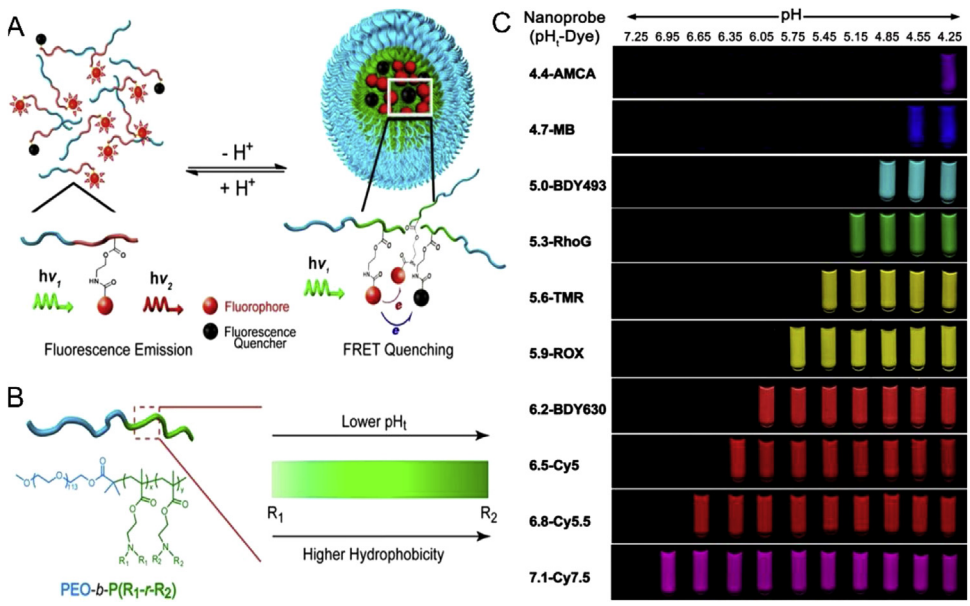


**Fig. 3.** Graphic sketch of ultra pH-sensitive (UPS) nanoprobes and random copolymer approach aimed at designing nanoprobes possessing tailored transition pH (pHt). pHt was magnificently adjusted through monitoring the hydrophobicity of the PR segment (A). Normalized relative fluorescence units (RFU) as a function of pH (B), and fluorescence images (C) for a library of UPS nanoprobes with every 0.3 increment of pH from pH 4 to 7.4.

Adapted with permission from ref [182].

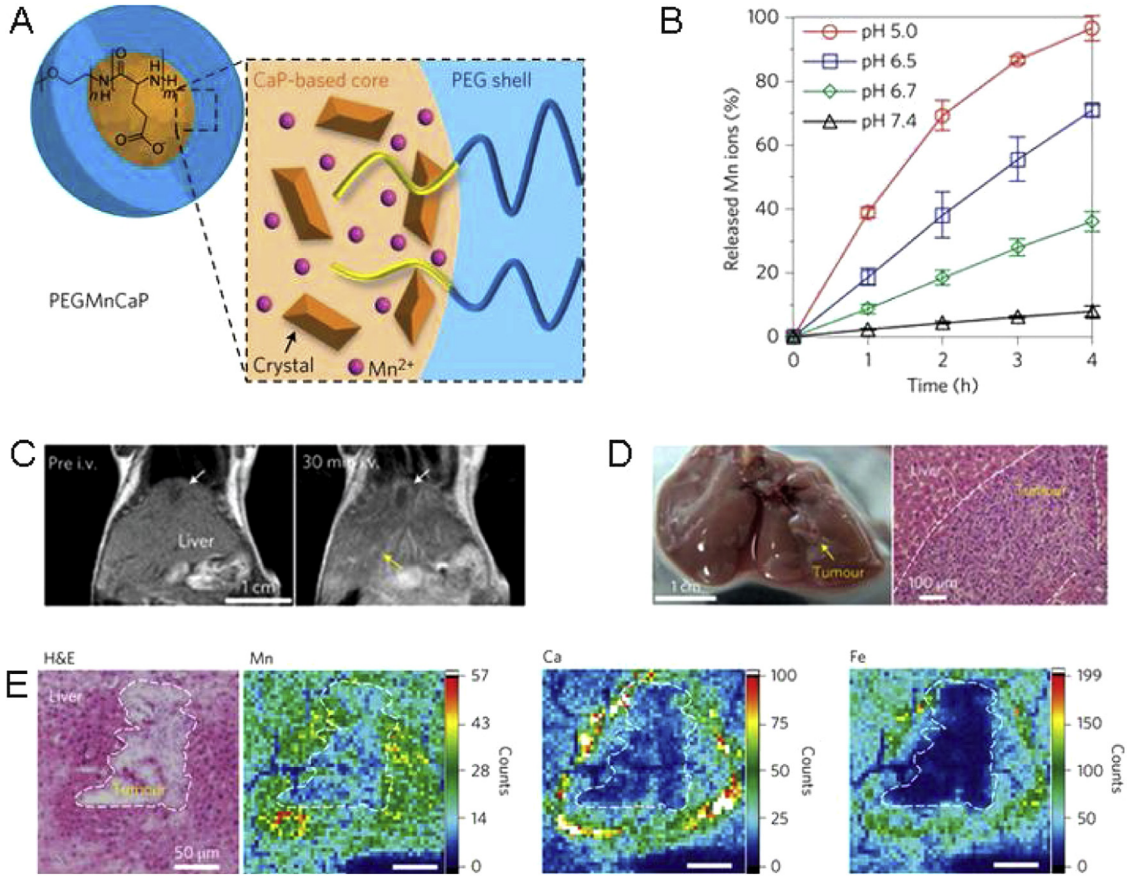


**Fig. 4.** Graphic sketch of the structure of the pH-sensitive nanoparticle (PEGMnCap) comprised of a PEG shell, Cap-based core and inner-trapped $Mn^{2+}$ (A). $Mn^{2+}$ releasing outline of PEGMnCap at diverse pH (B). *In vivo* MR imaging of liver metastasis exploiting PEGMnCap on mice bearing the metastatic C26 colon tumour (C). Images of liver metastasis and its H&E staining from an imaged mouse (D). Correlation of H&E stained liver metastasis and its micro distribution of PEGMnCap in liver metastasis scanned by μ-SR-XRF (E).

Adapted with permission from ref. [193].

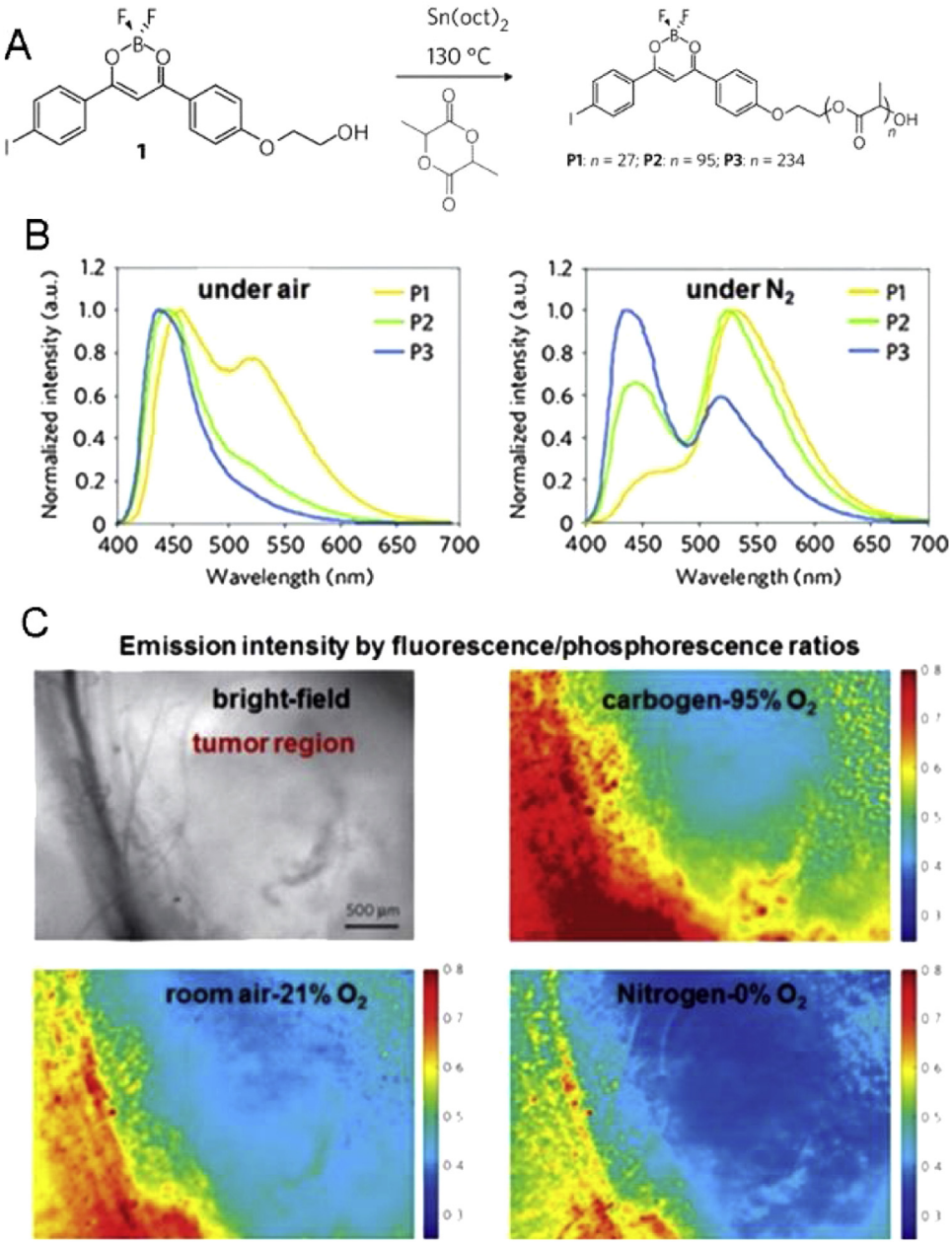


**Fig. 5.** Synthetic procedure and chemical structure of a dual-emissive polymer (BF2dbm(I)PLA) (A). The emission spectra of BF2dbm(I)PLA with different molecular weights under air or N2 (P1 = 2700 Da, P2 = 7300 Da, and P3 = 17,600 Da) (B). *In vivo* imaging of tumour hypoxia using P2 fabricated boron nanoparticles in mice bearing 4T1 breast cancer (C). A dorsal window chamber was used for hyperspectral imaging and emission intensity represents fluorescence/phosphorescence ratios under different breathing conditions.

Adapted with permission from [216].

expressed. Hence, the NTR level might be castoff towards analyzing the volume of hypoxia in TME. Aiming at scheming a fluorescent probe for detecting the NTR and NTR-catalyzed fluorescence quenching tactic was employed [209–211]. Li et al. testified an ultrasensitive fluorescent probe intended towards optical detection of NTR [211]. Two functional groups of the fluorescent probes a NTR-sensitive aromatic nitro group besides a fluorescent reporter.

Cyanine fluorescence emission of was quenched because of aromatic nitro group owing to its robust electron retraction effect besides recuperated following the reduction of nitro group by NTR (Fig. 6A). Remarkably, following the addition of 0.25 μg $mL^{-1}$ NTR the connecting groups as well as the position of the nitro fluorescence augmentation is approximately 110-times (Fig. 6B). Such a probe displayed significant sensitivity while detecting NTR in an A549 tumour *in vitro* (Fig. 6C) as well as *in vivo* (Fig. 6D). Substantial augmentation of NIR fluorescence was spotted in an A549 tumour 5 min following intratumoral injection of Cy7-1. The probe was not examined *via* systemic administration owing to poor pharmacokinetics. Aimed at imaging tumour hypoxia through systemic injection macromolecular as well as nanoparticle NTR-sensitive probes have been advanced [207]. Trivial molecules, for example, 2-nitroimidazole [212] as well as indolequinone [213] maybe reduced under tumour hypoxic environment, hence employed to paradigm bio-reduction stimulated fluorescence probes intended for hypoxia imaging group on the aromatic group significantly altered sensitivity of the NTR. Cy7-1 probe carrying as ester bond as well as nitro group at the para-phenyl position paraded superior NTR sensitivity.

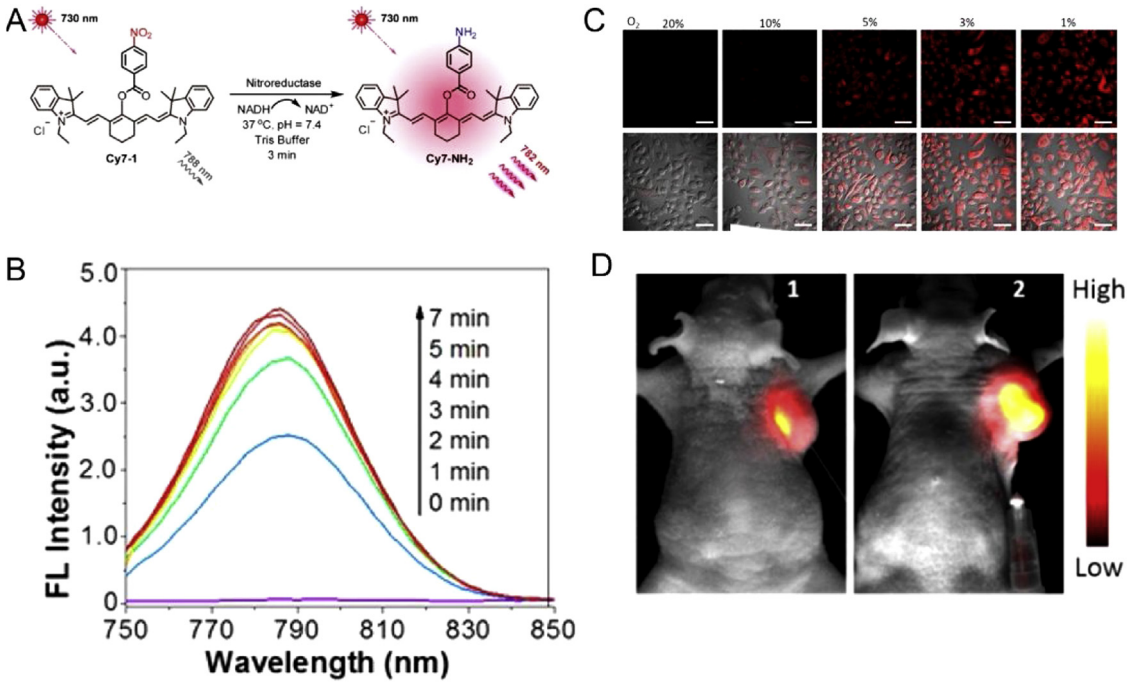


**Fig. 6.** Design of nitroreductase-responsive fluorescent probe Cy7-1 (A). The fluorescence spectral of Cy7-1 (10 μM) treated with nitroreductase (0.25 μg mL$^{-1}$) (B). *In vitro* fluorescence imaging of A549 cells incubated with Cy7-1 (5 μM) under different concentrations of $O_2$; scale bar = 60 μm (C). *In vivo* fluorescence imaging of mice bearing A549 tumours 5 min after intratumoral injection of Cy7-1 (20 μM) (tumour size: tumour 1 = 7 mm; tumour 2 = 12 mm) (D).
Modified with approval from Ref. [211].

*Tumour vasculture molecular imaging*

One of the most comprehensively reviewed physiognomies of the TME is the tumour vasculature. Judah Folkman in 1971 initially postulated that solid tumours lack adequate nourishment allocation so as to endure propagating plentiful active cancer cells, emphasizing angiogenesis impact in tumour growth [214]. Unalike an ordinary blood vessel having a healthy-systematized as well as an operative design, tumour vessels remain messy, erratically fashioned, muddled spread, haphazardly divided, besides complex [215]. In tumour vasculature, the manifesting biomolecules vary in nature as well as scale at dissimilar tumour phases. Biomarkers molecular imaging correlated through tumour angiogenesis could consent towards distinguishing tumour aggression, offering assistance towards treatment, besides monitoring vascular stabilization in antiangiogenic therapy.

*Integrin and VCAM-1 molecular imaging*

Integrins normally referred as cell adhesion molecules also function like cell adhesion receptors facilitating cell–matrix as well as cell–cell interactions, that remain connected with ECM proteins, growth factors, cytokines, as well as proteases. Non-covalently associated α and β subunits are the heterodimers which make the integrins. A variety of α as well as β subunits may amass into as a minimum as 24 distinctive heterodimers through diverse binding specifications as well as signalling features [217]. Expression of integrins remains engrossed within numerous cancer phases, for example, tumour development, succession, penetration, besides metastasis. Integrins for example $\alpha_5\beta_1$, $\alpha_v\beta_3$, and $\alpha_v\beta_5$ stand overexpressed on tumour blood vessels, nonetheless stay inadequately expressed on ordinary vessels. Aimed at the molecular imaging of tumour angiogenesis these overexpressed integrins can be castoff as targets. Numerous integrin-targeted imaging mediators stay advanced towards cancer detection as well as diagnosis, counting iron oxide or Gd-based MRI contrast agents [218], radiotracers aimed at PET or SPECT [219,220], fluorophores aimed at optical imaging [221,222], besides microbubbles aimed at US imaging [223] besides multimodal imaging agents [224]. Targeted liposomal particles which remained conjugated with Gd(III) chelates intended for the MRI of tumour angiogenesis were advanced by Sipkins et al. [225]. A targeting ligand such as biotinylated LM609 antibody happened to be employed aimed at precise attachment to $\alpha_v\beta_3$ integrin. Momentous MR contrast augmentation was witnessed inside the tumour of rabbits bearing squamous cell carcinoma (V2). Immunohistochemical staining for $\alpha_v\beta_3$ as well as LM609 exposed, association among targeting agents as well as their targets. The multivalent binding effects amongst the LM609 antibody and $\alpha_v\beta_3$ integrin could somewhat fund towards the elevated targeting effectiveness. In1984, Ruoslahti et al. revealed that RGD sequence (Arg-Gly-Asp), which remains as a fundamental component for intending an array of probes so as to target $\alpha_v\beta_3$ integrin. Cyclic RGD (cRGD) peptide displays superior *in vivo* stability, besides constructive conformation aimed at binding to a designated integrin as paralleled to linear RGD peptide. Intended at cancer molecular imaging RGD-founded imaging agents remain an encouraging rank of imaging probes [226]. Multivalent binding effect amongst the cRGD-targeted probes as well as $\alpha_v\beta_3$ integrin were validated through optical imaging with multimeric and monomeric probes [227]. *In vivo* optical imaging through tetrameric cRGD-targeted fluorescence probes paraded superior build-up, more extended retention, besides augmented contrast in $\alpha_v\beta_3$-positive tumours compared to the $\alpha_v\beta_3$-negative tumours [228]. The tumour contrast (tumour-to-skin ratio) through tetrameric probe was found to be almost two times superior compared with that of a monomeric probe in $\alpha_v\beta_3$-positive tumour at 4 h following injection. cRGD-targeted paramagnetic nanoparticles were verified for MR imaging of tumour angiogenesis as well as assessing treatment usefulness of antiangiogenic agents for example fumagillin [221,222].

*In vivo* targeting affinity as well as specificity of nanoparticles can be considerably affected by the shape of particle [229].

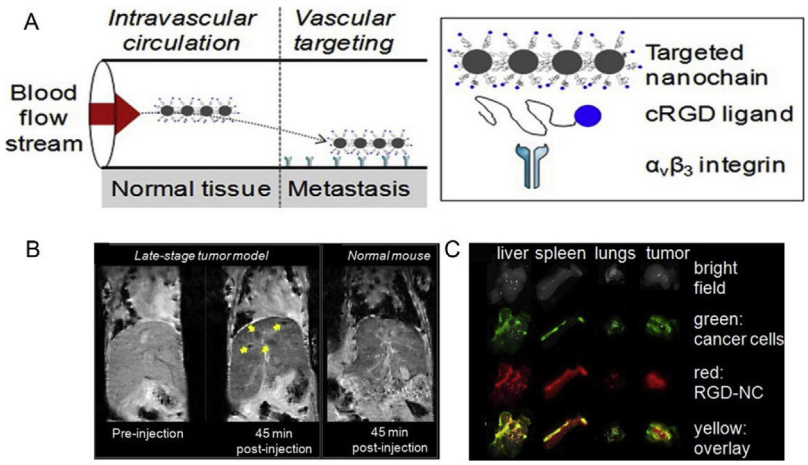


**Fig. 7.** Graphic design of the delivery of RGD-conjugated iron oxide nanochain (RGD-NC) to metastasis through vascular targeting (A). Illustrative T2-weighted MR images of the liver in normal as well as 4T1 metastatic mice employing a 9.4 T MRI. Dark spots specify metastatic tumours identified by the contrast agent (B). Maestro fluorescence images of dissected organs and tissues after injection of fluorophores-labelled RGD-NC nanoparticles (C).
Adapted with permission from [230].

A cRGD-targeted, chain-shaped iron oxide nanoparticle (RGD-NC) advanced by Peiris et al. aimed at identifying tumour metastasis through $T_2$-weighted MRI [230]. Nanochain remained acquired through the assemblage of iron oxide nanospheres *via* solid-phase chemistry besides step-by-step accumulation of NPs (Fig. 7A). MRI contrast agents such as RGD-NC offered a negative contrast towards $4T_1$ metastatic lesions in liver, hence shown as dark spots on the $T_2$-weighted MR images (Fig. 7B). Upon Maestro fluorescence imaging of a dissected tissues obtained from the mice injected with fluorophore-labelled RGD-NC established the elevated build-up of the targeted probes (red) in metastatic tumours (green) (Fig. 7C). Excellent targeting capability of these chain-shaped NPs in comparison to the spherical NPs could be attributed to their elevated aspect ratio besides flexibility of the geometrically boosted multivalent binding amongst the probes as well as targets on the tumour vasculature. Further Gd-based polymeric NPs aiming $\alpha_v\beta_3$ integrin were advanced as contrast agents aimed at MR molecular imaging of tumour angiogenesis [231,232]. Furthermore, excluding integrin, additional cell adhesion molecules, for example, endothelial vascular adhesion VCAM-1 were employed towards advancing tumour-targeted molecular imaging probes [233,234].

An exceedingly expressed protein on tumour vasculature is VCAM-1, facilitating the binding of tumour-associated macrophages to the vascular endothelium [169]. Aimed at the immediate discovery of brain metastases, Serres et al. advanced VCAM-1-targeted microparticles of iron oxide (MPIO) [234]. Iron oxide nanoparticle-based contrast agents were spotted, significantly at squatter concentration compared to the Gd-based agents owing to their elevated $T_2$ susceptibility [235]. For instance, MPIO-grounded MR contrast agents could offer elevated sensitivity amid a threshold through each single cell loaded with ~50 pg of iron at 1.5 T [236]. At the early phases of the brain metastasis, VCAM-1 up-regulation transpires. Brain metastasis MRI through the VCAM-MPIO fashioned and marked MR contrast consequence substitute as a focal hypointense areas on $T_2$-weighted images (Fig. 8A). The MRI contrast augmentation displayed similarity alongside brain metastases while being marked through immunohistochemistry (Fig. 8A–C). Quantity of hypointensities made through VCAM-MPIO amplified over time considerably (Fig. 8E–G) besides minute MPIO retention remained spotted in healthy mice injected by the identical agent (Fig. 8G). The average MRI-detectable 4T1 tumours included approximately $1 \times 10^3$ cells, nearly four times of the extent lesser than $1 \times 10^7$ cells of 2 mm diameter human brain metastasis. Nevertheless, micron-sized iron oxide NPs, for example, MPIO remain non-biodegradable besides they are not appropriate for human usage owing to safety apprehensions [237]. Together the small paramagnetic particles of iron oxide (SPIO) as well as the ultra-small SPIO possess lesser safety apprehensions and were used in patients [238].

*VEGF/VEGFR expression molecular imaging*

The key mediators of angiogenesis are vascular endothelial growth factors (VEGFs), that stand involved regarding the progress of numerous diseases. VEGFs exist as a clan of glycoproteins predominantly constituted by the VEGF-A, VEGF-B, VEGF-C, VEGF-D, as well as the placenta growth factor [239]. VEGF ligands tie to the endothelium-explicit tyrosine kinase receptors (VEGFR) besides activating the VEGF/VEGFR signalling pathway. Vital Supporting angiogenic factors stimulated by the necrotic as well as the hypoxic TME of several malignant tumours are VEGFs. Having been validated lately, that expression of VEGF-A displays a serious function in fashioning an immunosuppressive TME [240]. The insignificant clinical prognosis in cancer patients has been related to the overexpression of VEGF/VEGFR [241]. Antibodies such as (bevacizumab, cetuximab) [242] as well as the small molecules [243] in contradiction with VEGF, VEGFR, besides their complexes were employed in the clinic for anti-VEGF therapy. They were also employed towards advancing of the molecular imaging probes, counting PET as well as SPECT radio-tracers [244,245], fluorescent probes [246], US imaging microbubbles [223], MRI contrast agents [154], besides multimodal imaging agents [247].

A single-chain multimodal imaging agent founded on VEGF (scVEGF) was advanced in order to image the VEGFR present in tumour vasculature [247]. The Cys-tagged scVEGF remained categorized by distinctive correspondent molecules, counting with Cy5.5 dye aimed at NIRF imaging, a 99mTc complex for SPECT imaging, as well as a $^{64}$Cu chelator intended for the PET imaging (Fig. 9A). The correspondent molecules remained ascribed to scVEGF through a Cys-tag peptide, that didn't considerably alter the functioning of the scVEGF. In comparison to non-targeted probes, each of the scVEGF-targeted imaging probes specifically amassed in $4T_1$-Luc2 mouse tumours. Cy5.5-scVEGF Optical imaging afforded elevated contrast augmentation in the tumour as well as the fluorescence intensity continued virtually continuous over at least 7 days (Fig. 9B). SPECT imaging by 99mTc-scVEGF ensued in rather squat contrast augmentation present in tumour due to quick clear-

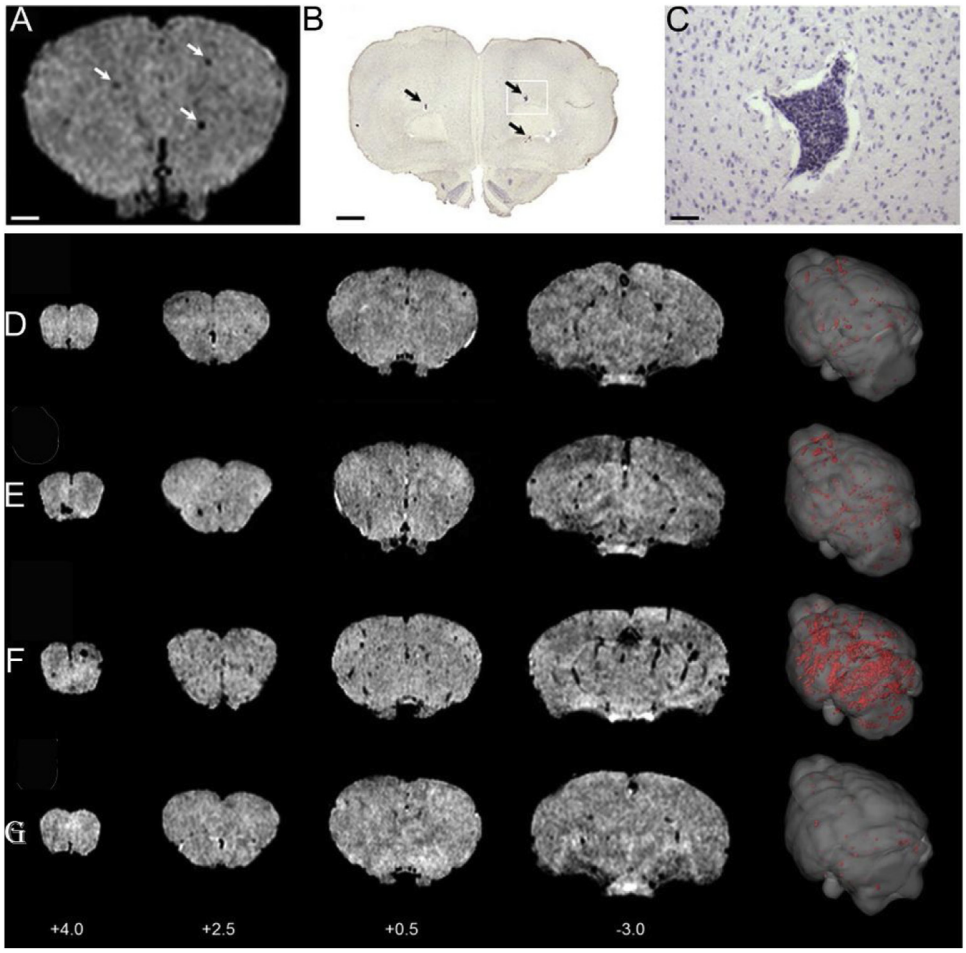


**Fig. 8.** VCAM-MPIO-enhanced MR imaging of brain metastases in a mouse 4T1 model. Co-localization of focal hypointensities (arrows) on $T_2$-weighted MR images (A) with brain metastases (arrows) detected by immunohistochemistry (B), and zoomed view (C) of box in (B). Representative MR images of mouse brain from the 3D dataset at days 5 (D), 10 (E), and 13 (F) after intra cardiac injection of 4T1 breast cancer cells. Intense focal hypointense areas (black) correspond to VCAM-MPIO binding. No specific binding was found in healthy mice injected with VCAM-MPIO (G). The spatial distribution of VCAM-MPIO binding (red) in the whole brain is reconstructed to 3D.
Adapted with permission from [234].

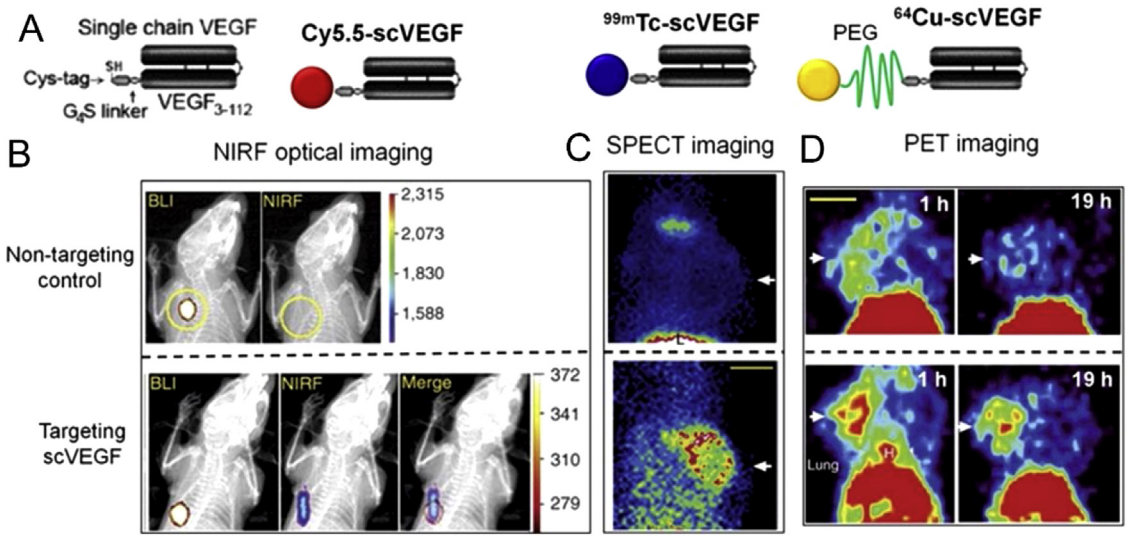


**Fig. 9.** Fundamental graphic illustration of Cys-tagged single-chain VEGF (scVEGF) and its conjugates with different reporting molecules for multimodal imaging (A). Molecular imaging of mice bearing 4T1-Luc breast tumours by different imaging modalities after injection of corresponding scVEGF-targeting (lower row) and non-targeting probe (upper row) (B, C). Bioluminescence imaging (BLI), NIRF fluorescent imaging and merged images (B). SPECT imaging of mice at 1 h after injection of 99mTc-labelled probe (C). PET imaging of mice at 1 h or 19 h after injection of $^{64}$Cu-labelled probe (D). White arrows point to tumour. Scale bar = 1 mm.
Adapted with permission from [247].

ance of 99mTc besides SPECT imaging furthermore disclosed a probe retention in the tumour remained exceedingly assorted but it did prevail in the tumour rim (Fig. 9C). In order produce the PET imaging agent $^{64}$Cu-scVEGF, PEG remained cast-off as a linker. In comparison to the non-PEGylated 99mTc-scVEGF probe, PEGylated, $^{64}$Cu-scVEGF probe displayed extended circulation in the blood as well as greater tumour buildup. Even 19 h following injection $^{64}$Cu-scVEGF PET imaging offered determined augmentation in the tumour (Fig. 9D). New tumour vasculature-related biomarkers, for example, phosphatidylserine (PS) as well as neuropilin-1 (NP-1) were employed to achieve tumour vasculature molecular imaging. A phospholipid (PS) which generally dwells around the internal leaflet of the plasma membrane, although its unprotected from tumour vasculature external surface [241]. PS-recognizing peptides [248], proteins [249], as well as antibodies [249,250] were employed for tumour vasculature molecular imaging is A transmembrane glycoprotein called as NP-1 works like a co-receptor for VEGFRs incites. Tumour progression is incited by NP-1 through controlling activities of numerous extracellular factors for example TGF-β, platelet-derived growth factor, besides hepatocyte growth factor [239]. In the tumour vasculature NP-1 is overexpressed thus its expression is connected to the tumour progression as well as poor patient prognosis. For SPECT, US, NIRF fluorescence, and MR imaging NP-1-targeting peptides as well as antibodies were advanced [251,252]. Fresh reports have revealed, imaging agents with heterodimeric peptides dual-targeting to VEGF as well as NP-1 are highly effective compared to an agent possessing a single peptide [253].

## TME responsive nanoconstructs for therapy

### *TME hypoxia responsive nanoconstructs for tumour therapy*

Recently, there have been huge headways in tumour biology understandings as well as its adjoining microenvironment. Areas having low oxygen intensities are generated by solid tumours, which are commonly dubbed as hypoxic areas. Such hypoxic zones bid an extraordinary prospect towards developing the targeted therapies. Hypoxia though not a unintentional by-product of the cellular environment owing to unrestrained tumour growth; somewhat its a continuously developing contestant in inclusive tumour growth as well as destiny. There is a changes in interstitial fluid pressure due to hypoxia, reduced pH as well as augmented production of reactive oxygen species (ROS). Hypoxic zones parade elevated interstitial fluid pressure owing to the presence of permeable vasculature in addition to irregular lymphatic drainage inside tumour.

A trait of the TME know as tumour hypoxia frequently transpires due to disordered equilibrium amid supply and $O_2$ ingesting in part of tumour growth as well as vascular abnormalities [254]. Up-to-date anticancer therapeutics counting chemotherapy, photodynamic therapy, as well as radiotherapy were found to be resisted by the tumour hypoxia [255,256]. To acclimatize with the hypoxic environment conditions, cancer cells undergo transcriptional activity of hypoxia-inducible factor-1α (HIF-1α), which includes angiogenesis, incursion, besides metastasis of cancer cells [257]. The HIF-1α was connected to resistance of chemotherapy through boosting the expression of P-glycoprotein (P-gp), a membrane efflux pump which identifies distinctive chemotherapeutic mediators besides passages them out of the cells, triggering the breakdown of chemotherapy [258]. Consequently, tumour hypoxia alteration is indispensable in order to elevate the effectiveness of cancer chemotherapy. For example, hyperbaric oxygen therapy, that encourages oxygen carriage from blood circulation towards hypoxic tumour tissue through growing the oxygen ($O_2$) pressure in plasma, could reinforce the chemotherapy [259]. Nevertheless, deprived of tumour-specific oxygen delivery, hyperbaric oxygen therapy might produce brutal harmful effects resulting due to extraordinary oxygen toxicity [260]. Therefore, its highly important to advance targeted oxygen nanocarrier aimed at ending tumour hypoxia alongside improved chemotherapy results. Latest studies show that $O_2$ shipping/breeding materials, for example, haemoglobin (Hb), perfluorohexane, plus manganese dioxide, might advance intratumoral $O_2$ supplementation as well as increase cancer therapeutic effectiveness [261–263]. Amongst such materials, Hb which is a natural protein present in the red blood cells and respinsible for the delivery of oxygen to the tissues. Hb regarde as a biosafe oxygen transporter inside nanosystems aimed at oxygen-boosted photodynamic therapy [261]. Intended for certain cancerous cell targeting, nanoparticles were generally tailored through targeting ligands (*e.g.*, peptides, antibodies, and nucleic acids) [264]. Presently, biomimetic cell membrane-based drug delivery systems garnered extra consideration in order to develop smart materials, for example, cancer cell membrane-coated nanoparticles, blood cell membrane-derived nanoparticles, besides platelet membrane-modified nanoparticles [265–267]. Through replication of the surface antigenic range from the cancer cells towards concocted nanovehicle, cancer cell membrane-biomimetic nanoparticles remained gifted by the capability of targeting to homologous tumour cells [268]. Such a method might consequence into a hopeful targeted nanodelivery procedure for cancer therapies.

### *Modulation of tumour hypoxia* via *oxygenation*

An impressive cure, that includes light as well as a photosensitizer (PS) is acknowledged as photodynamic therapy (PDT) [269,270]. From oxygen, PS might perhaps breed reactive oxygen species (ROS) in order to eradicate cells through the activation of light at a precise wavelength [271].

Nevertheless, hypoxia conditions limit the application of PDT in tumours. Moreover, $O_2$ ingesting throughout PDT might deteriorate tumour hypoxia, which would further decrease the PDT effectiveness like a brutal loop [272], what is more it could stimulate tumour metastasis [273] or therapy resistance [274,275]. In order to increase the PDT efficiency, its exceedingly appropriate to selectively increase the indigenous oxygen level in the tumour area. Cheng et al. testified oxygen self-enriching photodynamic therapy (Oxy-PDT) through loading of a near-infrared photosensitizer IR780 hooked on perfluoro-carbon nanodroplets [276]. An extra ordinarly suitable contender for transporting oxygen is perfluorocarbon, due to its extraordinary solubility of respiratory gases in perfluorocarbon [277,278]. NIR photosensitizer IR780 as well as perfluorohexane (PFH) have been engaged in order to prepare Lipid nano-droplets possessing PEG on the surface (Fig. 10A).

Afterwards PEGylation, nanodroplet size is about 200 nm, that is considered as appropriate to achieve passive targeting in tumour. On oxy-PDT treatment by 808 nm laser irradiation, oxygen supplemented in the PFH stood stimulated towards generating the cytotoxic singlet oxygen through IR780. Furthermore, it was discovered that the lifetime of $^1O_2$ in PFH (5-10-2s) is considerably longer compared to that in water (5-10-6s) as well as in the intracellular environment (6-10-7s). Oxy-PDT treatment by NIR laser irradiation indicated the maximum amount of $^1O_2$, and consequently the peak cell mortality (Fig. 10B and C). Further *in vivo* experiment demonstrated that Oxy-PDT displayed efficient tumour targeting because of EPR effect (Fig. 10E) besides enhanced inhibition of the tumour in comparison to the conventional PDT (Fig. 10F). Moreover, hollow $Bi_2Se_3$ nanoparticles have shown their capability to dispense perfluorocarbon aimed at improved radiotherapy [31]. Haemoglobin (Hb) which can bind with oxygen into oxygenated Hb was engaged as an oxygen carrier in order to encourage

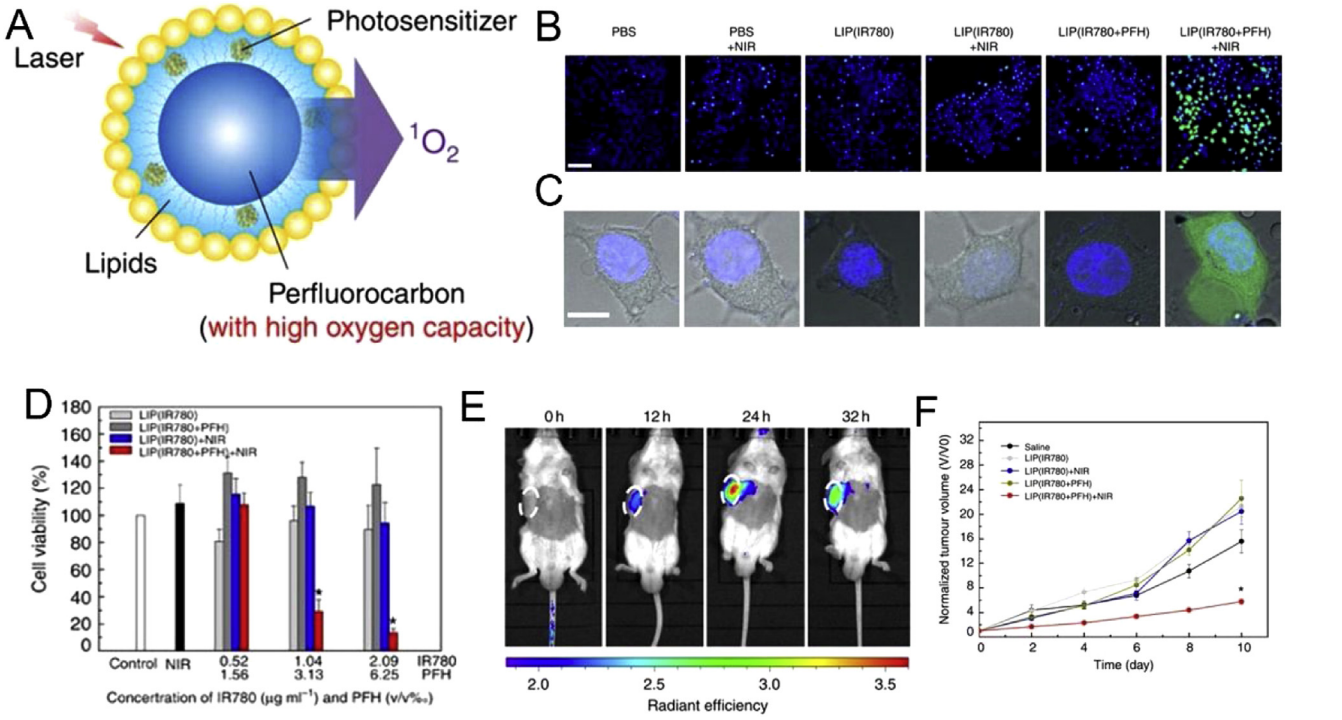


**Fig. 10.** (A) Graphic representation of the oxygen self-enriched photodynamic therapy (Oxy-PDT) NPs. (B and C) H2DCFDA were engaged to detect ROS generation by treating cells with several agents. Nuclei were stained with Hoechst 33342. Scale bar, 50 mm (B) and 10 mm (C). (D) Cell viability of CT-26 cells by the CCK-8 assay under hypoxic conditions. (E) Near-infrared fluorescence images of mice at different time points after intravenous injection of Oxy-PDT NPs. (F) Tumour therapy by single injection of Oxy-PDT NPs intravenously.

(Reprinted with permission from ref. [276]. Copyright 2015, Nature Publishing Group).

cancer therapy [279,280]. Zheng et al. [281] synthesized an $O_2$ self-sufficient ingenious liposome nanoplatform (LipoMB/$CaO_2$) intended for hypoxic tumour PDT under dual-stage light irradiation.

Meanwhile as demonstrated in (Fig. 11), in (LipoMB/$CaO_2$), hydrophilic PS methylene blue (MB) as well as $O_2$ supplier calcium peroxide ($CaO_2$) nanoparticles remained encapsulated into the aqueous cavity as well as a hydrophobic layer, correspondingly.

$CaO_2$ inside liposomes might sluggishly react with $H_2O_2$ or weak acid in order to discharge $O_2$ besides alleviating tumour hypoxia in tumour tissue. Following initial light irradiation, the liposomes were fragmented, thus additionally revealing $CaO_2$ to $H_2O$ and hastening $O_2$ production rate. Higher $O_2$ concentration will significantly advance PDT effectiveness following second light treatment. Additionally, downregulated hypoxia-inducible factor-1< (HIF-1<) as well as the vascular endothelial growth factor (VEGF) expression following tumour hypoxia improvement may perhaps shrink the tumour metastasis [282]. Dual-light irradiation treatment, higher $O_2$ production plus better-quality therapeutic efficiency towards hypoxic tumour by LipoMB/$CaO_2$ remained explored. The capability of $CaO_2$ NPs to control hypoxic environment was examined *in vitro* by means of mouse mammary carcinoma cells (4T1 cells). Reactive oxygen species (ROS)-ID hypoxia/oxidative stress detection kit was engaged in order to reproduce the intracellular hypoxia level. As displayed in confocal laser scanning microscopy (CLSM) images in (Fig. 12A), in hypoxic environment, durable red fluorescence (signified the stern hypoxia) was detected in the drug untreated as well as LipoMB treated 4T1 cells [283]. However in contarary to, 4T1 cells with Lipo$CaO_2$ besides LipoMB/$CaO_2$ treatments demonstrated fragile fluorescence, signifying the decent tumour hypoxia controll feature of $CaO_2$ nanoparticles. The $^1O_2$ production through $O_2$ self-sufficient LipoMB/$CaO_2$ nanoplatform in cancer cells were studied

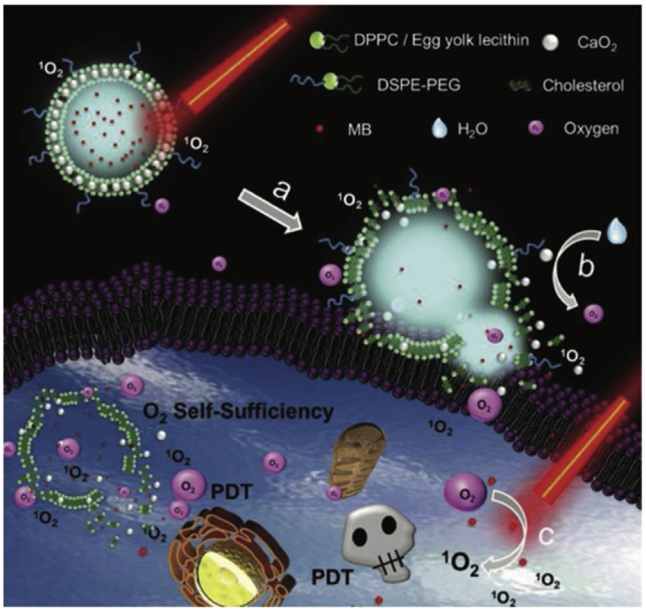


**Fig. 11.** Organization design of LipoMB/$CaO_2$ nanoplatform for $O_2$ self-sufficient PDT: (a) The $^1O_2$ activated by MB oxidized the phospholipid bilayer to break the liposome through the first stage short time irradiation; (b) Accelerated $O_2$ generation due to enhanced contact of $CaO_2$ with $H_2O$; (c) Improved PDT effect through the second stage long time light irradiation at the $O_2$ sufficient TME.

Adapted with permission from Ref. [281].

by means of 2′,7′-dichlorodihydrofluorescein diacetate (DCFH). As depicted in (Fig. 12B1-B4), almost no green fluorescence was noticed in untreated drug as well as Lipo$CaO_2$ treated cells in hypoxic environment, intendeding that the cells onself besides

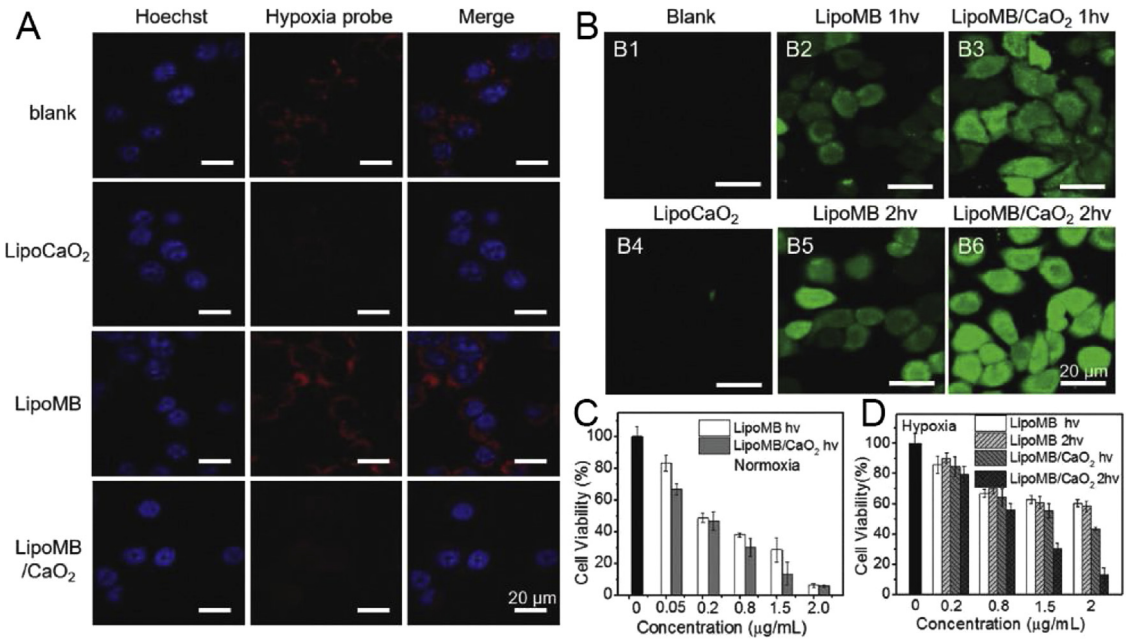


**Fig. 12.** (A) CLSM images of $CaO_2$-induced hypoxia reversion. (B) Intracellular ROS generation in 4T1 cells mediated by different samples and light treatments. (C) Cell viabilities of LipoMB and LipoMB/$CaO_2$ with single light irradiation cultured in normoxic environment. (D) Cell viabilities of LipoMB and LipoMB/$CaO_2$ with single or dual stage light irradiations cultured in hypoxic environment adapted with permission from ref. [283,284].

$CaO_2$ maught not generate $^1O_2$. Obvious green fluorescence was detected in LipoMB treated cells, demonstrating that though deficiency of $O_2$, MB might also produce definite amount of $^1O_2$ under 660 nm light irradiation (90 s, 30 mW $cm^{-2}$) (Fig. 12B2). However, the $O_2$ self-sufficient LipoMB/$CaO_2$ demonstrated an extra satisfying $^1O_2$ production capability under light irradiation since extremely bright fluorescence was exhibited in LipoMB/$CaO_2$ treated cells (Fig. 12B3). Overall light treatment time was equal (90 s) in (Fig. 12B2, B3, B5, B6). As depicted (Fig. 12B5), in comparison to the LipoMB 1hv group, no obvious green fluorescence augmentation was discovered in LipoMB 2hv group. Nonetheless, extremely robust fluorescence augmentation in LipoMB 2hv group was detected (Fig. 12B6), corroborated the suddenly better-quality $^1O_2$ generation of LipoMB/$CaO_2$ through dual-stage light irradiation accrediting to the higher oxygen level following first light irradiation. Drug phototoxicities over normoxic background were then tested. Depicting from (Fig. 12C), it was discovered that with 6 min of single light irradiation (660 nm, 30 mW $cm^{-2}$), LipoMB/$CaO_2$ presented considerably superior phototoxicity compared to LipoMB, with about 13.3% cell viability witnessed at the concentration of 1.5 μg $mL^{-1}$, although it was 28.5% for LipoMB. Such results signify that even under normoxic circumstance, the real time $O_2$ supplement *in situ* by $CaO_2$ nanoparticles might sharply advance PDT effectiveness at squat drug concentration. Additionally, phototoxicity of LipoMB/$CaO_2$ nanoplatform at hypoxic environment was verified (Fig. 12D), though phototoxicities of both LipoMB as well as LipoMB/$CaO_2$ were diminished, LipoMB/$CaO_2$ continuously presented greater cytotoxicity comapred to LipoMB owing to its elevated $O_2$ level by CaO [284].

Shi et al. [285] demonstrated a typical tumorous oxygenation prototype to overthrow the hypoxic tumour, by developing an implantable oxygen-generating depot, alginate pellets with catalase and $CaO_2$ inside (Fig. 13A). Mechanically, $CaO_2$ might act as the exogenous peroxide generator by the following chemical reaction (Fig. 13B) as $CaO_2 + 2H_2O = > Ca(OH)_2 + H_2O_2$. Afterwards, the hydrogen peroxide could be catalyzed by catalase to generate oxygen actively, vividly shrinking the tumorous hypoxic area (Fig. 13C). Mingled with the intra-venous DOX injection, the implant/DOX nanotherapy exhibited augmented tumour suppression outcome (Fig. 13D).

$H_2O_2$ as well as the insignificant acidity-responsive $MnO_2$ NPs show exceptional acts in fighting hypoxic tumours as an alternative class of inorganic nanomaterial. Coated by albumin polyelectrolyte, the $MnO_2$ core in A-$MnO_2$ NPs might be broken into $Mn^{2+}$ besides molecular oxygen beneath tumorous $H_2O_2$, overcoming the tumorous acidosis as well as the hypoxia (Fig. 14A–C) [254]. 2D $MnO_2$ nanosheets process similar functionality. From the materials perspective, 2D $MnO_2$ nanosheets remained attached with $NaYF_4$:Yb/Er/Tm upconversion NPs (UCSM), appeared with smart therapeutic as well as imaging proficiencies, particularly the synergistic photodynamic therapy as well as the radiotherapy [286]. The luminescence might be transformed into visible yellow lights through UCNPs upon radiation by NIR laser. Nevertheless, owing to the FRET effect amongst $MnO_2$ as well as the UCNP, the luminescence remained quenched. Upon delivery of UCSMs into the tumour area, $MnO_2$ nanosheets were reduced by means of the tumorous $H_2O_2$ under mild acidic TME, making $Mn^{2+}$ as well as plentiful oxygen molecules, and consequently the FRET effect was jammed and the unconverted luminescence remained regained (Fig. 14D). Moreover, improved $O_2$ level at tumour sites supports considerable synergistic therapy of PDT as well as the RT (Fig. 14E). Thus modulation of tumour hypoxia pivotal for realizing the improved therapeutic effect of PDT.

*Tumour hypoxia-responsive nanoconstructs for tumour therapy*

Hypoxia-sensitive activities in most of the moieties enclose nitroaryl or quinone functional groups were revealed by several organic funtional groups. Such organic moieties were broadly functional among the hypoxia-responsive nanomaterials aimed at tumour-specific nanotherapies. Park's group testified Hypoxia-responsive NPs (HR-NPs) carrying the DOX chemo drugs intended for the selective tumour chemotherapy were testfied by the Park's group [287].

In HR-NPs, hypoxia-responsive 2-nitroimidazole (NI) byproduct were conjugated on the backbone of the carboxymethyl dextran. Under tumorous hypoxic circumstances, representative peak dis-

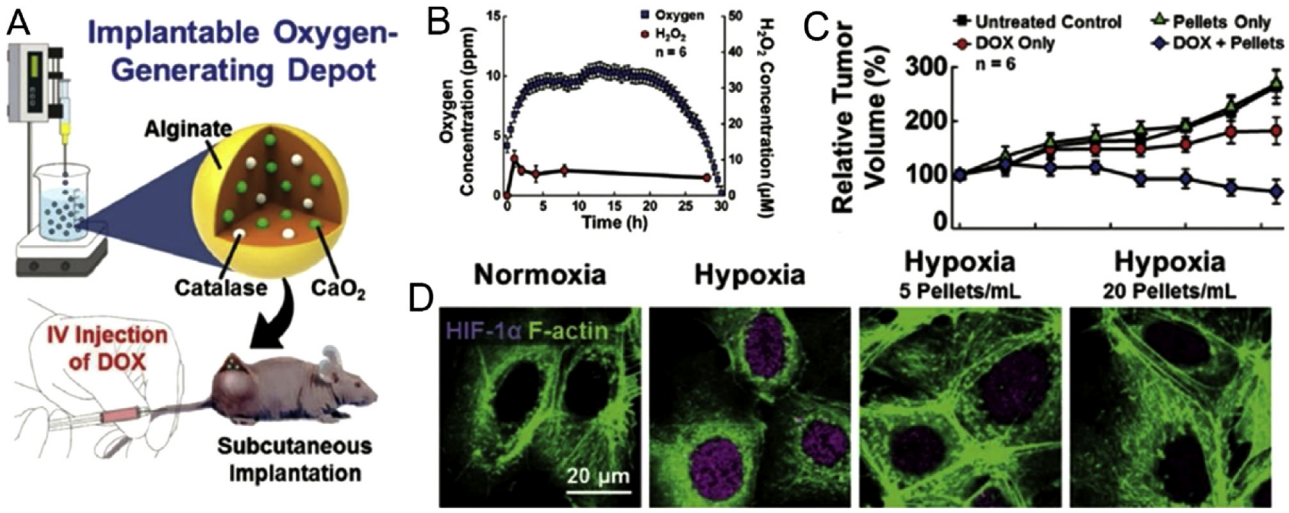


**Fig. 13.** (A) Schematic illustration of the implantable oxygen generating depot and therapeutic modality. (B) Production profiles of $O_2$ and $H_2O_2$ of the alginate pellets in assay buffer. (C) Confocal images of hypoxic marked 2D cells treated with the pellets under different oxygen conditions. (D) *In vivo* therapeutic performance of the pellets with or without the combined DOX chemotherapy.

Reproduced with permission from Ref. [285].

played a redshift ranging from the 325 nm to 278 nm (Fig. 15A) alongside a noticeably diminished zeta potential (Fig. 15B), clearly demonstrating conversion of the nitro functional group to amino functional group underneath hypoxic environments. Therefore, such conjugates might efficiently oblige as hypoxia- responsive nanoindicators. These HR-NPs might split under tumorous hypoxia hence thus discharge loaded DOX, therefore revealing ample heightened selectivity besides therapeutic result regarding hypoxia-allied diseases counting cancer too. An elusive strategy towards utilizing tumorous hypoxia, nitroimidazole remained emplaoyed in order to lock the photo trigger from photo releasing antitumor chemo drugs. Nitroimidazole experienced a hypoxia-specific nitro-to-amino reduction in order to trigger the coumarin photo trigger, ensuing into the next photoactivated fluorescence as well as the photo heterolysis of C-O bonds, besides consequent discharge of antitumor chemo drug (etoposide) simultaneously (Fig. 15C) [288]. In order to conjugate PEG-hexanethiol (PEG-C6) as well as the antitumor chemo drug combretastatin A-4 (CA4) to give PEG-C6-AZO-CA4 micelles afterwards self-assembly, hypoxia-responsive azobenzene (AZO) was used. Through reducing AZO groups in a reductive situation, for example, NADPH (Fig. 15D) [289], such micelles might additionally function as a DOX-delivery structure aimed at hypoxia-responsive CA4 as well as DOX co-releasing following the stripped PEG-C6-AZO-CA4/DOX nanoplatform upon hypoxia (Fig. 15E, F). Hypoxic property might perhaps also reduce the therapeutic efficacy of PDT as PDT is intensely oxygen-dependent [290].

Aimed at simultaneous light-responsive PDT as well as the hypoxia-responsive chemotherapy conjugated polymer-based nanocarrier (DOX/CP-NI NPs) was synthesized displaying incessant morphology plus size variations following irradiation for 5 min (Fig. 16A) [291]. In a standard analysis, indigenous hypoxia as well as the robust oxidative stresses inside the cells occurred afterwards treatment with the DOX/CP-NI under light irradiation. As the implanted polymers remained light-responsive, DOX release outlines displayed coherent reactions regarding light (Fig. 16B). *In vivo* therapeutic functioning of the DOX/CP-NI under light irradiation displayed meaningful tumour xenograft destruction synergistically (Fig. 16C). While as in another study targeting towards conquering the oxygen-dependency inside the tumour tissue, a PEGylated stimulating NP (SCNP) core-ZnO shell arrangement was produced (SZNP) [292]. Such an SCNP translates the irradiated X-ray towards the UV light successfully, shadowed by the photo bred transporter's separation in ZnO semiconductors The neighbouring water molecules auxiliarrly react with reactive photo generated holes in order to breed the toxic ·OH, dodging the considerable oxygen-dependence of conventional PDT (Fig. 16D). Given as evidence of such a concept of *in vitro* therapeutics, the SZNP provoke analogous cytotoxicity concerning HeLa cells under both normoxic (21% $O_2$) or hypoxic (2% $O_2$) condition (Fig. 16E).

In order to avoid hypoxia-stimulated chemo resistance, Lintao Cai et al. established a cancer cell membrane-biomimetic oxygen nanocarrier. While as explained in (Fig. 17A), Hb as well as doxorubicin (DOX) were encapsulated in poly (lactic-co-glycolic acid) (PLGA) to give a core, in which the cancer cell membrane and PEGylated phospholipid(1,2-distearoyl-sn-glycero-3-phosphoe-thanolamine-N-maleimide(polyethylene glycol 2000), DSPE-PEG were enclosed in order to construct a homologous targeting nanoparticles (DHCNPs, denoting to as DOX/Hb loaded PLGA-cancer cell membrane nanoparticles). Regarding the experimental uses, oxy-DHCNPs were acquired through the oxygenation of the synthetic DHCNPs with pure oxygen stream. Through the retention of cell membrane proteins over the surface of MCF-7 cells (human breast cancer cells from Michigan Cancer Foundation), oxy-DHCNPs steered towards exceedingly precise self-recognition towards the homologous cells. Besides, theese oxy-DHCNPs might realize $O_2$ self-adequacy in tumour besides downregulate HIF-1α, multidrug resistance gene 1 (MDR1), as well as the P-gp, that considerably hindered DOX spread in the hypoxic tumour cells. Consequently, DHCNPs promoted the intracellular DOX buildup besides exhibiting extraordinary chemo-cytotoxicity upon hypoxic cancer cells (Fig. 17B).

In order to examine the influence of DHCNPs-founded $O_2$ source upon hypoxia-induced chemo-resistance *in vivo*, immunofluorescence staining of tumour portions alongside hypoxyprobe was executed aimed at mapping the tumour hypoxia [293].

As shown in Fig. 18A, group treated with DCNPs without $O_2$ supply exhibited significant hypoxia spreading in tumour as well as weak FL intensity of DOX. Through dissimilarity with the $O_2$ interference, hypoxia dispersal in DHCNPs group diminished considerably, besides DOX spread in the hypoxia-reduced region, demonstrating the $O_2$ mediation of DHCNPs comforted tumour hypoxia as well as enhanced the DOX buildup inside tumour. In tumour P-gp expression assay was reviewed through WB analysis

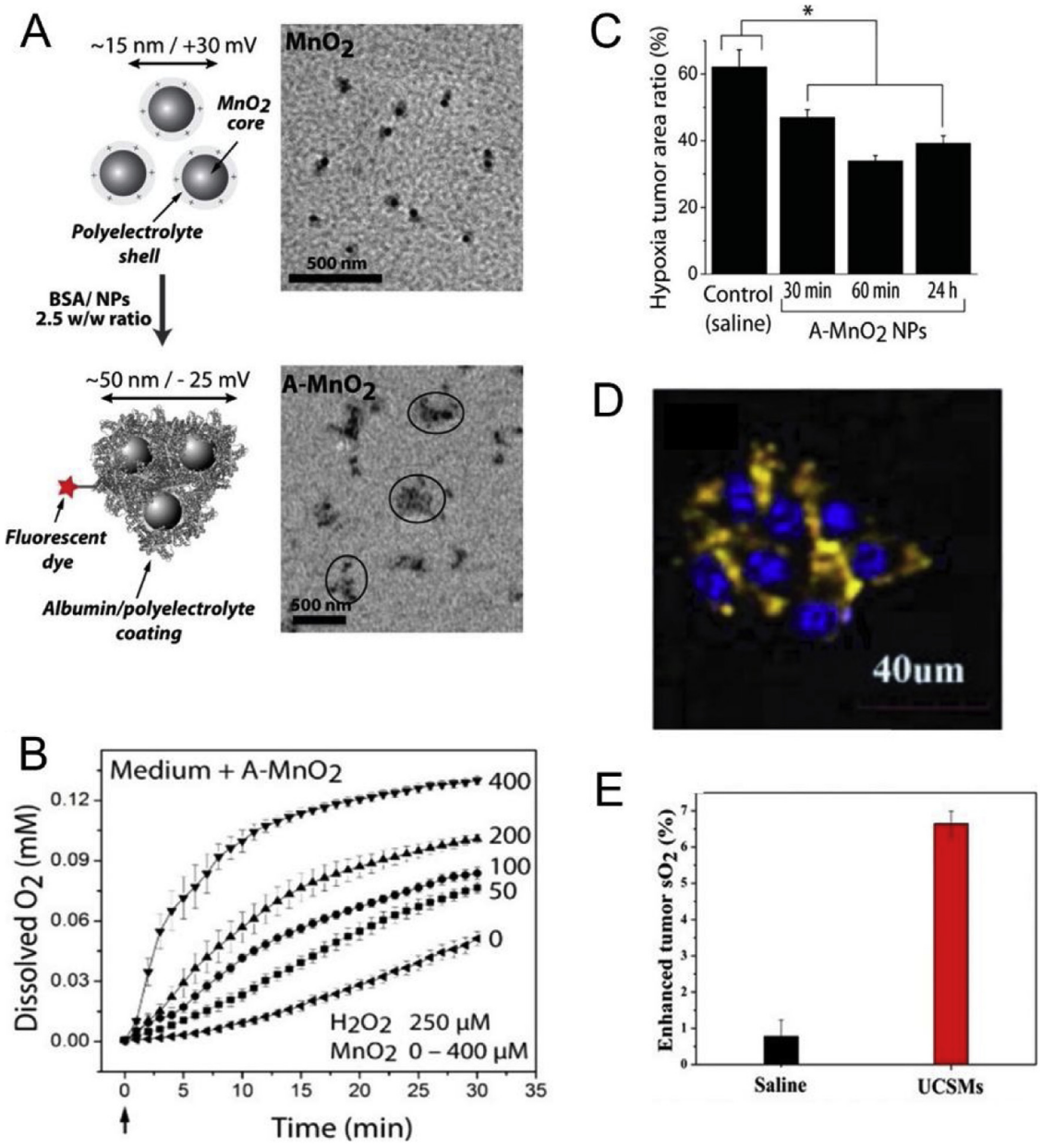


**Fig. 14.** (A) Graphic sketch and corresponding TEM images of as prepared $MnO_2$ core and albumin/polyelectrolyte coated $MnO_2$ NPs (A-$MnO_2$ NPs). (B) Oxygen production profiles of A-$MnO_2$ NPs of varied concentrations under the presence of $H_2O_2$. (C) Hypoxic tumour area judging from the immunohistochemistry images of EMT6 tumours treated with A-$MnO_2$ NPs for varied time periods. Reproduced with permission [254]. Copyright 2014, American Chemical Society. (D) Confocal images of NIR irradiated fluorescence profiles of DAPI stained 4T1 cells incubated with UCSMs intelligent nanoplatform for 20 h. (E) Tumour vascular oxygen levels after injected with saline and UCSMs. Reproduced with permission [286]. Copyright 2015, Wiley-VCH Verlag GmbH.

(Fig. 18B). Remarkably, the P-gp in tumour treated with DHCNPs was down-regulated in comparison to that off DCNPs group. The outcome revealed the means of homologous targeted oxygen delivery on transgression tumour hypoxia-induced chemo resistance. Throughout 30 d treatments tumour volume was measured and calculated (Fig. 18C). The efficiency of DCNPs was extra strong compared to the those of the DCNPs, free DOX, as well as phosphate buffered saline (PBS), that flopped to efficiently prevent growth of the tumour. Nevertheless, owing to the collaboration among the homologous targeted delivery as well as efficient $O_2$ intervention, the DHCNPs group demonstrated the solidest tumour prevention, which was discovered through comparison of the relative tumour volume of the DHCNPs group ($3.94 \pm 0.51$) as wel as the DCNPs group ($6.49 \pm 0.70$). Furthermore, Founded upon the tumour growth the survival curve for each treated group was valued (Fig. 18D). On day 30th mice treated with PBS as well as the free DOX were all dead, whereas DNPs group exhibited 33.3% survival at 30 d post-treatment. At the end of experiment the DCNPs as well as the DHCNPs treated mice realized 100% survival. Thus it designated that all the DCNPs and DHCNPs encouraged an outstanding therapeutic effectiveness through the homologous targeting capability as well as the $O_2$ supply competence. No obvious variation in mice weight were dectected in all treated groups. These different categories of hypoxia responsive nanoconstructs discussed above present an encouring prospect in for future advancement in cancer therapy by targetting tumour hypoxia by improving the oxygenation of tumour mircoenvironment thus augmenting the effeciency of PDT.

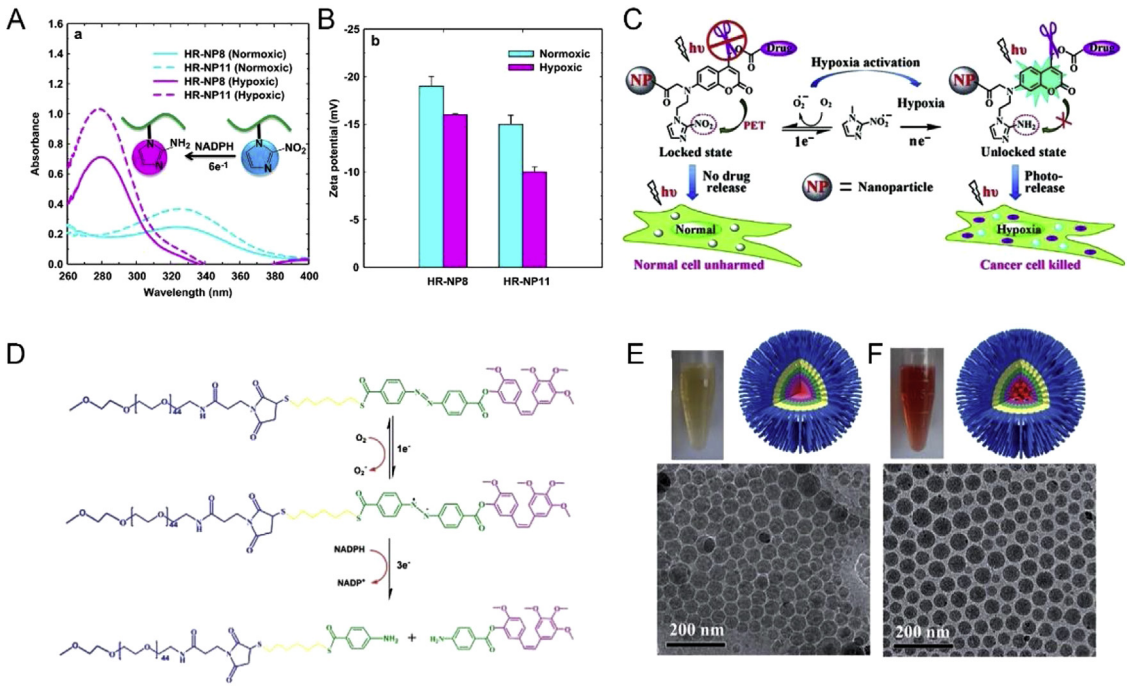


**Fig. 15.** (A) Absorption spectra of HR-NPs incubated under hypoxia and normoxic conditions for 3 h. Measurements were performed in PBS buffer containing 100.10-6 m NADPH as an electron donor (The inset shows the conversion of NI into 2-aminoimidazole). (B) Zeta potentials of HR-NPs incubated under hypoxic and normoxic conditions with 100.10-6 m NADPH as electron donor. Reproduced with permission from ref. [287]. Copyright 2013, Elsevier Ltd. (C) Schematic illustration of the hypoxia-activated photo trigger releasing drug specifically in tumour. Reproduced with permission from ref. [288]. Copyright 2013, Wiley-VCH Verlag GmbH. (D) The mechanism of the bond cleavage of AZO in PEG-C6-AZO-CA4 micelles. (E) Cryo-TEM images of PEG-C6-AZO-CA4/DOX micelles and (F) disassembled PEG-C6-AZO-CA4 micelles. Reproduced with permission from Ref. [289] Copyright 2015, The Royal Society of Chemistry.

*TME pH responsive nanoconstructs*

The trivial acidic character has been regarded as the greatest archetypal TME inside the tumour tissues besides the variation in the tissue pH is interrelated to several pathological developments [182]. It has been normally assumed, acidity of this kind instigates after build-up of the lactate ($pK_a$ = 3.86), metabolite of the exaggerated aerobic glycolysis (Warburg effect) [295]. Moreover, during the citric acid cycle, glutamine molecules are metabolized, ensusing the creation of lactate (glutaminolysis) [296]. following a highly-recognized and some reprogrammed oncogenes, these tumour cells enable the $Na^+/H^+$ exchangers [297], carbonic anhydrase-9 [298], as well as the mono-carboxylate carriers [299] to sustain this kind of acidic nature, shaping the tumour extracellular pH values to be in the range of 6.0–7.0 besides tumour intracellular pH values to be within the range of 6.0–6.5 [300]. From the tissue pH MRI it was understood through picturing the signal intensities of the hyperpolarized bicarbonate ($^{13}HCO_3-$) as well as $^{13}CO_2$ utilizing the dynamic nuclear polarization technique. These outcomes acknowledged the fact that average pH value of tumour interstitials was significantly lesser compared to its adjoining tissues [300]. Such an minor acidic character has been engaged aimed at multipurpose nanomedical theranostics, for example, micro metastasis tracking [301], imaging of concealed tumour malignancy [193], precise identification of pathological conditions of tumour [193,302], stimuli-responsive drug release [303], as well as tumour-specific chemotherapy [304,305]. Some lysosomal enzymes may be activated by acidic extracellular pH. Furthermore, the acidic microenvironment may further upsurge drug resistance besides affecting the tumour metastasis [306,307]. In oder to overcome such effects, its very significant to advance a nanosystems which can control the tumour extracellular pH. Here we have categorized the pH responsive nanoparticles into two groupings: inorganic ones and organic ones.

*pH sensitive inorganic NPs for tumour therapy*

Recently the inorganic NPs started to attract growing courtesy for cancer cure because of reasonable as well as outstandingly controllable production, aside from effortlessness of their functionalization. Inorganic NPs, for example, acid soluble calcium carbonate ($CaCO_3$) [262,308], calcium phosphate (CaP) [309] as well as manganese dioxide ($MnO_2$) [286] have materialized as outstanding contenders aimed at realizing the pH-responsive cancer therapy. The Achilefu's group produced $CaCO_3$ NPs in order to control the TME [308]. $CaCO_3$ may decay progressively inside the mild acidic environment (pH B 6.8) into $Ca^{2+}$ and $CO_2$, and the pH can be controlled by annihilating protons simultaneously.

Tumour inhibition effect of these NPs was further established during the animal experimentation. Besides, Liu's group loaded $Mn^{2+}$-chelated Ce6 (Ce6(Mn)) plus DOX hooked on $CaCO_3$ through co-precipitation technique, then customized the monodisperse $CaCO_3$ NPs alongside PEG (Fig. 19A) [262]. The 100 nm sized Ce6(Mn)@$CaCO_3$-PEG sluggishly decayed at pH 6.5 besides dissociating promptly at pH 5.5. When Ce6 (Mn) was discharged from $CaCO_3$, it was observed that the $Mn^{2+}$ $T_1$-weighted magnetic resonance (MR) signal were considerably augmented (Fig. 19C). Such type of NPs should be efficaciously employed in order to realize the imaging guided therapy. Another type of pH responsive biomaterial such as CaP has been extensively employed for siRNA as well as drug delivery. CaP is nontoxic in comparison to $CaCO_3$, biocompatible besides degradable in the early lysosome [310]. Nonetheless, CaP's exceedingly charged surface is comfortable towards binding with the proteins, which limits the blood circulation life of CaP. In addition, $MnO_2$ is also pH sensitive, and it can generate oxygen and relieve tumour hypoxia by reacting with $H_2O_2$. Such inorganic pH responsive nanoconatructs present a promising potential for cancer therapy *via* precise responsive to the acidic pH in the TME.

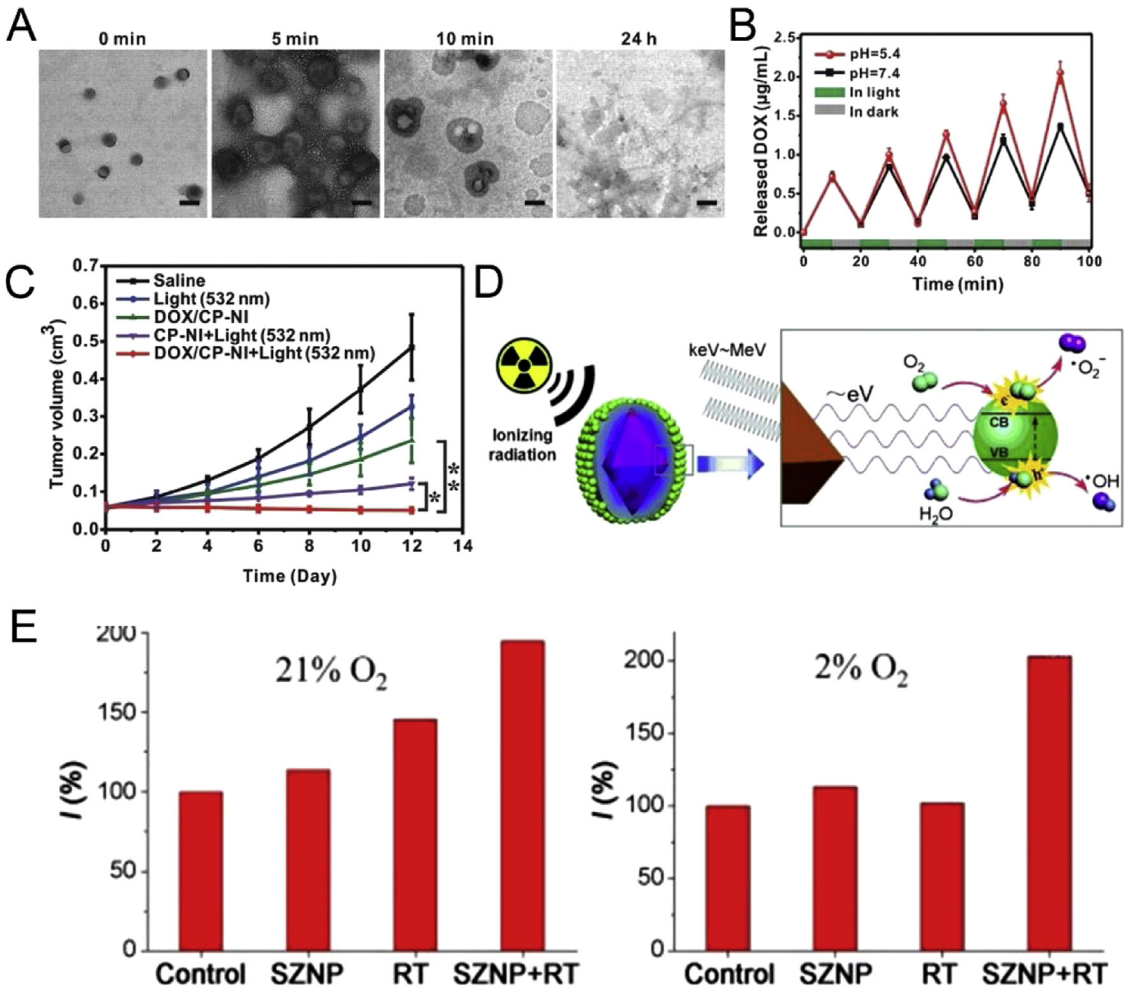


**Fig. 16.** (A) TEM images of DOX/CP-NI NPs in varied time periods after 5 min light irradiation. (B) The light-responsive DOX releasing profiles of DOX/CP-NI under different pH values and light conditions. (C) *In vivo* therapeutic performance of DOX/CP-NI towards HeLa xenografts. Reproduced with permission [291]. Copyright 2016, Wiley-VCH Verlag GmbH (D) Schematic illustration of X-ray mediated photodynamic therapy with diminishing oxygen dependency. (E) *In vitro* cytotoxicity profiles of SZNP towards HeLa tumour cells under normoxic and hypoxic conditions. Reproduced with permission [292]. Copyright 2015, Wiley-VCH Verlag GmbH.

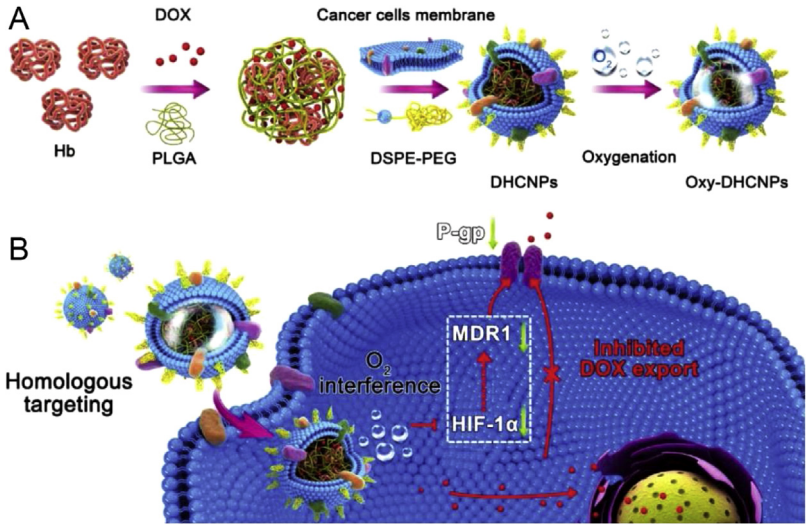


**Fig. 17.** The design as well as the functions of DOX/Hb loaded PLGA-cancer cell membrane nanoparticles (DHCNPs) for homologous targeting and $O_2$ interference. (A) Synthesis of oxy-DHCNPs. DHCNPs were prepared by extrusion with preformed DOX/Hb-PLGA NPs, DSPE-PEG, and MCF-7 cancer cell membrane, and then were oxygenated to obtain oxy-DHCNPs. (B) Cellular functions of DHCNPs, including homologous targeting, downregulation of predictive markers Fig. 24 MDR1, and P-gp), and inhibited DOX export. Adapted with permission from Ref. [294].

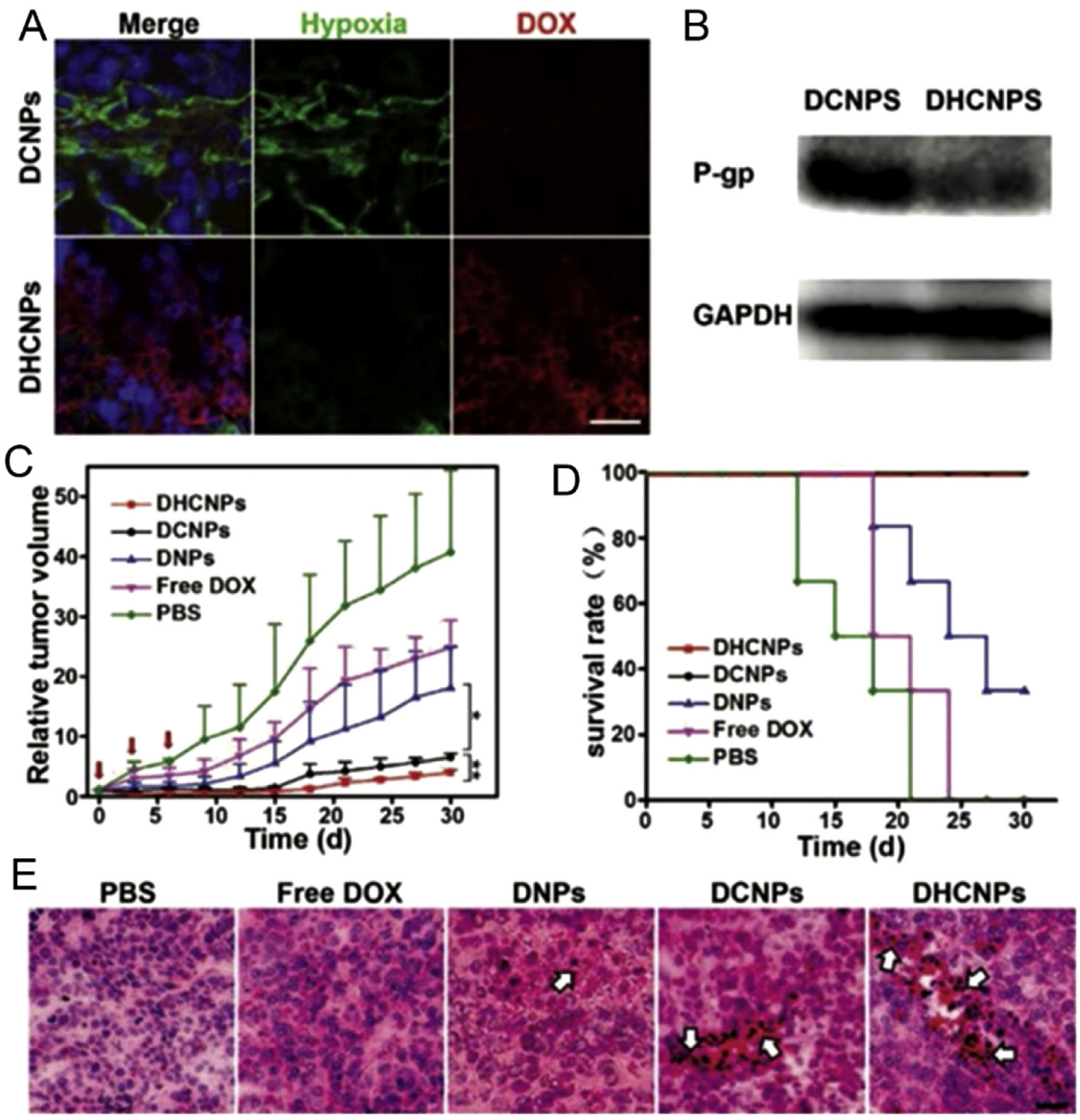


**Fig. 18.** Antitumor effect of DHCNPs based on chemotherapy mediated by homologous targeting and $O_2$ interference. All the nanoparticles were oxygenated before experiments (DOX dose = 2.5 mg $kg^{-1}$). (A) Fluorescent imaging of hypoxic probe (green) and DOX (red) in tumour sections at 24 h after intravenous injection of DHCNPs (scale bar 25 μm). (B) P-gp expression in tumour treated with DCNPs and DHCNPs. (C) MCF-7 tumour growth curves of different treated groups (scale bar 50 μm). (D) Survival rates of tumour-bearing mice in various groups. (E) H&E stained histological sections of tumour at 3 d after treatments with PBS, free DOX, DNPs, DCNPs, and DHCNPs. Statistical *P*-values: $^{*}P < 0.05$, $^{**}P < 0.01$.

Adapted with permission from Ref. [294].

*pH responsive polymers for tumour therapy*

Countless pH-responsive polymers were advanced during these preceding years intended for the tumour targeted delivery. Maximum of these polymers have been responsive towards somewhat low acidic conditions (pH 4.5–5.5) besides they only could react in endo-/lysosome pH. Polymers activated near the tumour extracellular environment (pH 6.5–7.0) have been extremely looked-for recently [311]. A typical linker 2-Propionic-3-methylmaleic anhydride (CDM) might be split inside a trivial acidic environment (pH B 6.8). Platinum (Pt) prodrug was conjugated on poly(amidoamine) (PAMAM) through an ester bond by Wang's group, besides afterwards employed CDM towards connecting the (PAMAM/Pt) as well as polycaprolactone (PCL) [312].

Through the buidup of the PCL-CDM-PAMAM/Pt, PEG-b-PCL as well as PCL, they fabricated iCluster/Pt NPs having diameter of nearly about 100 nm (Fig. 20A). In physiological milieu such iCluster/Pt NPs remain stable and maybe disintegrated into infinitesimal PAMAM/Pt dendrimers inside the acidic TME through the splitting of DCM (Fig. 20B–D). Following the entery of dendrimers into the tumour cells, the Pt drug might promptly discharged after encountering a redox environment. In order to supervise infiltration of such NPs insde the acidic TME, a PCL block of the hydrophobic core stayed branded by rhodamine B (RhB, red) besides PAMAM was branded by the fluorescein (Flu, green). As shown in the (Fig. 20E), almost null green fluorescence was noticed inside the internal area yet after even 24 h incubation with cluster/Pt NPs deprived of CDM. Nevertheless, green signals were definitely perceived uniformly inside the internal as well as the edge of the spheroids afterward 24 h incubation for iCluster/Pt NPs. Moreover, such iCluster/Pt NPs considerably hindered tumour growth as well as the sustained the average survival time of the A549R cisplatin-resistant human lung tumour model in mice (Fig. 20F) Reversible protonation/deprotonation techniques were also applied in order to design the strategy of pH sensi-

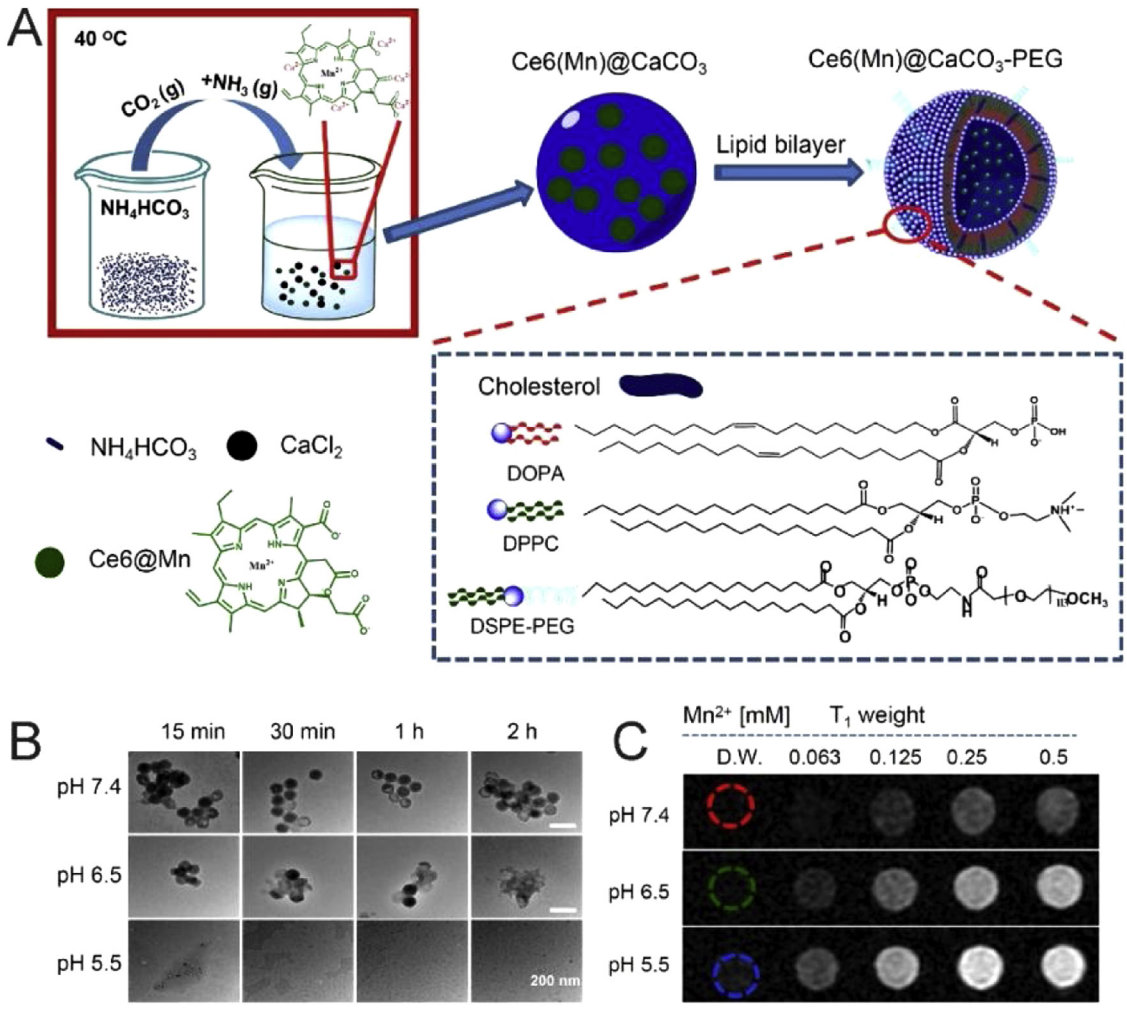


**Fig. 19.** (A) Outlines exhibiting the synthesis and structure of Ce6(Mn)@$CaCO_3$-PEG NPs. (B) TEM images of Ce6(Mn)@ $CaCO_3$-PEG immersed with different pH values (5.5, 7.4 and 6.5) PBS buffers after various times. (C) T1-Weighted MR images of Ce6(Mn)@$CaCO_3$-PEG with different concentrations and different pH values after 4 h incubation. Reprinted with permission from Ref. [262].

tive polymers [186]. Zwitterionic-to-cationic charge conversion blocks, for example, acylsulfonamide [313], carboxybetaine [314] as well as phosphorylcholine [315], remain as admirable contenders. For instance, Mizuhara et al. advanced pH-responsive zwitterionic ligand founded over alkoxyphenyl acylsulfonamide, that might preserve neutrality in physiological conditions besides becoming positively charged in the TME (pH of 6.5) carrying an affiliated augmentation of cellular uptake [313]. L-Histidine (His), which is an amino acid possessing a pH of 6.5, besides being a characteristic protonation/deprotonation ligand to sensitive to trivial acidic tumour pH [43]. Bae's group advanced a micelle from polyHis-b-PEG and poly(L-lactic acid) (pLLA)-b-PEG-b-polyHis-biotin [43,316], then the DOX was encapsulated in the micelle. As shrank under the pH value 7.0, maximum of the biotin molecules was wide-open over surface due to ionization of polyHis besides interaction with the cells. The micelles damaged, ensuing into the heightened drug release as the pH value lower than 6.5. Lately, an ultrasensitive pH-responsive fluorescent micellar structure inclosing tertiary amine substituents as a pH detector has been testified by Gao's group [317]. These NPs can briskly counter to the variance of less than 0.25 pH units in the tumour extracellular microenvironment. Herein these pH responsive polymer nanocontructs discussed above display a significant invio and *in vitro* therapeutic improvement by tragetting the pH fluctuations in the TME.

*$H_2O_2$ responsive nanoconstructs for tumour therapy*

Under extraordinary oxidative stresses environemnt tumour cells instigated the overexpression of the superoxide anion radicals, hydroxyl radicals, as well as the hydrogen peroxide [318]. Such ROS instigate *via* an distinctive oxygen metabolic pathways in the mitochondria, peroxisomes, as well as in the endoplasmic reticulum, *etc.* [319]. Through the reduction of oxygen molecules in the electron transport train inside the mitochondria these superoxide anion radicals were regularly produced, insinuating into the notable oxidative potential in cancer cells [320]. In order to thwart these hostile oxidative stresses, tumour cells have to be coerced in order to maintain the reduction potential *via* expression of the redox species such as superoxide dismutase (SOD), catalase, GSH, besides glutathione peroxidase, *etc.* [321]. The overexpressed SOD might efficiently react with super-oxide anion radicals in order to produce the $H_2O_2$ as well as $O_2$ disproportionally, mitigating the oxidative stresses through transformation of the exceedingly oxidative species into less oxidative ones [322,323]. $H_2O_2$ buidup was manipulated as an impulsive activator intended for the chemotherapy through responsive drug release [324,303], endogenous $O_2$ maker [286], as well as new impelling energy supply aimed at drug-releasing nanomotors [325].

In order to achieve $H_2O_2$ responsive drug release, ultras-mall (5 nm) Ag NPs which acted as nanolids towards capping the

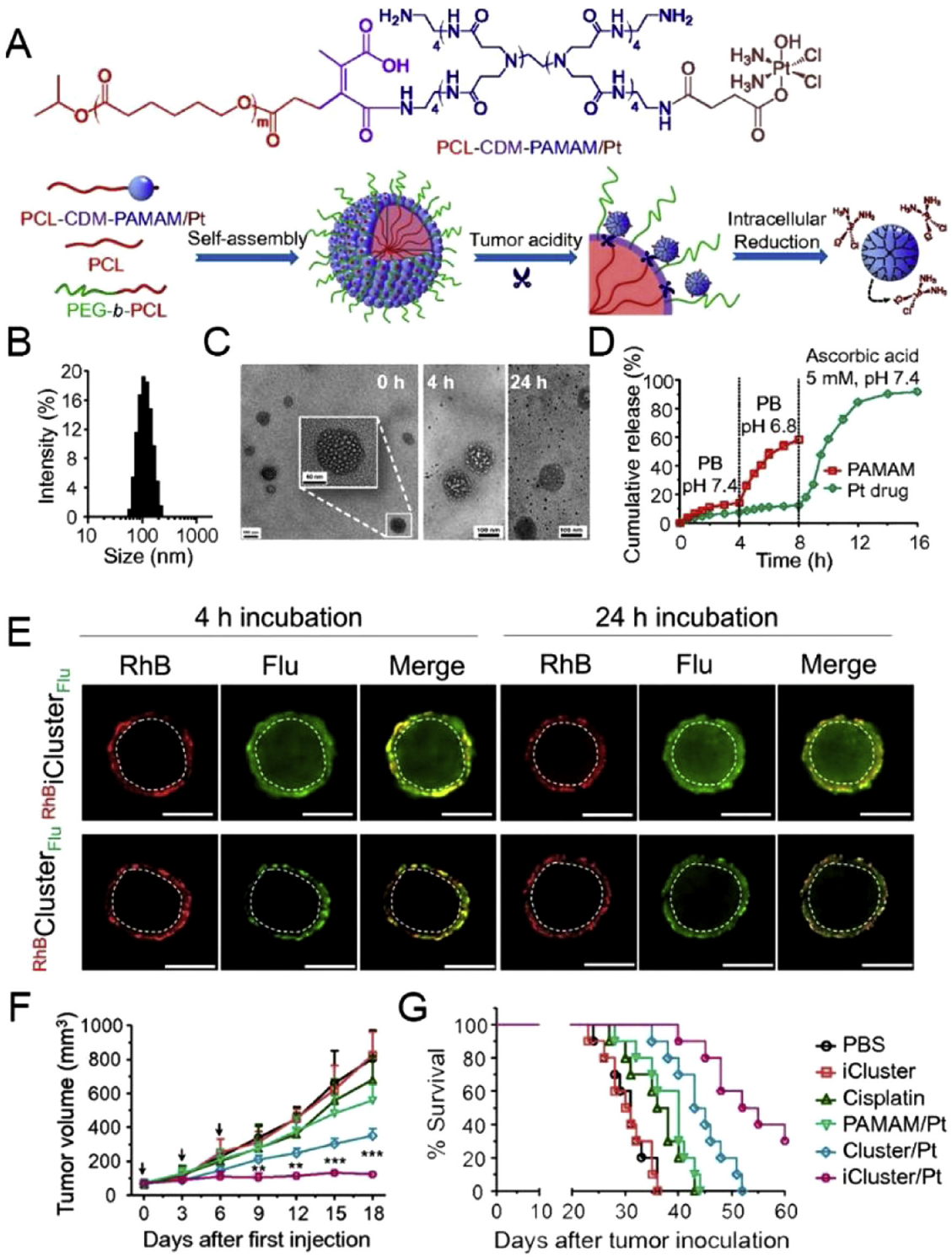


**Fig. 20.** (A) Chemical structure of PCL-CDM-PAMAM/Pt and the mechanism of the self-assembly Pt-containing pH-instable clustered (iCluster/Pt) NPs in response to the tumour environment. (B) Size distribution of iCluster/Pt measured by DLS. (C) TEM images of iCluster/Pt and Cluster/Pt immersed with PBS at pH 6.8 for various amounts of time. (D) *In vitro* release profiles of PAMAM (green line) and platinum drug (red line) from iCluster. (E) Multicellular spheroid model of BxPC-3 cells to confirm the penetration of RhBiClusterFlu and RhBClusterFlu at pH 6.8 after 4 h or 24 h incubation (scale bar = 200 μm). (F) Inhibition of A549R cisplatin-resistant human lung cancer model by iCluster/Pt. Mice were i.v. administered an equivalent platinum dose of 1.5 mg $kg^{-1}$ on days 0, 3, and 6. (G) Kaplan–Meier plots of the animal survival in 4T1 tumour mice ($n = 10$). Mice were treated at a platinum dose of 3 mg $kg^{-1}$ *via* i.v. administration on days 10, 15, and 20 after tumour inoculation.
(Reprinted with permission from Ref. [312]. Copyright 2016, National Academy of Science).

drug-encapsulated passages of mesoporous silica NPs (MSN) stood established (Fig. 21A) [324]. When exposed to the tumorous $H_2O_2$, such Ag nanolids may cumulative resuting in the larger particles thus the caps located at the end of these nanochannels of MSN maybe detached (Fig. 21B), ensuing the discharge of the encapsulated drugs (Fig. 21C). Backed by the catalase $H_2O_2$ also functions

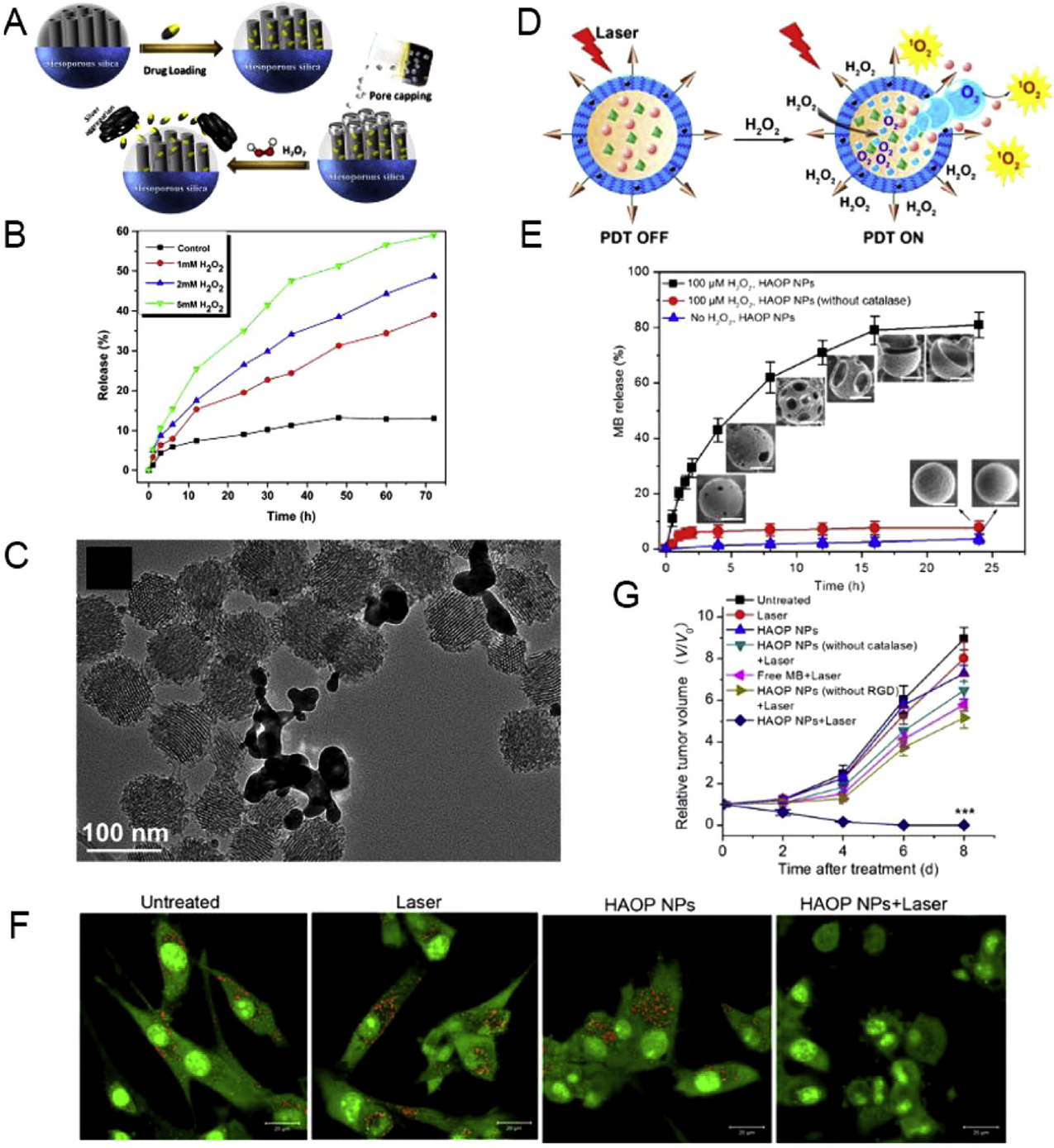


**Fig. 21.** (A) Graphic designs of Ag nanolids-capped and drug encapsulated MSN as well as $H_2O_2$-responsive drug release. (B) TEM image of Ag@MSNs treated with 10 X$10^{-3}$ m $H_2O_2$. (C) Releasing profiles of Rhodamin 6G from Ag@R6G@MSNs in the presence of varied concentrations of $H_2O_2$. Reproduced with permission from Ref. [324] Copyright 2014, American Chemical Society. (D) Schematic illustration of HAOP NPs for $H_2O_2$-activatable and $O_2$-evolving photodynamic therapy. (E) $H_2O_2$-responsive releasing profiles of photosensitizer MB from HAOP NPs. (F) Confocal fluorescence images of acridine orange staining U87-MG cells under different treatments. (G) *In vivo* therapeutic performances of HAOP NPs. Reproduced with permission from Ref. [326]. Copyright 2015, American Chemical Society.

as an *in situ* oxygen producer in order to augment PDT [326], manganese oxide ($MnO_2$) [286] as well as the Au NPs *etc.* Acting as an ideal prototype, natural enzyme catalase, photosensitizer methylene blue (MB), black hole quencher-3 (BHQ-3) have been concurrently encapsulated and hooked on to the PLGA to give an $H_2O_2$-activatable besides $O_2$-evolving photodynamic (HAOP) nanoplatform (Fig. 21D) [326]. BHQ-3 Functioned as a "switch" so as to control the photosensitizer MB. Precisely, when encapsulated on HAOP NPs, the $^1O_2$ production from MB was "switched off" *via* BHQ-3 through Förster resonance energy transfer (FRET) effect. Upon delivery of the nanoparticles intp the tumorous region, $H_2O_2$ in tumour cells might penetrate inside the HAOP NPs. Upon catalysis through the catalase, $H_2O_2$ was successfully disintegrated to produce $O_2$, stimulating splitting of the PLGA shells, that diminished the FRET effect as well as endorsed MB release (Fig. 21E). Consequently, upon the activation of the photosensitzer which acted as "switched on". During the external light irradiation, $^1O_2$ was abundantly bred from the MB, that later on induced tumour PDT

besides hence inviting cell apoptosis thru a lysosome-mediated pathway (Fig. 21F, G). In addition to $O_2$ generation, $H_2O_2$ also contributed in the discharge of seceral other gas molecules for example CO. Manganese carbonyl $Mn_2(CO)_{10}$ encapsulating hollow MSN (MnCO@hMSN) remained engaged as alternative antitumor nanoplatform. Such NPs might disparate the intratumoral $H_2O_2$ into ·OH, through the application of an efficient Fenton-like catalytic performance. The released ·OH may additionally assault the Mn coordination centre, ensuing the $H_2O_2$-responsive discharge of the CO. Such a comibination of the chemodynamic therapy as well as CO-mediated gas therapy revealed great tumour-therapeutic efficacy both *in vitro* as well as *in vivo* [327]. These $H_2O_2$ responsive nanoconstructs catalyze $H_2O_2$, which is disintegrated to produce $O_2$ inside tumour microenvironemt thereby augmenting the cancer therapeutic efficency by relieving the tumour tissue of its hypoxia.

*Glutathione-responsive nanoconstructs for tumour therapy*

In an extremely oxidative microenvironment the tumour cells thrive as discussed in the previous section. Through upregulation of the anti-oxidative biomolecules, for example, glutathione, tumour cells thwart the damaging effects of such oxidative stresses [318]. Glutathione disulfide/glutathione redox combine (GSSG/2GSH) could be employed to act as a significant marker of intracellular redox environment [328]. As an outcome, the intratumoral GSH levels rests at $0.5–10 \times 10^{-3}$ M intracellularly, four-folds higher in comparison to that of the ordinary tissues [329]. This type of reducing microenvironment aids nanotherapies through GSH reductive responsiveness. In a latest work reported by Shi and his coworkers, they verified a anticancer drug DOX loaded Mn-HMSN model (DOX@PEG/Mn-HMSN) intended for the tumour-specific GSH/pH-responsive chemotherapy [330]. The produced DOX@PEG/Mn-HMSN NPs unveiled outstanding GSH/pH-responsive outline about biodegradation hence consequently fast-tracked DOX liberation. Such an tumour exclusive stimuli-responsive stratagem offers adequate therapeutic conclusion alongside elevated chemotherapeutic biosafety in contradiction of tumour xenografts. *In vivo* biodegradability concern of inorganic nanomaterials subsequent to transporting as well as discharging the therapeutic drugs reamins as one of the gravest apprehensions in the realizaton into clinical transformation. Furthermore, scaffold organic-inorganic combination grants these amalgamated mesoporous organosilica nanoparticles (MONs) as well as HMONs with exclusive reductive GSH responsive biodegradability though disulfide bonds (S-S) hybridization. This type of intratumoral GSH-responsive biodegradability drug delivery nanoplatforms facilitates canny besides operative tumour nanotherapies alongside assuring clinical translations [331]. The charateristic feature of this GSH reductive responsiveness offers extra pivotal trait aimed at the antitumoral nanotherapies. As GSH function like a major reductive species, these biomolecules are possibly radical hunters functioning in contradiction of the deadly weapons, for example, Fenton reaction. Through instantaneous depletion of such biomolecules, the therapeutic functioning of ROS-facilitated antitumor nanotherapies may be improved. This types of encouraging and multifunctional responsiveness brightens the imminent maturities of the TME-sponsored nanotherapies.

*Extra cellular matrix responsive (ECM) nanoconstructs for tumour therapy*

For tissue morphogenesis, the extracellular matrix acts as a scaffold. The ECM is mainly constituted of the vastly interlocked collagen fibres as well as allied large glycoproteins, proteoglycans together with various proteins which control tissue homeostasis, organ growth besides tissue lesion [332]. Many components in tumour ECM are factors responsible for the growth besides cell migration in solid tumours [333]. Due to manifestation of the excessive collagen yield, a amplified level of lysyl oxidase (LOX), as well as an augmented integrin receptors, solid tumours possess dense extracellular matrix to facilitate the transmission of extracellular signals towards cells, that results into the escalation of the solid stress in the tumours, besides squeezes tumour blood vessels in order to lessen tumour perfusion [115]. Moreover, a profuse tumour ECM also precludes the infiltration of the NPs, decreasing tumour treatment effectiveness. Alteration of the tumour ECM offers a substitute tactic for augmenting cancer therapy. One such technique is to engage the enzymes, for example, hyaluronidase (HAase) and collagenase, towards vitiating matrix structure [334].

TME was modulated by the Liu's group through supervision of HAase, that splits hyaluronan, considere to be a key ECM constituent in tumours (Fig. 22A) [335]. The C18PMH-PEG-Ce6 nanomicelles were synthesized as well as co-administered alongside HAase-PEG into mice aimed at cancer treatment. Both tumour vascular density as well as effective vasculature exhibited enlargement following HAase injection, encouraging intensified perfusion in the tumour. Subsequent to the treatment by HAase, hypoxia stained signals turn out to be visibly lesser inside entire tumour paralleled to control group (Fig. 22B), besides the tumour growth was approximately entirely subdued (Fig. 22C, D). A recombinant human hyaluronidase PH20 (rHuPH20) customized with PLGA-PEG NPs were devloped by the Cheng's group [336]. rHuPH20 may damage hyaluronic acid in order to augmented NP infiltration inside the tumour (Fig. 22E). NPs compressed by the DOX might proficiently prevent tumour development as well as foster tumour survival rate (Fig. 22F). As verified by the fluorescence imaging that HA on a diffusion path NPs were damaged whereas the signal of HA existed reserved inside the ordinary tissue. The signal of HPEG-PH20-NP could be evidently perceived throughout the surrondings of the blood vessels inside tumour (Fig. 22G).

Jerveratrum alkaloid cyclopamine is an naturally arising steroidal, which could impede the hedgehog signalling pathway (Hh) through operating over SMO receptor [337]. Testified by the Zhang et al, cyclopamine may disorder tumour extracellular fibronectins, expand tumour blood vessels besides spreading the tumour perfusion. Cyclopamine as well as the paclitaxel encapsulated PEG-PLA NPs might modify extracellular matrix accumulation, advance pancreatic cancer tumour perfusion as well as accomplish momentous tumour development hindrance. Oligosaccharides of hyaluronan (oHA) are be able to unsettle the HA matrix by switching HA for the binding on CD44 [338]. Gao's group synthesized oHA-lipid-PTX NPs, that may proficiently unsettle tumour HA matrix besides boosting drug delivery inside cells [339]. Synthetic peptide sequence Bz-Arg-Arg-p-nitroanilide can be cleaved by Bromelain and digested the extracellular matrix [340]. Tasciotti's group customized MSNs alongside bromelain then discovered an improved diffusion of MSNs inside tumour extracellular matrix [341]. Extracellular matrix penetration depth is improved by another enzyme collagenase through contravention of the peptide bonds in collagens [342]. Goodman et al. advanced polystyrene NPs immobilized with collagenase [343]. The collagenase treatment of spheroids ensued in a notably amplified infiltration of polystyrene NPs. Giorgio's group also validated the collagenase-functionalized superparamagnetic NPs have the capability to damage the extracellular matrix aimed at superior interstitial mobility [344]. Lately, the Vallet-Regí group constructed hybrid MSN NPs clipped onto collagenase-polymeric nanocapsules towards advancing their tumour infiltration [345]. Such polymeric nanocapsules defend the collagenase against proteolytic degradation as well as hydrolysis during circulation inside bloodstream although permitting collagenase discharge at tumour pH in order to augment tumour matrix deprivation. ECM-related inhibitors

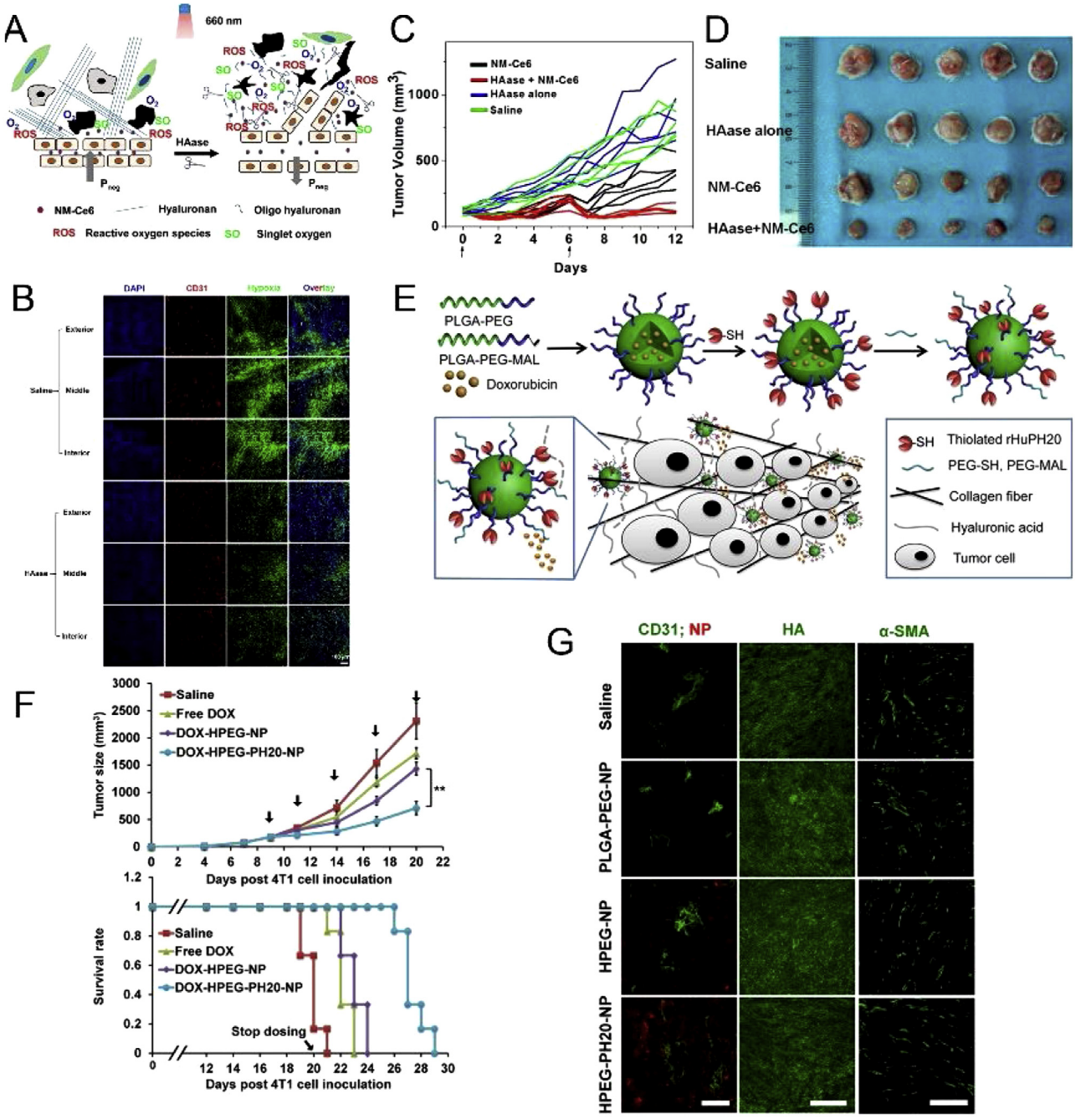


**Fig. 22.** (A) Outline displaying the strategy to modulate the TME by HAase. (B) Tumour slices immunofluorescence imaging by treatment with 1500 U HAase. Red: blood vessels; green: hypoxic regions; blue: nuclei. (C) Tumour inhibition under various treatments with saline, HAase alone, PDT alone, and PDT plus HAase at days 0 and 6. PDT effect is obviously enhanced by administration of HAase. (D) *Ex vivo* tumour pictures of the same study described in (C). (E) Scheme of synthesizing hyaluronidase-modified nanocarrier by conjugating thiolated rHuPH20 on the first PEG layer followed by anchoring the second PEG layer. (F) Tumour growth inhibition curves and survival rate plots for 4T1 tumour-bearing mice treated with either saline, free DOX, DOX-HPEG or DOX-HPEG-PH20 NPs at 2 mg $kg^{-1}$ equivalent dose of DOX. (G) Staining of sectioned tumour tissues collected 24 h post-injection of saline or various NP formulas. Scale bar: 50 μm (left); 200 μm (middle); 100 μm (right). (A–D) was reprinted with permission from Ref. [335]. Copyright 2016, American Chemical Society. (E–G) was reprinted with permission from Ref. [336]. Copyright 2016, American Chemical Society).

possess capability to be used as a cancer therapeutic mediators although few among them for example MMP inhibitors has been unsuccessful clinically [346]. Topoisomerase I inhibitor topotecan and the cardiac glycoside digoxin are two types of drugs exhibiting anticancer properties through plummeting tumour fibrosis as well as inhibiting HIF1a build-up besides being verified in preclinical models. During the Phase II clinical test of the digoxin are currently being run over men having recurring prostate cancer (Clinical Trials. gov, number: NCT01162135). Furthermore, a preliminary clinical test of topotecan (ClinicalTrials.gov, number: NCT00182676) in patients at advanced cancer stages and HIF1a over-expression shown on tumour biopsy was lately stated in which HIF1a protein levels were unnoticeable in the post-treatment biopsy samples from four of seven patients who were studied, and diminished tumour blood flow was witnessed in 70% of patients by contrast-enhanced dynamic magnetic resonance imaging [347]. Volociximab, IgG4 monoclonal antibody (mAb) *versus* a5b1 integrin, was assessed in phase I analysis inside the solid

tumours [348]. Though its antitumor activities were not established, its decent safety profile revived assessment of this drug in arrangement with chemotherapy in non-small cell lung cancer [349]. This arrangement exhibited some effectiveness bearing in mind that 24% of patients realized a fractional response besides 52% stable disease with a safe toxicity profile.

*Immune responsive nanoconstructs for tumour therapy*

In our body, immune responses play vital roles. Immunotherapy known as a far-reaching group comprising anti-cancer therapies which exploit body's immune system to achieve cancer treatment, that could boost unambiguous besides a resilient anticancer responses [350]. The immune system has to be activated first for efficacious therapy, these effector cells get swelled besides being intimated towards the tumour tissue. Ultimately, tumour cells get demolished [351]. Nevertheless, cancerous cells couls perhaps get away from such immune responses, as well as the TME might extraordinarily inhibit such developments [69]. NPs considered as the suitable contenders towards stimulating the antitumor immune responses intended for the immunotherapy. NPs after being dispensed into tumour tissue, cquire the capability for modulating the immunosuppressed TME besides activation of the immune system. Another stratagem concering the cancer therapy is the transport of immunostimulatory drugs into antitumor immune cells. Antigens are regarded as the molecules which could incite an immune response on the behalf of host organism amid an extraordinary degree of specificity [352]. NPs could well be used as carriers towards delivering the antigens in order to initiate antitumor immune responses. Paralleled alongside tradirional chemotherapies, immunotherapy requisites squat dosages of antigens for activating the immune responses, besides lessening the harmful effects of the anticancer drugs.

In order treat prevailing cancer NPs might be cast-off as therapeutic cancer vaccine. The competence and the overpower pertinent tissue barriers besides proficiently delivering the therapeutic cancer vaccines into specific tissue targets has been discrived as the key towards designing tumour vaccine transport techniques. Key locatons of the antigen-presenting cells (APCs)Lymph nodes, could be engaged as sites for the targetted intended for the vaccine delivery. DCs may prompt antigen-specific cytotoxic T cells, that inturn can provoke an efficient anti-tumour response [353]. Towards achieving an efficient vaccine delivery into the lymph nodes, transporter has to be taken up into lymphatic vessels then to be held inside the draining lymph nodes. Transporter size is very perilous thus it must be less than 100 nm so as to enhance the carriers uptake into the lymphatic vessels [354]. Zhang's group devised a nanovaccine which dispensed 30 nm a-Ap-FNP so as to developed DCs straightforwardly [355]. Moreover, an adjuvant, a pharmacological or immunological agent, may augment effectiveness of a vaccine. NPs that ship both tumour antigens as well as the adjuvants could be premeditated so as to co-deliver vaccine constituents [70]. Hybrid NPs having several function can combine diverse immune effectors were devised so as to ovethrow the immuno-inhibitory feature of TME besides endorsing the immunotherapy.

A hydrophobic small molecule inhibitor of the immune suppressive cytokine transform growth factor-b (TGF-b) as well as the the T cell mitogenic cytokine interleukin-2 (IL-2) were encapsulated to form a nanoscale liposomal polymeric gels (nLGs) by Fahmy's group, (Fig. 23A) [356]. Such a polymer is able to release TGF-b inhibitor (SB505124) besides IL-2 into TME, instigating an noteworthy lessening of the tumour growth (Fig. 23B and C). Furthermore, their group also employed dual-labelled nLGs prepared through integration of the fluorescein-labelled PEG-phosphoethanolamine into the lipid membrane of rhodamine-loaded nLGs witht an aim to gauge transferring of the particles against transferring of the consignment. As shown, both the vehicle and consignment were hoarded into the subcutaneous tumours and lung metastases (Fig. 23D). Consequently, such a method could dispense both hydrophilic as well as the hydrophobic immunomodulators towards boosting the antitumor endeavour *versus* subcutaneous as well as the metastatic melanomas. Huan's group employed lipid-calcium-phosphate (LCP) NPs in order to provoke the antigen-specific immune response as well as liposome-protamine-hyaluronic acid (LPH) NPs for delivering siRNA [357]. Deliverin of the siRNA through the usage of LPH NPs ensued into the effective bargain of TGF-b in the late stage TME. TGF-b down-regulation encouraged the vaccine effectiveness besides subding the tumour growth beyond vaccine treatment unaccompanied.

*Nutrient depletion responsive nanoconstructs for tumour therapy*

Throughout the course of propagation of the malignant tumour cells, energy carrying molecules such as (ATPs), nucleotides, fatty acids, membrane lipids together with amino acids remain exceedingly necessitated [358]. Throughout the mammoth angiogenesis, these nutrients could be voraciously consumed and afterwards broken down by tumour cells so as to get the energy besides stocking it for the tumour proliferation, growth, as well as the metastasis following the protocols of the associated metabolic contrivances. Purposefully, *via* direct utilization (*e.g.*, exhausting, identifying, besides transforming) such copious nutrients, numerous effective nano therapeutic stratgies were advanced for treating the tumour cells. Through entire depletion of the ATP molecules around tumour area, alkylating agent 3-bromopyruvate realizes effectual prevention of the malignant tumour (2–3 cm) [359]. Pluronic block copolymers have been validated towards rendering a indispensable function in ATP depleting with EC50 < 0.01%, which antitheses the multidrug resistance of cancer cells while being presently under Phase II clinical trials [360]. Depletion, additional nutrients, for example d-glucose as well as the glutamine, remain as the vital refills aimed at tumour development. Aerobic glycolysis inside the proliferating tumour cells was observed by Warburg initially in 1956, thru which simply 4 moles ATP were produced per molecule of d-glucose metabolized (Warburg effect) [361]. Defiantly, ordinary tissue cells exploited d-glucose in an added profitable oxidative phosphorylation pathway, that creates 36 moles ATP per molecule of d-glucose metabolized. Actually, tumour cells aggressively express a sizable volume of glucose carriers, involving facilitative glucose transporters as well as sodium reliant on glucose carriers inteded for intracellular uptake of d-glucose [362]. Through such a strategy why multiplying tumour cells should acclimatize towards such an inferiorly operative metabolism pathway stands mysterious. Hitherto it might be conjectured that tumour cells spectacle more reliance onto glucose nutrient compared to the ordinary tissue cells. Since production of nucleotides relies on the glucose thru pentose phosphate shunt through glycolysis process. Glutamine remains firstly disintegrated through the glutaminolysis after being dispensed into mitochondria for tricarboxylic acid cycle, at that point, citrate is produced aimed at additional fatty acids synthesis [363].

If nutrients are taken under control the inflated glucose-dependent character compels tumour cells into a susceptible position. Investigators have thus recommended numerous famishing-type of nanotherapeutics so as to fight tumour cells thru glucose-depleting stratagem. Considering a modest nonetheless an efficient approach, Zhao et al. modified glucose oxidase (GOx or GOD, E.C number: 1.1.3.4) through poly(FBMA-co-OEGMA) so as to achieve a nanogels, that might function towards the tumour starvation as well as peroxide-mediated oxidation nanotherapy [364].

They established that through the polymers modification, activity of theenzymes might be fully maintained, the therapeu-

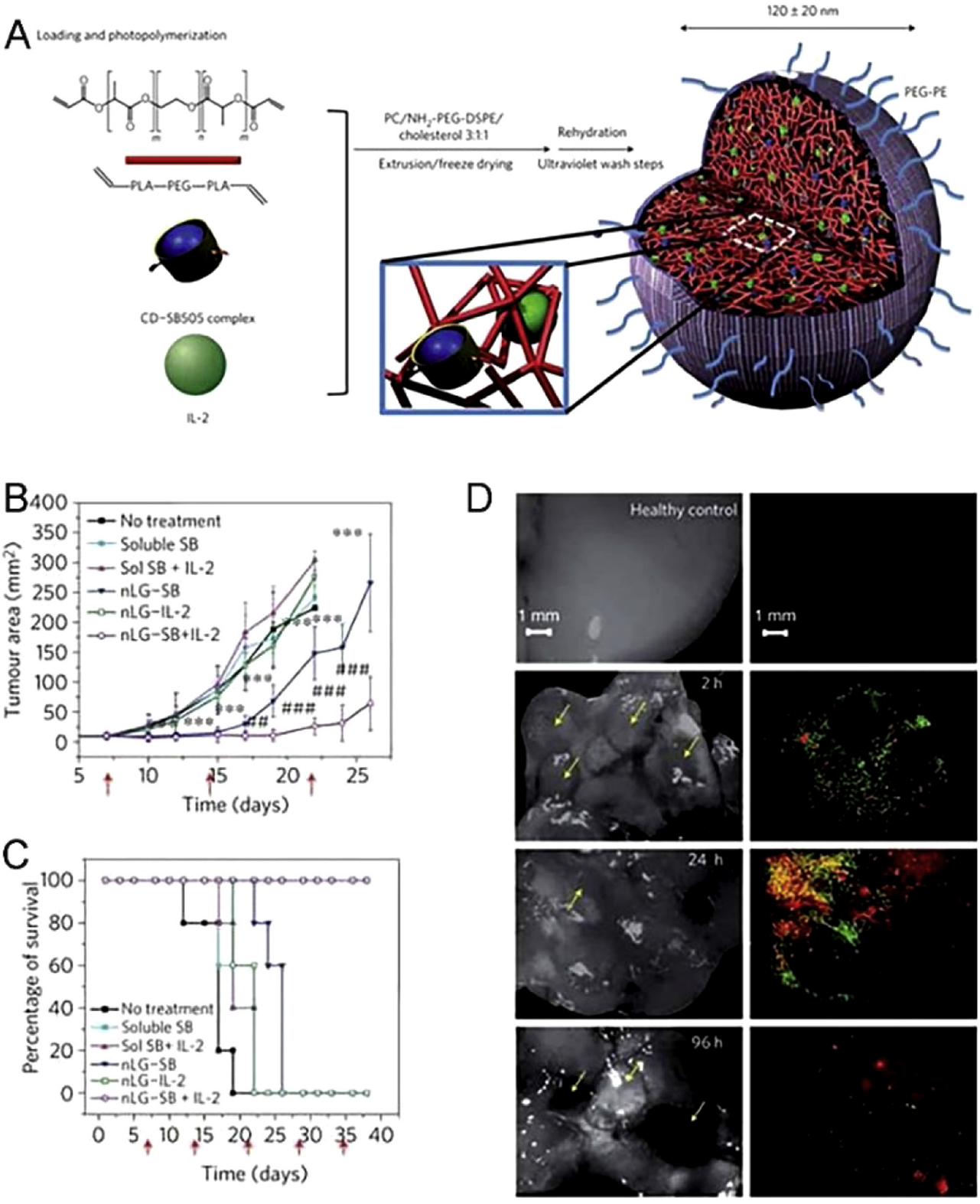


**Fig. 23.** (A) The synthesis and structure of NPs by entrapment of the drug-loaded CD (blue) and the IL-2 (green) in the polymer matrix (red). (B) Plot of B16 melanoma tumour area *vs.* time after intratumoral injection of different formulas. Tumours in the nLG-SB and nLG-SB + IL-2 groups were significantly smaller when compared against all other groups from day 12 to day 22. (C) Survival rate of mice from the same study given in (B). (D) Analysis of lung tissues under bright field and fluorescent microscopy demonstrate the presence of both lipid carrier (green) and rhodamine payload (red) around individual lung tumours at early time points post injection.
(Reprinted with permission from Ref. [356]. Copyright 2012, Nature Publishing Group).

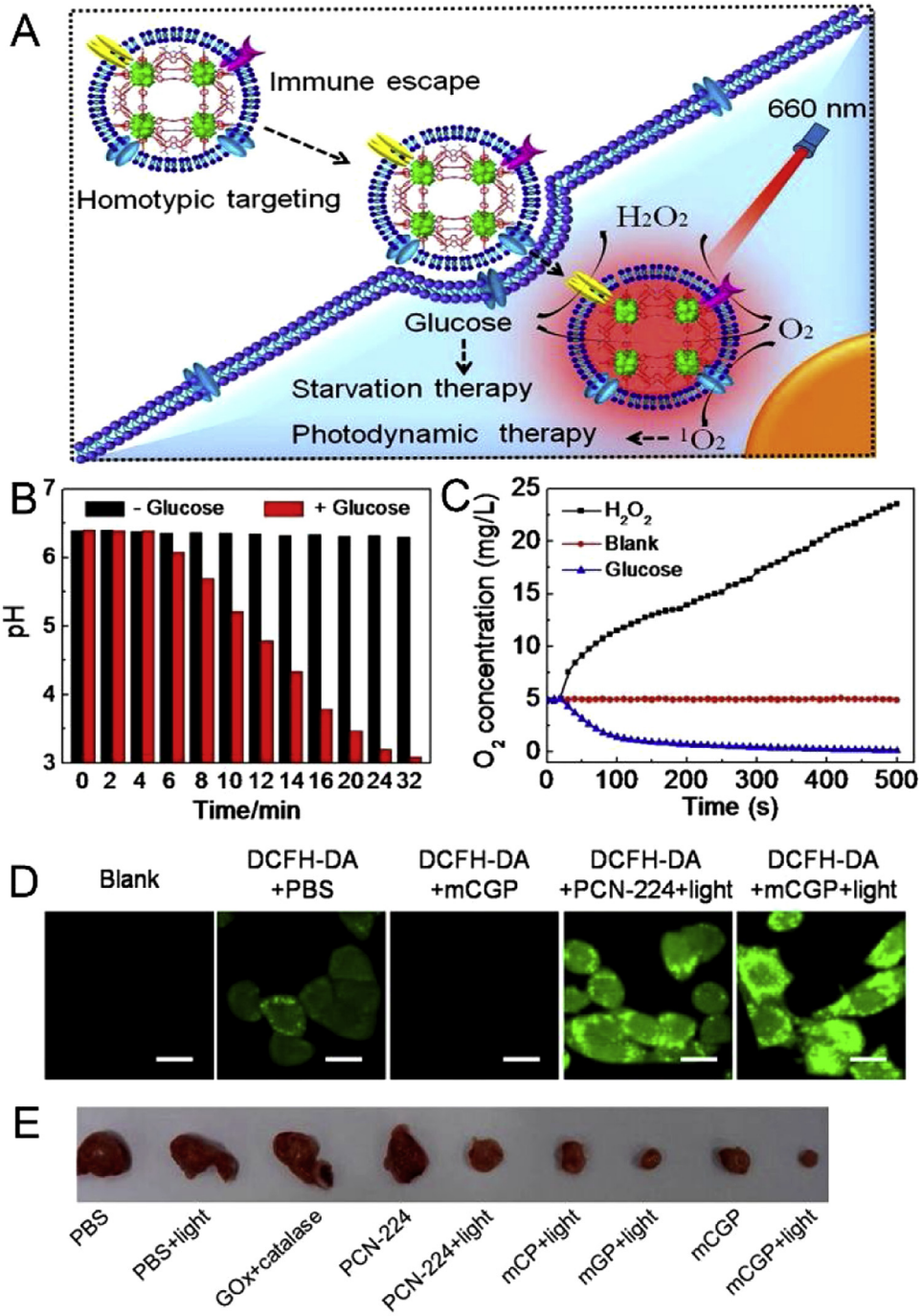


**Fig. 24.** (A) Therapeutic representations of mCGP for tumour starvation and photodynamic therapy. (B) Time-course acidity profiles of mCGP solution with or without the addition of glucose. (C) Oxygen releasing profiles of mCGP solution in the presence of peroxide or glucose. (D) Confocal images of 4T1 tumour cells stained with $^1O_2$ fluorescence probe DCFH-DA after incubation and irradiation under varied conditions. (E) Digital photographs of dissected tumour after the therapeutic treatments under varied conditions.

Reproduced with permission [364]. Copyright 2017, American Chemical Society.

tic functioning *versus* melanoma thus stood augmented. For an alternative strategy, membrane-veiled porphyrin metal-organic framework-based bioreactor (mCGP) enclosing GOx as well as catalase were made-up so as to aim for the synergistic starvation therapy besides photodynamic therapy (Fig. 24A) [364]. As a prototypical, GOx signified as the glucose depriver as well as the hydrogen peroxide ($H_2O_2$) initiator concurrently (Fig. 24B). The freed $H_2O_2$ could be catalyzed *via* catalase so as to achieve an ample oxygen generation (Fig. 24C). Consequently, on irradiation by 660 nm laser, the porphyrin metal-organic framework (PCN-224), aiding and functioning like a nanophotosensitizer, might efficiently switch molecular oxygen towards foriming the toxic singlet oxygen ($^1O_2$) aimed at tumour PDT. The 2′,7′-dichlorofluorescein diacetate (DCFH-DA) stained in 4T1 tumour cells dislosed the generation of toxic $^1O_2$ species (Fig. 24D) besides the operative therapeutic functioning of the mCGP bioreactor remained demonstrated *in vivo* (Fig. 24E). Furthermore, the glucose oxidase could well be useful in successive catalytic reactions intended at tumour therapeutics.

Fan and associates proposed a successively functioning biomolecule (GOD besides l-arginine) inside a hollow mesoporous

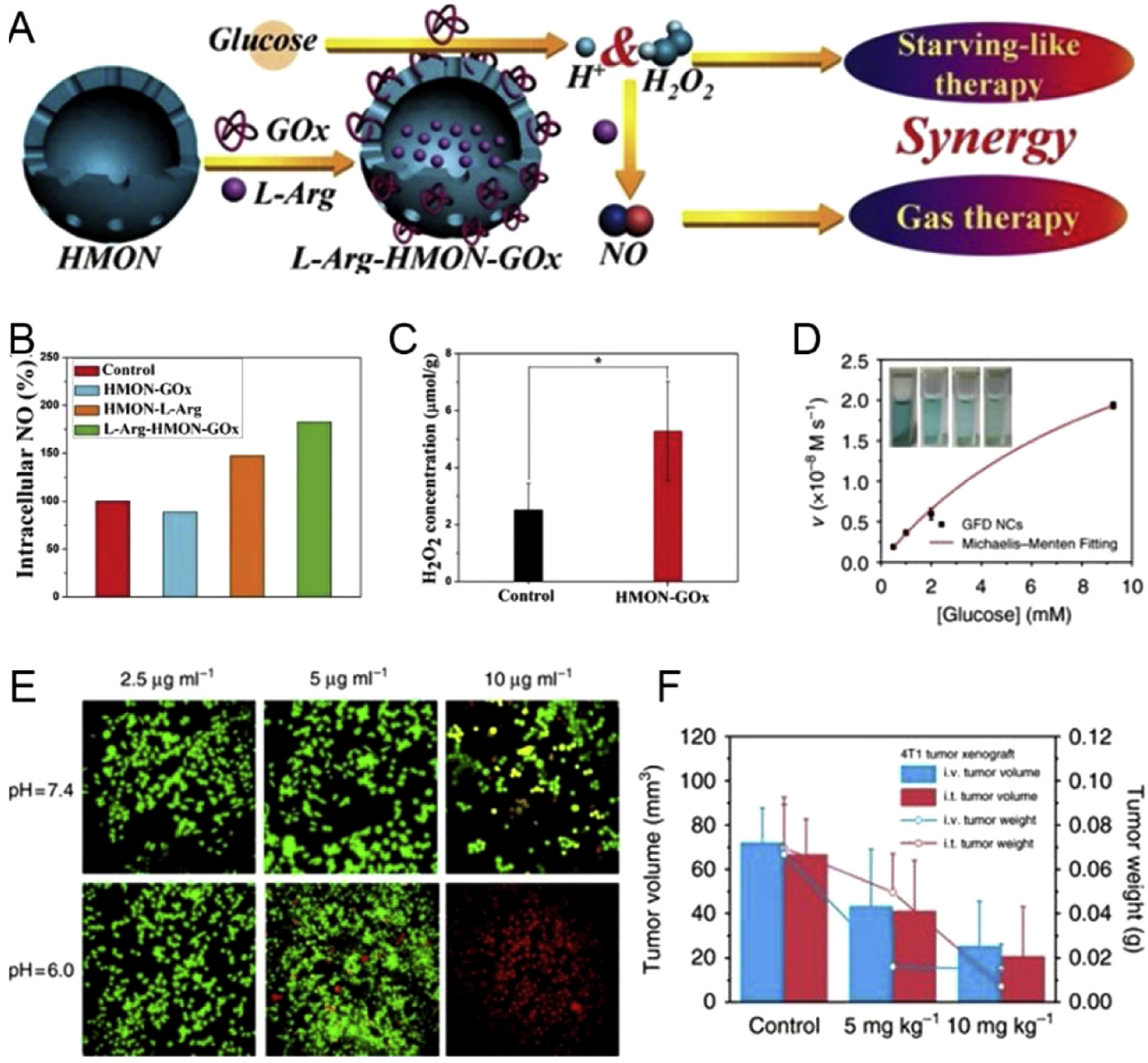


**Fig. 25.** (A) Synthetic route of l-Arg-HMON-GOx for the synergistic cancer starving-like/gas therapy. (B) Quantitative evaluation of intracellular generation of NO in U87MG cells. (C) Variation of $H_2O_2$ concentration in U87MG tumours in 4 h post injection of HMON-GOx. Reproduced with permission from Ref. [365,368]. Copyright 2017, Wiley-VCH Verlag GmbH. (D) *In vitro* colorimetric assay of hydroxyl radical formation using 3,3,5,5-Tetramethylbenzidine (TMB) as an indicator. (E) CLSM images of viable and dead cell distributions after coincubation with GFD NCs at varied concentrations under neutral and acidic conditions for 4 h. (F) *In vivo* 4T1 mammary tumour suppression experiment of varied doses of GFD NCs injected intratumorally and intravenously. Reproduced with permission from Ref. [366].

organosilica NPs (HMONs) in order to achieve the simultaneous starving-like as well as gas therapies (Fig. 25A) through a sequential generations of the $H_2O_2$ and nitric oxides (NO) (Fig. 25B, C) [365]. On behalf of an additional efficient pattern, Jianlin Shi's group recently contrived chronologically functioning biological-chemical nanocatalysts grounded on dendritic mesoporous silica NPs (GOD-$Fe_3O_4$@DMSN nanocatalysts, GFD NCs) regarding the hydroxyl radicals (·OH)-mediated tumour nanotherapy (Fig. 25D-F) [366]. These kinds of GOD approved hearsays bids a fascinating role of dual assisnation with one shot as GOD catalyzed an $H_2O_2$-forming reaction in which the d-glucose nutrient was exhausted although the level of intracellular $H_2O_2$ was thus raised. These bred $H_2O_2$ molecules later functioned as NO and ·OH manufacturers. Moreover, such freed $H_2O_2$ molecules could be employed towards aiming the drug responsive delivery [367] besides production of the $O_2$ [326]. Up-to-date advancement about the nutrient-depleting nanotherapies largely emphasis over the profuse glucose nutrient by means of the natural enzyme GOD. Even though GOD bestows extremely catalytic recital in exhausting glucose, the long-lasting biosafety contours were not yet gauged. Moreover, such a comprehensive mechanism of the approved nutrient metabolism rests ambiguous thu need to be further comprehensively investigated. Furthermore, the glucose-depleting tactics, nanotherapies centred on other nutrients (*e.g.*, glutamine, amino acids) responsive strategies have were rarely reported.

*Enhanced permeability and retention effect*

Tumorous cells characteristically parade extravagant development as well as propagation. In order to quench their plea of massive blood supply, tumour cells overexpress angiogenesis factors for example vascular endothelial growth factor (VEGF) as a mean towards amplifying the manufacturing of blood vessels intended for the nutrients as well as oxygen uptake [368]. Such a

neovasculature is usually made from the inadequately allied faulty endothelial cells amid extensive fenestrations besides crashed lymphatic drainage [369]. Such an far-reaching angiogenesis may thus steer towards the hypervasculature as well as enhanced permeability that remains fully recognized as the enhanced permeability and retention (EPR) effect in Scheme 3 [370]. This type of EPR effect can afford choosy methods to achieve nanotherapeutics since nanoparticles (NPs) with definite sizes remain aided towards penetrating inside the tumour tissues in a considerably superior magnitude compared to that of in ordinary tissues, that might realize a protracted retention time in order to wield therapeutic effects [371]. Angiogenesis as well as the EPR effect institute a vital model for nanomedicines and nanotherapies *versus* tumour as such results might facilitate a series of assaults on tumours through specifically attacking tumour tissue plus instigating therapeutic utilities through nanosystems.

The leakage window of tumour neovasculature fluctuates from 50 to 800 nm subject to the tumour categories and development stages. It is commonly thought that NPs with size of about 5–200 nm performing superior EPR effect, as NPs smaller than 5 nm are to be effortlessly removed through urinary excretion [372] whereas NPs bigger than 200 nm might be speedily taken by reticuloendothelial system in spleens as wellas in livers [373]. Moreover, a specific shape as well as surface alteration were shown to affect EPR effect significantly. It remains established that spherical NPs incline towards tailing a laminar flow pattern to arrive at the surface of the vasculature wall but rod and tube shaped NPs might provoke a stormy flow pattern of blood inside vessels, offering additional prospects towards crossing the gaps on the vascular wall [374]. Surface features for example charges as well as the surface alterations were reported to affect the EPR effect [375]. Regarded as a distinctive inorganic drug nanocarrier, mesoporous silica NPs (MSNs) were established that the process of polyethylene glycol modification (PEGylation) might award MSNs with a brush-like conformation and far lessen negative charging, that might advance its biocompatibility besides diminish phagocytosis, ensuing into a heightened plasma circulation time as well as tougher EPR effect as paralleled to MSNs deprived of PEGylation [376]. Fascinatingly, NPs possessing a marginally negative-charged surface incline towards seepaging from the macrophage endocytosis, supporting extra well-organized tumour accumulations.

Though investigators established that NPs might pierce in side the tumour tissue thru EPR effect, the competence of tumour build-ups nevertheless lingered at fairly low (<10% by intravenous injection). Stratagems towards advancing the tumour build-up, for example, size optimization besides active targeting were advanced. Nevertheless, the effective augmentation happens to be less substantial as otherwise anticipated. Additional works have to be dedicated towards conquering the build-up barricade through EPR effect together with discovering additional tumour buildup approaches.

## Conclusion and outlook

This review wishes to summarize and bring about an assessment over the strategies of the therapeutic NPs through manipulating of the TME. NPs bid countless latent profits which have now opened up for applications in the clinic. The TME offers several new-fangled stratagems for cancer treatment. Hence, a deep-rooted insight over the genuine situations as well as communications involved in the TME theatres a momentous responsibility for manufacturing the intelligent NPs. While as TME remains scrutinized from last several years, in what ways to scheme NPs and making the use of the TME remains yet in its beginning, besides there are numerous difficulties in order to design an efficient therapeutic NPs intended for the clinical cancer therapy.

TME constitutes a vibrant structure experiencing unambiguous amendments throughout cancer development commanding ultimately towards the metastatic spreading that remains the vital cause of death among the cancer patients. TME is made up of a cellular compartment that contains stromal fibroblasts, penetrating immune cells, the blood as well as lymphatic vascular networks, besides a non-cellular component comprising of ECM. Inside the TME all of its components support its propagation besides incursion of the tumour through yielding growth factors, chemokines, matrix-degrading enzymes as well as supporting tumour cells. A well thoughtful consideration of tumour-host cell communications, furthermore its cell-ECM communications, might assist in comprehending of the biological activity liable for tumour development thus improving the cancer therapies. Treatments which target the TME components carry a benefit comprising, prohibition of non-tumour cells which remain genetically steady in comparison to the tumour cells, that may advance diverse mutation throughout cancer development which is primarily blamable for drug resistance. As has been reported that cells might alter certain biological physiognomies whole being chosen by tumour cells since there happens to be a subtle equilibrium amongst their prohibitory action against tumour endorsing task. Classification of the biological variations so as to aim these fundamental molecular thespians in TEM is regarded as a significant step for anticancer treatment. Multitargeted methodologies, offering a concurrent prohibition of numerous TME constituents, might bid a supplementary competent towards the treatment of the cancer through by-passing such difficulties.

The TME-assisted nanotherapies depend deeply over feebly investigated contrivance of the TME. Though numerous over productive metabolites, for example, glucose, $H_2O_2$, as well as GSH were acknowledged, essential mechanism of their unambiguous expressions yet relics as ambiguous. Paralleled alongside ordinary tissues, solid tumour contains an exclusive microenvironment comprising vascular abnormalities, hypoxia, low pH, besides a compact tumour ECM, that was researched upon so as to formulate new-fangled therapeutic NPs. Variation as well as the utilization of the TME through NPs stands validated. Since cancer remains a multifaceted disease, a stratagem which pools different treatment functions jointly entertains palpable benefits on and over a single treatment method. As an example, a single NP drug delivery arrangement could be intended towards modulating the tumour pH as well as stimulating the oxygen concentration simultaneously. Its highly conceivable in order combining the pH responsive drug release with active dual targeting systems (For example RGD as well as transferrin). Its thought-provoking that certain multipurpose drug delivery techniques trait a large diameter of (100 nm) towards augmenting tumour vascular extravasation through EPR effect, besides consequently releasing trivial NPs inside the neighbourhood of the tumour to advance tumour infiltration. Accordingly, advance in the intelligent nanomaterials which exploit unique tumour traits might steer us towards a momentous advancement in NP founded cancer therapy.

While gaining the understanding of the therapeutic result of the TME-aided nanotherapies, it is found that disastrous effects against tumour cells remain significantly reliant on the nanoparticle buildups inside the tumour region, propelled by the EPR effect whereas small buildup efficacy of significantly lesser than 10% (through i.v. administration) through EPR effect saddens the scientific society. Approaches, for example, PEGylation, size/shape modulation, besides active targeting were used towards extending the particulate plasma circulation besides enhancing the tumour buildups, however, such profits linger restricted as well as less cost-effective. Thus, tactics for tumour build-up approaches along with

amplified EPR competence might donate such nanotherapies with considerably enriched drug bioavailability besides alleviating the nanoparticle administration. Insufficient destructive choosiness similarly hampers maturity of TME-aided nanotherapies. Though diminishing of the glucose nutrient in tumour nanotherapies might meaningfully quell the development as well as the propagation of tumour cells, meanwhile, still, the nutrient load adjoining tumour tissue could be aggravated, additionally prompting stern hostile bearings besides tumour metastasis. Furthermore, in trivial acidity-responsive nanotherapies, inconsistency of pH value amongst tumour tissue as well as ordinary tissues is somewhat insignificant, thus efficacy of trivial acidity-responsive nanotherapies is marginally little somewhat. Considering material perspective, logical strategy as well as a well-ordered production of exceedingly responsive or manifold responsive nanoplatforms demand to be unified so as to increase the tumour therapeutic choosiness among the destructive functioning of TME-aided nanotherapies. Lastly, further grave topographies in TME remain to be discovered and explored. For instance, as there is a plea for amino acids as well as the lipids of thriving tumour cells throughout reproductions. Obstructing ingestion of such species has been anticipated to hinder the propagation of tumour cells considerably. Furthermore, as we tumour cells remain bordered with enormous magnitude of immune cells for example dendritic cells, B cells, as well as T cells. Such immune cells are anticipated to disturb the TME in long-drawn-out physiognomies through delivering particular agents. Nevertheless, nanotherapies aided with such unique qualities in TME yet remain to be in infancy. Additional research has to be dedicated comprehensively towards maturing new-fangled characters of TME besides conforming TEM-aided nanotherapies.

Regarded as one of the fundamental trait of tumour, TME was documented as a vital target aimed at the designing of necessary theranostic approaches/modalities intended for fighting cancer. The occurrence as well as the profligate advance of nanomedicine additionally endorse the progress of the TME-responsive cancer theranostics. While there remains a number of precarious concerns and tasks have been presented in the TME-enabled nanotherapy, like advanced implementations besides predictable theranostic results have disclosed their extraordinary possibilities for additional clinical rendition, that remains to be vastly thought to carve a novel approach aimed at concurrently realizing the extraordinary theranostic functioning besides alleviating the injurious unexpected result on cancer treatment. In brief, our review deliberated upon exploiting of the TME through NPs in order to achieve cancer therapy. The exploitation of TME-sensitive NPs carries a potential in cancer therapy. Certainly, prodigious headway was previously made concerning this ambition. Preferably, a therapeutic NP structure must be capable of delivering payloads precisely to the tumour what is more be destroyed devoid of complex harmful effects to the body. Additionally, this work yet quietly proceeding towards developing a new-fangled NP structures particularly aimed at the TME.

## Acknowledgement

Financial supports from the National Natural Science Foundation of China (NSFC 51772059, 51602072, 51720105015, 51332008 and 51575528), the Projects for Science and Technology Development Plan of Jilin Province (20170414003GH and 20160101300JC), and the Fundamental Research funds for the Central Universities are greatly acknowledged.

## References

[1] D.F. Quail, J.A. Joyce, Nat. Med. 19 (2013) 1423–1437.
[2] F. Danhier, O. Feron, V. Preat, J. Control. Release 148 (2010) 135–146.
[3] Y. Huang, J. Yuan, E. Righi, W.S. Kamoun, M. Ancukiewicz, J. Nezivar, M. Santosuosso, J.D. Martin, M.R. Martin, F. Vianello, P. Leblanc, L.L. Munn, P. Huang, D.G. Duda, D. Fukumura, R.K. Jain, M.C. Poznansky, Proc. Natl. Acad. Sci. USA 109 (2012) 17561–17566.
[4] J.A. Joyce, D.T. Fearon, Science 348 (2015) 74–80.
[5] N. Chan, I.M. Pires, Z. Bencokova, C. Coackley, K.R. Luoto, N. Bhogal, M. Lakshman, P. Gottipati, F.J. Oliver, T. Helleday, E.M. Hammond, R.G. Bristow, Cancer Res. 70 (2010) 8045–8054.
[6] Y. Sun, J. Campisi, C. Higano, T.M. Beer, P. Porter, I. Coleman, L. True, P.S. Nelson, Nat. Med. 18 (2012) 1359–1368.
[7] T. Chanmee, P. Ontong, K. Konno, N. Itano, Cancers 6 (2014) 1670–1690.
[8] C.H. Chang, J. Qiu, D. O'Sullivan, M.D. Buck, T. Noguchi, J.D. Curtis, Q. Chen, M. Gindin, M.M. Gubin, G.J. van der Windt, E. Tonc, R.D. Schreiber, E.J. Pearce, E.L. Pearce, Cell 162 (2015) 1229–1241.
[9] G. Song, Y. Chen, C. Liang, X. Yi, J. Liu, X. Sun, S. Shen, K. Yang, Z. Liu, Adv. Mater. 28 (2016) 7143–7148.
[10] K. Hasegawa, A. Suetsugu, M. Nakamura, T. Matsumoto, T. Kunisada, M. Shimizu, S. Saji, H. Moriwaki, M. Bouvet, R.M. Hoffman, Anticancer Res. 36 (2016) 4443–4448.
[11] J. Kim, H.R. Cho, H. Jeon, D. Kim, C. Song, N. Lee, S.H. Choi, T. Hyeon, J. Am. Chem. Soc. 139 (2017) 10992–10995.
[12] W. Zhu, Z. Dong, T. Fu, J. Liu, Q. Chen, Y. Li, R. Zhu, L. Xu, Z. Liu, Adv. Funct. Mater. 26 (2016) 5490–5498.
[13] J. Yu, C. Yang, J. Li, Y. Ding, L. Zhang, M.Z. Yousaf, J. Lin, R. Pang, L. Wei, L. Xu, F. Sheng, C. Li, G. Li, L. Zhao, Y. Hou, Adv. Mater. 26 (2014) 4114–4120.
[14] T. Zander, M. Scheffler, L. Nogova, C. Kobe, W. Engel-Riedel, M. Hellmich, I. Papachristou, K. Toepelt, A. Draube, L. Heukamp, R. Buettner, Y.D. Ko, R.T. Ullrich, E. Smit, R. Boellaard, A.A. Lammertsma, M. Hallek, A.H. Jacobs, A. Schlesinger, K. Schulte, S. Querings, E. Stoelben, B. Neumaier, R.K. Thomas, M. Dietlein, J. Wolf, J. Clin. Oncol. 29 (2011) 1701–1708.
[15] J.J.G.X. Yang, I.J. Rowland, A. Javadi, S.A. Hurley, V.Z. Matson, D.A. Steeber, S. Gong, ACS Nano 4 (2010) 6805–6817.
[16] Z.-X.C.L.-S. Lin, J. Li, K.-M. Ke, S.-S. Guo, H.-H. Yang, G.-N. Chen, J. Mater. Chem. B 2 (2014) 1031–1037.
[17] Z.L.F. Kong, D. Luan, X. Liu, K. Xu, B. Tang, Anal. Chem. 88 (2016) 6450–6456.
[18] Q. Chen, C. Liang, X. Sun, J. Chen, Z. Yang, H. Zhao, L. Feng, Z. Liu, Proc. Natl. Acad. Sci. USA 114 (2017) 5343–5348.
[19] K. Kiyose, K. Hanaoka, D. Oushiki, T. Nakamura, M. Kajimura, M. Suematsu, H. Nishimatsu, T. Yamane, T. Terai, Y. Hirata, T. Nagano, J. Am. Chem. Soc. 132 (2010) 15846–15848.
[20] S. Zschaeck, R. Haase, N. Abolmaali, R. Perrin, K. Stutzer, S. Appold, J. Steinbach, J. Kotzerke, D. Zips, C. Richter, V. Gudziol, M. Krause, K. Zophel, M. Baumann, Acta Oncol. (Stockholm, Sweden) 54 (2015) 1355–1363.
[21] S.M. Weis, D.A. Cheresh, Nat. Med. 17 (2011) 1359–1370.
[22] N.E. Sounni, A. Noel, Clin. Chem. 59 (2013) 85–93.
[23] W. Yin, L. Yan, J. Yu, G. Tian, L. Zhou, X. Zheng, X. Zhang, Y. Yong, J. Li, Z. Gu, Y. Zhao, ACS Nano 8 (2014) 6922–6933.
[24] X. Qian, S. Shen, T. Liu, L. Cheng, Z. Liu, Nanoscale 7 (2015) 6380–6387.
[25] T. Liu, S. Shi, C. Liang, S. Shen, L. Cheng, C. Wang, X. Song, S. Goel, T.E. Barnhart, W. Cai, Z. Liu, ACS Nano 9 (2015) 950–960.
[26] T. Liu, C. Wang, W. Cui, H. Gong, C. Liang, X. Shi, Z. Li, B. Sun, Z. Liu, Nanoscale 6 (2014) 11219–11225.
[27] T. Liu, C. Wang, X. Gu, H. Gong, L. Cheng, X. Shi, L. Feng, B. Sun, Z. Liu, Adv. Mater. 26 (2014) 3433–3440.
[28] Y. Yong, L. Zhou, Z. Gu, L. Yan, G. Tian, X. Zheng, X. Liu, X. Zhang, J. Shi, W. Cong, W. Yin, Y. Zhao, Nanoscale 6 (2014) 10394–10403.
[29] L. Cheng, C. Yuan, S. Shen, X. Yi, H. Gong, K. Yang, Z. Liu, ACS Nano 9 (2015) 11090–11101.
[30] L. Cheng, S. Shen, S. Shi, Y. Yi, X. Wang, G. Song, K. Yang, G. Liu, T.E. Barnhart, W. Cai, Z. Liu, Adv. Funct. Mater. 26 (2016) 2185–2197.
[31] G. Song, C. Liang, X. Yi, Q. Zhao, L. Cheng, K. Yang, Z. Liu, Adv. Mater. 28 (2016) 2716–2723.
[32] D. Hanahan, R.A. Weinberg, Cell 144 (2011) 646–674.
[33] F. Chen, X. Zhuang, L. Lin, P. Yu, Y. Wang, Y. Shi, G. Hu, Y. Sun, BMC Med. 13 (2015) 45.
[34] M. Labelle, R.O. Hynes, Cancer Discov. 2 (2012) 1091–1099.
[35] H. Peinado, S. Lavotshkin, D. Lyden, Semin. Cncer Biol. 21 (2011) 139–146.
[36] J.J. Tomasek, G. Gabbiani, B. Hinz, C. Chaponnier, R.A. Brown, Nat. Rev. Mol. Cell. Biol. 3 (2002) 349–363.
[37] R. Kalluri, M. Zeisberg, Nat. Rev. Cancer 6 (2006) 392–401.
[38] A. Orimo, P.B. Gupta, D.C. Sgroi, F. Arenzana-Seisdedos, T. Delaunay, R. Naeem, V.J. Carey, A.L. Richardson, R.A. Weinberg, Cell 121 (2005) 335–348.
[39] M.G. Procopio, C. Laszlo, D. Al Labban, D.E. Kim, P. Bordignon, S.H. Jo, S. Goruppi, E. Menietti, P. Ostano, U. Ala, P. Provero, W. Hoetzenecker, V. Neel, W.W. Kilarski, M.A. Swartz, C. Brisken, K. Lefort, G.P. Dotto, Nat. Cell. Biol. 17 (2015) 1193–1204.
[40] A. Lochter, S. Galosy, J. Muschler, N. Freedman, Z. Werb, M.J. Bissell, J. Cell Biol. 139 (1997) 1861–1872.
[41] D.W. Powell, R.C. Mifflin, J.D. Valentich, S.E. Crowe, J.I. Saada, A.B. West, Am. J. Physiol. 277 (1999) C1–C9.
[42] I.V. Pinchuk, J.I. Saada, E.J. Beswick, G. Boya, S.M. Qiu, R.C. Mifflin, G.S. Raju, V.E. Reyes, D.W. Powell, Gastroenterology 135 (2008) 1228–1237, 1237.e1221-1222.
[43] K. Lee, C.M. Nelson, Int. Rev. Cell. Mol. Biol. 294 (2012) 171–221.
[44] A. Nawshad, D. Lagamba, A. Polad, E.D. Hay, Cells Tissues Organs 179 (2005) 11–23.

[45] A. Moustakas, C.H. Heldin, J. Cell. Sci. 118 (2005) 3573–3584.
[46] P. Carmeliet, Nat. Med. 9 (2003) 653–660.
[47] G.L. Wang, B.H. Jiang, E.A. Rue, G.L. Semenza, Proc. Natl. Acad. Sci. USA 92 (1995) 5510–5514.
[48] G.L. Semenza, Nat. Rev. Cancer 3 (2003) 721–732.
[49] S. Leoni, F. Piscaglia, I. Serio, E. Terzi, I. Pettinari, L. Croci, S. Marinelli, F. Benevento, R. Golfieri, L. Bolondi, Digest. Liver Dis. 46 (2014) 549–555.
[50] J.I. Bardos, M. Ashcroft, BioEssays 26 (2004) 262–269.
[51] F.M. Richards, Expert Rev. Mol. Med. 2001 (2001) 1–27.
[52] D.F. Higgins, K. Kimura, M. Iwano, V.H. Haase, Cell Cycle (Georgetown, Tex.) 7 (2008) 1128–1132.
[53] H.Y. Jung, L. Fattet, J. Yang, Clin. Cancer Res. 21 (2015) 962–968.
[54] D.J. Ceradini, A.R. Kulkarni, M.J. Callaghan, O.M. Tepper, N. Bastidas, M.E. Kleinman, J.M. Capla, R.D. Galiano, J.P. Levine, G.C. Gurtner, Nat. Med. 10 (2004) 858–864.
[55] G.O. Ahn, J.M. Brown, Angiogenesis 12 (2009) 159–164.
[56] R.N. Kaplan, B. Psaila, D. Lyden, Cancer Metast. Rev. 25 (2006) 521–529.
[57] J.M. Roodhart, M.H. Langenberg, J.S. Vermaat, M.P. Lolkema, A. Baars, R.H. Giles, E.O. Witteveen, E.E. Voest, Neoplasia (New York, N.Y.) 12 (2010) 87–94.
[58] G.T. Motz, G. Coukos, Nat. Rev. Immunol. 11 (2011) 702–711.
[59] C.H. Heldin, K. Rubin, K. Pietras, A. Ostman, Nat. Rev. Cancer 4 (2004) 806–813.
[60] D. Hanahan, L.M. Coussens, Cancer Cell 21 (2012) 309–322.
[61] A. Mantovani, P. Allavena, A. Sica, F. Balkwill, Nature 454 (2008) 436–444.
[62] L. Gamelin, O. Capitain, A. Morel, A. Dumont, S. Traore, B. Anne le, S. Gilles, M. Boisdron-Celle, E. Gamelin, Clin. Cancer. Res. 13 (2007) 6359–6368.
[63] L. Yang, Y. Pang, H.L. Moses, Trends. Immunol. 31 (2010) 220–227.
[64] E.J. Wherry, M. Kurachi, Nat. Rev. Immunol. 15 (2015) 486–499.
[65] A.C. Anderson, N. Joller, V.K. Kuchroo, Immunity 44 (2016) 989–1004.
[66] S.L. Topalian, C.G. Drake, D.M. Pardoll, Curr. Opin. Immunol. 24 (2012) 207–212.
[67] J. Galon, A. Costes, F. Sanchez-Cabo, A. Kirilovsky, B. Mlecnik, C. Lagorce-Pages, M. Tosolini, M. Camus, A. Berger, P. Wind, F. Zinzindohoue, P. Bruneval, P.H. Cugnenc, Z. Trajanoski, W.H. Fridman, F. Pages, Science 313 (2006) 1960–1964.
[68] C.S. Hinrichs, S.A. Rosenberg, Immunol. Rev. 257 (2014) 56–71.
[69] J.C. Becker, M.H. Andersen, D. Schrama, P. Thor Straten, Cancer Immunol. Immunother. 62 (2013) 1137–1148.
[70] J.M. Silva, M. Videira, R. Gaspar, V. Preat, H.F. Florindo, J. Control. Release 168 (2013) 179–199.
[71] Yoshiko Takeuchi, Hiroyoshi Nishikawa, Role of regulatory T cells in cancer immunity, Int. Immunol. 28 (2016) 401–409.
[72] R. Noy, J.W. Pollard, Immunity 41 (2014) 49–61.
[73] Y. Pei, Y. Yeo, J. Control. Release 240 (2016) 202–211.
[74] J. Cook, T. Hagemann, Curr. Opin. Pharmacol. 13 (2013) 595–601.
[75] B.Z. Qian, J.W. Pollard, Cell 141 (2010) 39–51.
[76] K. Palucka, J. Banchereau, Nat. Rev. Cancer 12 (2012) 265–277.
[77] G. Jego, A.K. Palucka, J.P. Blanck, C. Chalouni, V. Pascual, J. Banchereau, Immunity 19 (2003) 225–234.
[78] K.Q. Tran, J. Zhou, K.H. Durflinger, et al., J. Immunother. 31 (2008) 742–751.
[79] N. Kadowaki, S. Antonenko, S. Ho, M.C. Rissoan, V. Soumelis, S.A. Porcelli, L.L. Lanier, Y.J. Liu, J. Exp. Med. 193 (2001) 1221–1226.
[80] T.L. Whiteside, Springer, 2006, pp. 103–124.
[81] T. Kitamura, B.Z. Qian, J.W. Pollard, Nat. Rev. Immunol. 15 (2015) 73–86.
[82] P. Tsou, H. Katayama, E.J. Ostrin, S.M. Hanash, Cancer. Res. 76 (2016) 5597–5601.
[83] A.J. Gunderson, L.M. Coussens, Exp. Cell Res. 319 (2013) 1644–1649.
[84] D.I. Bellovin, B. Das, D.W. Felsher, Adv. Exp. Med. Biol. 734 (2013) 91–107.
[85] V. Kumar, S. Patel, E. Tcyganov, D.I. Gabrilovich, Trends Immunol. 37 (2016) 208–220.
[86] J.E. Talmadge, D.I. Gabrilovich, Nat. Rev. Cancer 13 (2013) 739–752.
[87] H. Katoh, M. Watanabe, Mediat. Inflamm. 2015 (2015) 159269.
[88] K. Hida, N. Maishi, D.A. Annan, Y. Hida, Int. J. Mol. Sci. 19 (2018) 1272.
[89] E. Vivier, S. Ugolini, D. Blaise, C. Chabannon, L. Brossay, Nat. Rev. Immunol. 12 (2012) 239–252.
[90] E. Vivier, D.H. Raulet, A. Moretta, M.A. Caligiuri, L. Zitvogel, L.L. Lanier, W.M. Yokoyama, S. Ugolini, Science 331 (2011) 44–49.
[91] M.J. Smyth, D.I. Godfrey, Nat. Immunol. 1 (2000) 459–460.
[92] A. Birbrair, T. Zhang, Z.M. Wang, M.L. Messi, A. Mintz, O. Delbono, Clin. Sci. 128 (2015) 81–93.
[93] A. Armulik, G. Genove, C. Betsholtz, Dev. Cell 21 (2011) 193–215.
[94] D. Keskin, J. Kim, V.G. Cooke, C.C. Wu, H. Sugimoto, C. Gu, M. De Palma, R. Kalluri, V.S. LeBleu, Cell Rep. 10 (2015) 1066–1081.
[95] C. Lu, M.M. Shahzad, M. Moreno-Smith, Y.G. Lin, N.B. Jennings, J.K. Allen, C.N. Landen, L.S. Mangala, G.N. Armaiz-Pena, R. Schmandt, A.M. Nick, R.L. Stone, R.B. Jaffe, R.L. Coleman, A.K. Sood, Cancer Biol. Ther. 9 (2010) 176–182.
[96] Y. Yonenaga, A. Mori, H. Onodera, S. Yasuda, H. Oe, A. Fujimoto, T. Tachibana, M. Imamura, Oncology 69 (2005) 159–166.
[97] C.A. Dumitru, H. Gholaman, S. Trellakis, K. Bruderek, N. Dominas, X. Gu, A. Bankfalvi, T.L. Whiteside, S. Lang, S. Brandau, Int. J. Cancer 129 (2011) 859–869.
[98] Y.C. Chong, G.H. Heppner, L.A. Paul, A.M. Fulton, Cancer Res. 49 (1989) 6652–6657.
[99] B. Amulic, C. Cazalet, G.L. Hayes, K.D. Metzler, A. Zychlinsky, Ann. Rev. Immunol. 30 (2012) 459–489.
[100] P. Lu, K. Takai, V.M. Weaver, Z. Werb, Cold spring harb, Perspect. Biol. 3 (2011).
[101] R.O. Hynes, Science 326 (2009) 1216–1219.
[102] W. Guo, F.G. Giancotti, Nat. Rev. Mol. Cell Biol. 5 (2004) 816–826.
[103] N. Ahmed, J. Niu, D.J. Dorahy, X. Gu, S. Andrews, C.J. Meldrum, R.J. Scott, M.S. Baker, I.G. Macreadie, M.V. Agrez, Oncogene 21 (2002) 1370–1380.
[104] M. Ferrari, Nat. Rev. Cancer 5 (2005) 161–171.
[105] R.K. Jain, T. Stylianopoulos, Nat. Rev. Clin. Oncol. 7 (2010) 653–664.
[106] P. Baluk, H. Hashizume, D.M. McDonald, Curr. Opin. Genet. Dev. 15 (2005) 102–111.
[107] J.A. Nagy, H.F. Dvorak, Clin. Exp. Metast. 29 (2012) 657–662.
[108] Y. Huang, T. Stylianopoulos, D.G. Duda, D. Fukumura, R.K. Jain, Cancer Res. 73 (2013) 7144–7146.
[109] B.B. Cerqueira, A. Lasham, A.N. Shelling, R. Al-Kassas, Eur. J. Pharm. Biopharm. 97 (2015) 140–151.
[110] V.P. Torchilin, Handb. Exp. Pharmacol. (2010) 3–53.
[111] V. Torchilin, Adv. Drug. Del. Rev. 63 (2011) 131–135.
[112] K. Greish, Methods Moll. Biol. 624 (2010) 25–37.
[113] H. Maeda, H. Nakamura, J. Fang, Adv. Drug. Deliv. Rev. 65 (2013) 71–79.
[114] M.K. Danquah, X.A. Zhang, R.I. Mahato, Adv. Drug. Deliv. Rev. 63 (2011) 623–639.
[115] V.P. Chauhan, T. Stylianopoulos, J.D. Martin, Z. Popovic, O. Chen, W.S. Kamoun, M.G. Bawendi, D. Fukumura, R.K. Jain, Nat. Nanotechnol. 7 (2012) 383–388.
[116] H. Meng, M. Xue, T. Xia, Z. Ji, D.Y. Tarn, J.I. Zink, A.E. Nel, ACS Nano 5 (2011) 4131–4144.
[117] P. Decuzzi, B. Godin, T. Tanaka, S.Y. Lee, C. Chiappini, X. Liu, M. Ferrari, J. Control. Release 141 (2010) 320–327.
[118] H. Kobayashi, R. Watanabe, P.L. Choyke, Theranostics 4 (2013) 81–89.
[119] C. Fu, T. Liu, L. Li, H. Liu, D. Chen, F. Tang, Biomaterials 34 (2013) 2565–2575.
[120] S.B.L.H.L. Kim, H.J. Jeong, D.W. Kim, RSC Adv. 4 (2014) 31318–31322.
[121] J.A. Champion, Y.K. Katare, S. Mitragotri, J. Control. Release 121 (2007) 3–9.
[122] X. Huang, L. Li, T. Liu, N. Hao, H. Liu, D. Chen, F. Tang, ACS Nano 5 (2011) 5390–5399.
[123] N.P. Truong, M.R. Whittaker, C.W. Mak, T.P. Davis, Exp. Opin. Drug. Deliv. 12 (2015) 129–142.
[124] P. Kolhar, A.C. Anselmo, V. Gupta, K. Pant, B. Prabhakarpandian, E. Ruoslahti, S. Mitragotri, Proc. Natl. Acad. Sci. USA 110 (2013) 10753–10758.
[125] D.A. Christian, S. Cai, O.B. Garbuzenko, T. Harada, A.L. Zajac, T. Minko, D.E. Discher, Mol. Pharma 6 (2009) 1343–1352.
[126] F. Alexis, E. Pridgen, L.K. Molnar, O.C. Farokhzad, Mol. Pharma 5 (2008) 505–515.
[127] S. Hirn, M. Semmler-Behnke, C. Schleh, A. Wenk, J. Lipka, M. Schaffler, S. Takenaka, W. Moller, G. Schmid, U. Simon, W.G. Kreyling, Eur. J. Pharm. Biopharma 77 (2011) 407–416.
[128] C. He, Y. Hu, L. Yin, C. Tang, C. Yin, Biomaterials 31 (2010) 3657–3666.
[129] N.M.O.B.-S.a.L.A, S. Lowe, Polym. Chem. 6 (2015) 198–212.
[130] R.P. Garay, R. El-Gewely, J.K. Armstrong, G. Garratty, P. Richette, Exp. Opin. Drug. Deliv. 9 (2012) 1319–1323.
[131] A. Abuchowski, T. van Es, N.C. Palczuk, F.F. Davis, J. Biolo. Chem. 252 (1977) 3578–3581.
[132] A. Abuchowski, J.R. McCoy, N.C. Palczuk, T. van Es, F.F. Davis, J. Biol. Chem. 252 (1977) 3582–3586.
[133] P. Kingshott, H. Thissen, H.J. Griesser, Biomaterials 23 (2002) 2043–2056.
[134] R. Gref, M. Luck, P. Quellec, M. Marchand, E. Dellacherie, S. Harnisch, T. Blunk, R.H. Muller, Colloids Surf. B Biointerfaces 18 (2000) 301–313.
[135] S. Jiang, Z. Cao, Adv. Mater. 22 (2010) 920–932.
[136] H. Amano, T. Ikeda, M. Toda, R. Okubo, T. Yabe, I. Watanabe, D. Saito, Int. Heart J. 57 (2016) 285–291.
[137] K. Yoshimoto, T. Hirase, J. Madsen, S.P. Armes, Y. Nagasaki, Macromol. Rapid Commun. 30 (2009) 2136–2140.
[138] B. Wang, T. Blin, A. Kakinen, X. Ge, E.H. Pilkington, J.F. Quinn, M.R. Whittaker, T.P. Davis, P.C. Ke, F. Ding, Polym. Chem. 7 (2016) 6875–6879.
[139] R.L. Chia-Chih Chang, C. Ryan, Hayward, Todd Emrick, Macromolecules 41 (2015) 7843–7850.
[140] S.L. Wei Yang, Tao Bai, Andrew J. Keefa, Lei Zhang, Jean-Rene-Menye, Yuting Li, Shaoyi Jiang, Nano Today (2014) 10–16.
[141] C.M. Hu, R.H. Fang, K.C. Wang, B.T. Luk, S. Thamphiwatana, D. Dehaini, P. Nguyen, P. Angsantikul, C.H. Wen, A.V. Kroll, C. Carpenter, M. Ramesh, V. Qu, S.H. Patel, J. Zhu, W. Shi, F.M. Hofman, T.C. Chen, W. Gao, K. Zhang, S. Chien, L. Zhang, Nature 526 (2015) 118–121.
[142] L. Gu, D.J. Mooney, Nat. Rev. Cancer 16 (2016) 56–66.
[143] W. Gao, C.M. Hu, R.H. Fang, B.T. Luk, J. Su, L. Zhang, Adv. Mater. 25 (2013) 3549–3553.
[144] R. Palomba, A. Parodi, M. Evangelopoulos, S. Acciardo, C. Corbo, E. de Rosa, I.K. Yazdi, S. Scaria, R. Molinaro, N.E. Furman, J. You, M. Ferrari, F. Salvatore, E. Tasciotti, Sci. Rep. 6 (2016) 34422.
[145] H. Sun, J. Su, Q. Meng, Q. Yin, L. Chen, W. Gu, P. Zhang, Z. Zhang, H. Yu, S. Wang, Y. Li, Adv. Mater. 28 (2016) 9581–9588.
[146] H. Maeda, Bioconjug. Chem. 21 (2010) 797–802.
[147] J.D. Byrne, T. Betancourt, L. Brannon-Peppas, Adv. Drug. Deliv. Rev. 60 (2008) 1615–1626.
[148] N. Bertrand, J. Wu, X. Xu, N. Kamaly, O.C. Farokhzad, Adv. Drug. Deliv. Rev. 66 (2014) 2–25.
[149] Y.H. Bae, K. Park, J. Control. Release 153 (2011) 198–205.
[150] G. Zhao, B.L. Rodriguez, Int. J. Nanomed. 8 (2013) 61–71.

[151] D.R. Senger, D.T. Connolly, L. Van de Water, J. Feder, H.F. Dvorak, Cancer Res. 50 (1990) 1774–1778.
[152] S. Goel, 6 (2014) 21677–21685.
[153] K. Chen, Z.B. Li, H. Wang, W. Cai, X. Chen, Eur. J. Nucl. Med. Mol. Imaging 35 (2008) 2235–2244.
[154] M.A. Abakumov, N.V. Nukolova, M. Sokolsky-Papkov, S.A. Shein, T.O. Sandalova, H.M. Vishwasrao, N.F. Grinenko, I.L. Gubsky, A.M. Abakumov, A.V. Kabanov, V.P. Chekhonin, Nanomedicine 11 (2015) 825–833.
[155] M.F. Hawthorne, Angew. Chem. Int. Ed. 32 (1993) 950–984.
[156] J.D. Hood, M. Bednarski, R. Frausto, S. Guccione, R.A. Reisfeld, R. Xiang, D.A. Cheresh, Science 296 (2002) 2404–2407.
[157] R.O. Hynes, Cell 69 (1992) 11–25.
[158] W. Cai, D.W. Shin, K. Chen, O. Gheysens, Q. Cao, S.X. Wang, S.S. Gambhir, X. Chen, Nano Lett. 6 (2006) 669–676.
[159] N. Graf, D.R. Bielenberg, N. Kolishetti, C. Muus, J. Banyard, O.C. Farokhzad, S.J. Lippard, ACS Nano 6 (2012) 4530–4539.
[160] M.S. Shive, J.M. Anderson, Adv. Drug. Deliv. Rev. 28 (1997) 5–24.
[161] J.C.X. Cun, S. Ruan, L. Zhang, J. Wan, Q. He, H. Gao, ACS Appl. Mater. Interfaces 7 (2015) 27458–27466.
[162] F. Chen, H. Hong, S. Goel, S.A. Graves, H. Orbay, E.B. Ehlerding, S. Shi, C.P. Theuer, R.J. Nickles, W. Cai, ACS Nano 9 (2015) 3926–3934.
[163] F. Yan, H. Wu, H. Liu, Z. Deng, H. Liu, W. Duan, X. Liu, H. Zheng, J. Control. Release 224 (2016) 217–228.
[164] S. Goel, F. Chen, H. Hong, H.F. Valdovinos, R. Hernandez, S. Shi, T.E. Barnhart, W. Cai, ACS Appl. Mater. Interfaces 6 (2014) 21677–21685.
[165] Z. Zhen, W. Tang, Y.J. Chuang, T. Todd, W. Zhang, X. Lin, G. Niu, G. Liu, L. Wang, Z. Pan, X. Chen, J. Xie, ACS Nano 8 (2014) 6004–6013.
[166] M. Schlesinger, G. Bendas, Int. J. Cancer 136 (2015) 2504–2514.
[167] N. Patel, B.A. Duffy, A. Badar, M.F. Lythgoe, E. Arstad, Bioconjug. Chem. 26 (2015) 1542–1549.
[168] S. Gosk, T. Moos, C. Gottstein, G. Bendas, Biochim. Biophys. Acta 1778 (2008) 854–863.
[169] Q. Chen, X.H. Zhang, J. Massague, Cancer Cell 20 (2011) 538–549.
[170] H. Cao, Z. Zhang, S. Zhao, X. He, H. Yu, Q. Yin, Z. Zhang, W. Gu, L. Chen, Y. Li, J. Control. Release 205 (2015) 162–171.
[171] X. He, H. Yu, X. Bao, H. Cao, Q. Yin, Z. Zhang, Y. Li, Adv. Healthc. Mater. 5 (2016) 439–448.
[172] R. Weissleder, Science 312 (2006) 1168–1171.
[173] M.A. Pysz, S.S. Gambhir, J.K. Willmann, Clin. Radiol. 65 (2010) 500–516.
[174] H.J. Kong, D.J. Mooney, Nat. Rev. Drug Discov. 6 (2007) 455–463.
[175] R.N. Kaplan, S. Rafii, D. Lyden, Cancer Res. 66 (2006) 11089–11093.
[176] N.L.A.L.K. Bell, S.H. Lee, J.R. Griffiths, NMR Biomed. 24 (2011) 612–635.
[177] M.F. Penet, B. Krishnamachary, Z. Chen, J. Jin, Z.M. Bhujwalla, Adv. Cancer Res. 124 (2014) 235–256.
[178] J.V. Frangioni, J. Clin. Oncol. 26 (2008) 4012–4021.
[179] Z. Zhou, Z.R. Lu, Wiley interdisciplinary reviews, Nanomed. Nanobiotechnol. 5 (2013) 1–18.
[180] M.L. James, S.S. Gambhir, Physiol. Rev. 92 (2012) 897–965.
[181] R. Cairns, I. Papandreou, N. Denko, Mol. Cancer Res. 4 (2006) 61–70.
[182] I.F. Tannock, D. Rotin, Cancer Res. 49 (1989) 4373–4384.
[183] X. Zhang, Y. Lin, R.J. Gillies, J. Nucl. Med. 51 (2010) 1167–1170.
[184] Y. Kato, S. Ozawa, C. Miyamoto, Y. Maehata, A. Suzuki, T. Maeda, Y. Baba, Cancer Cell Int. 13 (2013) 89.
[185] T.A.C.V. Estrella, M. Lloyd, J. Wojtkowiak, H.H. Cornnell, A. Ibrahim-Hashim, K. Bailey, Y. Balagurunathan, J.M. Rothberg, B.F. Sloane, J. Johnson, R.A. Gatenby, R.J. Gillies, Cancer Res. 73 (2013) 1524–1535.
[186] Y. Wang, K. Zhou, G. Huang, C. Hensley, X. Huang, X. Ma, T. Zhao, B.D. Sumer, R.J. DeBerardinis, J. Gao, Nat. Mater. 13 (2014) 204–212.
[187] M. Wang, Y. Wang, K. Hu, N. Shao, Y. Cheng, Biomater. Sci. 3 (2015) 480–489.
[188] K.S. Kim, W. Park, J. Hu, Y.H. Bae, K. Na, Biomaterials 35 (2014) 337–343.
[189] X. Wang, D. Niu, Q. Wu, S. Bao, T. Su, X. Liu, S. Zhang, Q. Wang, Biomaterials 53 (2015) 349–357.
[190] X. Ma, J. Am. Chem. Soc. 136 (2014) 11085–11092.
[191] K. Zhou, H. Liu, S. Zhang, X. Huang, Y. Wang, G. Huang, B.D. Sumer, J. Gao, J. Am. Chem. Soc. 134 (2012) 7803–7811.
[192] C. Wang, Y. Wang, Y. Li, B. Bodemann, T. Zhao, X. Ma, G. Huang, Z. Hu, R.J. DeBerardinis, M.A. White, J. Gao, Nat. Commun. 6 (2015) 8524.
[193] P. Mi, D. Kokuryo, H. Cabral, H. Wu, Y. Terada, T. Saga, I. Aoki, N. Nishiyama, K. Kataoka, Nat. Nanotechnol. 11 (2016) 724–730.
[194] V.S. Lelyveld, E. Brustad, F.H. Arnold, A. Jasanoff, J. Am. Chem. Soc. 133 (2011) 649–651.
[195] A. Bertin, A.-I. Michou-Gallani, J.-L. Gallani, D. Felder-Flesch, Toxicol. In Vitro 24 (2010) 1386–1394.
[196] K. Ruan, G. Song, G. Ouyang, J. Cell. Biochem. 107 (2009) 1053–1062.
[197] P. Vaupel, L. Harrison, Oncologist 9 (Suppl 5) (2004) 4–9.
[198] Y. Kim, Q. Lin, P.M. Glazer, Z. Yun, Curr. Mol. Med. 9 (2009) 425–434.
[199] N. Rohwer, T. Cramer, Drug Resist. Updates 14 (2011) 191–201.
[200] B.A. Teicher, Cancer Metast. Rev. 13 (1994) 139–168.
[201] J.M. Brown, W.R. Wilson, Nat. Rev. Cancer 4 (2004) 437–447.
[202] M.R. Horsman, L.S. Mortensen, J.B. Petersen, M. Busk, J. Overgaard, Nat. Rev. Clin. Oncol. 9 (2012) 674–687.
[203] X.-d. Wang, O.S. Wolfbeis, Chem. Soc. Rev. 43 (2014) 3666–3761.
[204] H. Xiang, J. Cheng, X. Ma, X. Zhou, J.J. Chruma, Chem. Soc. Rev. 42 (2013) 6128–6185.
[205] M.-M. Wu, J.-Y. Wang, R. Sun, C. Zhao, J.-P. Zhao, G.-B. Che, F.-C. Liu, Inorg. Chem. 56 (2017) 9555–9562.
[206] V. Mirabello, F. Cortezon-Tamarit, S.I. Pascu, Front. Chem. 6 (2018).
[207] J. Napp, T. Behnke, L. Fischer, C. Wurth, M. Wottawa, D.M. Katschinski, F. Alves, U. Resch-Genger, M. Schaferling, Anal. Chem. 83 (2011) 9039–9046.
[208] S. Kizaka-Kondoh, H. Konse-Nagasawa, Cancer Sci. 100 (2009) 1366–1373.
[209] E. McCormack, E. Silden, R.M. West, T. Pavlin, D.R. Micklem, J.B. Lorens, B.E. Haug, M.E. Cooper, B.T. Gjertsen, Cancer Res. 73 (2013) 1276–1286.
[210] J. Zhang, H.W. Liu, X.X. Hu, J. Li, L.H. Liang, X.B. Zhang, W. Tan, Anal. Chem. 87 (2015) 11832–11839.
[211] Y. Li, Y. Sun, J. Li, Q. Su, W. Yuan, Y. Dai, C. Han, Q. Wang, W. Feng, F. Li, J. Am. Chem. Soc. 137 (2015) 6407–6416.
[212] K. Okuda, Y. Okabe, T. Kadonosono, T. Ueno, B.G. Youssif, S. Kizaka-Kondoh, H. Nagasawa, Bioconjug. Chem. 23 (2012) 324–329.
[213] K. Tanabe, N. Hirata, H. Harada, M. Hiraoka, S. Nishimoto, Chembiochem 9 (2008) 426–432.
[214] S.M. Ehsan, K.M. Welch-Reardon, M.L. Waterman, C.C.W. Hughes, S.C. George, Integr. Biol. 6 (2014) 603–610.
[215] B.J. Vakoc, R.M. Lanning, J.A. Tyrrell, T.P. Padera, L.A. Bartlett, T. Stylianopoulos, L.L. Munn, G.J. Tearney, D. Fukumura, R.K. Jain, B.E. Bouma, Nat. Med. 15 (2009) 1219–1223.
[216] G. Zhang, Nat. Mater. 8 (2009) 747–751.
[217] S.M. Albelda, C.A. Buck, FASEB J. 4 (1990) 2868–2880.
[218] M. Tan, Z.R. Lu, Theranostics 1 (2011) 83–101.
[219] A.J. Beer, H. Kessler, H.J. Wester, M. Schwaiger, Theranostics 1 (2011) 48–57.
[220] Z. Liu, H. Liu, T. Ma, X. Sun, J. Shi, B. Jia, Y. Sun, J. Zhan, H. Zhang, Z. Zhu, F. Wang, J. Nucl. Med. 55 (2014) 989–994.
[221] C. Zhang, M. Jugold, E.C. Woenne, T. Lammers, B. Morgenstern, M.M. Mueller, H. Zentgraf, M. Bock, M. Eisenhut, W. Semmler, F. Kiessling, Cancer Res. 67 (2007) 1555–1562.
[222] Z. Cheng, Y. Wu, Z. Xiong, S.S. Gambhir, X. Chen, Bioconjug. Chem. 16 (2005) 1433–1441.
[223] C.R. Anderson, J.J. Rychak, M. Backer, J. Backer, K. Ley, A.L. Klibanov, Invest. Radiol. 45 (2010) 579–585.
[224] Y. Zhang, Y. Yang, W. Cai, Theranostics 1 (2011) 135–148.
[225] D.A. Sipkins, D.A. Cheresh, M.R. Kazemi, L.M. Nevin, M.D. Bednarski, K.C. Li, Nat. Med. 4 (1998) 623–626.
[226] F. Danhier, A. Le Breton, V. Preat, Mol. Pharma 9 (2012) 2961–2973.
[227] I. Dijkgraaf, A.Y. Rijnders, A. Soede, A.C. Dechesne, G.W. van Esse, A.J. Brouwer, F.H. Corstens, O.C. Boerman, D.T. Rijkers, R.M. Liskamp, Org. Biomol. Chem. 5 (2007) 935–944.
[228] Z.H. Jin, V. Josserand, S. Foillard, D. Boturyn, P. Dumy, M.C. Favrot, J.L. Coll, Mol. Cancer 6 (2007) 41.
[229] C.R. Anderson, X. Hu, H. Zhang, J. Tlaxca, A.E. Decleves, R. Houghtaling, K. Sharma, M. Lawrence, K.W. Ferrara, J.J. Rychak, Invest. Radiol. 46 (2011) 215–224.
[230] P.M. Peiris, R. Toy, E. Doolittle, J. Pansky, A. Abramowski, M. Tam, P. Vicente, E. Tran, E. Hayden, A. Camann, A. Mayer, B.O. Erokwu, Z. Berman, D. Wilson, H. Baskaran, C.A. Flask, R.A. Keri, E. Karathanasis, ACS Nano 6 (2012) 8783–8795.
[231] J.A. Park, J.Y. Kim, Y.J. Lee, W. Lee, S.M. Lim, T.J. Kim, J. Yoo, Y. Chang, K.M. Kim, ACS Med. Chem. Lett. 4 (2013) 216–219.
[232] Z. Zhou, Z. Han, Z.R. Lu, Biomaterials 85 (2016) 168–179.
[233] S. Hernot, S. Unnikrishnan, Z. Du, T. Shevchenko, B. Cosyns, A. Broisat, J. Toczek, V. Caveliers, S. Muyldermans, T. Lahoutte, A.L. Klibanov, N. Devoogdt, J. Control. Release 158 (2012) 346–353.
[234] S. Serres, M.S. Soto, A. Hamilton, M.A. McAteer, W.S. Carbonell, M.D. Robson, O. Ansorge, A. Khrapitchev, C. Bristow, L. Balathasan, T. Weissensteiner, D.C. Anthony, R.P. Choudhury, R.J. Muschel, N.R. Sibson, Proc. Natl. Acad. Sci. USA 109 (2012) 6674–6679.
[235] A.J. Beer, M. Schwaiger, Cancer Metast. Rev. 27 (2008) 631–644.
[236] C. Heyn, J.A. Ronald, S.S. Ramadan, J.A. Snir, A.M. Barry, L.T. MacKenzie, D.J. Mikulis, D. Palmieri, J.L. Bronder, P.S. Steeg, T. Yoneda, I.C. MacDonald, A.F. Chambers, B.K. Rutt, P.J. Foster, Magn. Reson. Med. 56 (2006) 1001–1010.
[237] N. Singh, G.J.S. Jenkins, R. Asadi, S.H. Doak, Nano Rev. 1 (2010).
[238] R.A. Heesakkers, A.M. Hovels, G.J. Jager, H.C. van den Bosch, J.A. Witjes, H.P. Raat, J.L. Severens, E.M. Adang, C.H. van der Kaa, J.J. Futterer, J. Barentsz, Lancet Oncol. 9 (2008) 850–856.
[239] L.M. Ellis, D.J. Hicklin, Nat. Rev. Cancer 8 (2008) 579–591.
[240] T. Voron, O. Colussi, E. Marcheteau, S. Pernot, M. Nizard, A.L. Pointet, S. Latreche, S. Bergaya, N. Benhamouda, C. Tanchot, C. Stockmann, P. Combe, A. Berger, F. Zinzindohoue, H. Yagita, E. Tartour, J. Taieb, M. Terme, J. Exp. Med. 212 (2015) 139–148.
[241] R.T.P. Poon, S.T. Fan, J. Wong, J. Clin. Oncol. 19 (2001) 1207–1225.
[242] N. Ferrara, K.J. Hillan, H.P. Gerber, W. Novotny, Nat. Rev. Drug Discov. 3 (2004) 391–400.
[243] M. Zangari, E. Anaissie, A. Stopeck, A. Morimoto, N. Tan, J. Lancet, M. Cooper, A. Hannah, G. Garcia-Manero, S. Faderl, H. Kantarjian, J. Cherrington, M. Albitar, F.J. Giles, Clin. Cancer Res. 10 (2004) 88–95.
[244] M.A. Deri, B.M. Zeglis, L.C. Francesconi, J.S. Lewis, Nucl. Med. Biol. 40 (2013) 3–14.
[245] H. Hong, F. Chen, Y. Zhang, W. Cai, Adv. Drug Deliv. Rev. 76 (2014) 2–20.
[246] A.G. Terwisscha van Scheltinga, G.M. van Dam, W.B. Nagengast, V. Ntziachristos, H. Hollema, J.L. Herek, C.P. Schroder, J.G. Kosterink, M.N. Lub-de Hoog, E.G. de Vries, J. Nucl. Med. 52 (2011) 1778–1785.
[247] M.V. Backer, Z. Levashova, V. Patel, B.T. Jehning, K. Claffey, F.G. Blankenberg, J.M. Backer, Nat. Med. 13 (2007) 504–509.

[248] M. Wuest, A. Perreault, J. Kapty, S. Richter, C. Foerster, C. Bergman, J. Way, J. Mercer, F. Wuest, Nucl. Med. Biol. 42 (2015) 864–874.
[249] H. Zhou, J.H. Stafford, R.R. Hallac, L. Zhang, G. Huang, R.P. Mason, J. Gao, P.E. Thorpe, D. Zhao, J. Biomed. Nanotechnol. 10 (2014) 846–855.
[250] L. Zhang, H. Zhou, O. Belzile, P. Thorpe, D. Zhao, J. Control. Release 183 (2014) 114–123.
[251] G.K. Feng, R.B. Liu, M.Q. Zhang, X.X. Ye, Q. Zhong, Y.F. Xia, M.Z. Li, J. Wang, E.W. Song, X. Zhang, Z.Z. Wu, M.S. Zeng, J. Control. Release 192 (2014) 236–242.
[252] H. Zhang, S. Tam, E.S. Ingham, L.M. Mahakian, C.Y. Lai, S.K. Tumbale, T. Teesalu, N.E. Hubbard, A.D. Borowsky, K.W. Ferrara, Biomaterials 56 (2015) 104–113.
[253] H. Wu, H. Chen, D. Pan, Y. Ma, S. Liang, Y. Wan, Y. Fang, Mol. Imaging Biol. 16 (2014) 781–792.
[254] P. Prasad, C.R. Gordijo, A.Z. Abbasi, A. Maeda, A. Ip, A.M. Rauth, R.S. DaCosta, X.Y. Wu, ACS Nano 8 (2014) 3202–3212.
[255] C. Liu, H. Dong, N. Wu, Y. Cao, X. Zhang, ACS Appl. Mater. Interfaces 10 (2018) 6991–7002.
[256] Y. Ikeda, H. Hisano, Y. Nishikawa, Y. Nagasaki, Mol. Pharma 13 (2016) 2283–2289.
[257] D.M. Gilkes, G.L. Semenza, D. Wirtz, Nat. Rev. Cancer 14 (2014) 430–439.
[258] D. Samanta, D.M. Gilkes, P. Chaturvedi, L. Xiang, G.L. Semenza, Proc. Natl. Acad. Sci. USA 111 (2014) E5429–E5438.
[259] I. Moen, L.E. Stuhr, Target. Oncol. 7 (2012) 233–242.
[260] Y.L. Chen, Y.N. Zhang, Z.Z. Wang, W.G. Xu, R.P. Li, J.D. Zhang, Brain Res. 1635 (2016) 180–189.
[261] Z. Luo, M. Zheng, P. Zhao, Z. Chen, F. Siu, P. Gong, G. Gao, Z. Sheng, C. Zheng, Y. Ma, L. Cai, Sci. Rep. 6 (2016) 23393.
[262] Z. Dong, L. Feng, W. Zhu, X. Sun, M. Gao, H. Zhao, Y. Chao, Z. Liu, Biomaterials 110 (2016) 60–70.
[263] X. Song, L. Feng, C. Liang, K. Yang, Z. Liu, Nano Lett. 16 (2016) 6145–6153.
[264] T. Sun, Y.S. Zhang, B. Pang, D.C. Hyun, M. Yang, Y. Xia, Angew. Chem. Int. Ed. 53 (2014) 12320–12364.
[265] L. Rao, L.L. Bu, B. Cai, J.H. Xu, A. Li, W.F. Zhang, Z.J. Sun, S.S. Guo, W. Liu, T.H. Wang, X.Z. Zhao, Adv. Mater. 28 (2016) 3460–3466.
[266] Y. Zhai, J. Su, W. Ran, P. Zhang, Q. Yin, Z. Zhang, H. Yu, Y. Li, Theranostics 7 (2017) 2575–2592.
[267] Q. Hu, C. Qian, W. Sun, J. Wang, Z. Chen, H.N. Bomba, H. Xin, Q. Shen, Z. Gu, Adv. Mater. 28 (2016) 9573–9580.
[268] H. Tian, Z. Luo, L. Liu, M. Zheng, Z. Chen, A. Ma, R. Liang, Z. Han, C. Lu, L. Cai, Adv. Funct. Mater. (2017) 1703197.
[269] A. Gulzar, J. Xu, D. Yang, L. Xu, F. He, S. Gai, P. Yang, Dalton Trans. 47 (2018) 3931–3939.
[270] A. Casas, G. Di Venosa, T. Hasan, B. Al, Curr. Med. Chem. 18 (2011) 2486–2515.
[271] Z. Zhou, J. Song, L. Nie, X. Chen, Chem. Soc. Rev. 45 (2016) 6597–6626.
[272] V.H. Fingar, P.K. Kik, P.S. Haydon, P.B. Cerrito, M. Tseng, E. Abang, T.J. Wieman, Br. J. Cancer 79 (1999) 1702–1708.
[273] J.T. Erler, K.L. Bennewith, M. Nicolau, N. Dornhofer, C. Kong, Q.T. Le, J.T. Chi, S.S. Jeffrey, A.J. Giaccia, Nature 440 (2006) 1222–1226.
[274] Y. Wang, Y. Xie, J. Li, Z.H. Peng, Y. Sheinin, J. Zhou, D. Oupický, ACS Nano 11 (2017) 2227–2238.
[275] T.I. Simsek, Y. Deniz, T. Abdurrahman, G. Gurcan, A.E.U, Angew. Chem. Int. Ed. 55 (2016) 2875–2878.
[276] Y. Cheng, H. Cheng, C. Jiang, X. Qiu, K. Wang, W. Huan, A. Yuan, J. Wu, Y. Hu, Nat. Commun. 6 (2015) 8785.
[277] C.I. Castro, J.C. Briceno, Artif. Organs 34 (2010) 622–634.
[278] Y. Que, Y. Liu, W. Tan, C. Feng, P. Shi, Y. Li, H. Xiaoyu, ACS Macro Lett. 5 (2016) 168–173.
[279] J. Liu, P. Du, H. Mao, L. Zhang, H. Ju, J. Lei, Biomaterials 172 (2018) 83–91.
[280] Z. Pengfei, Z. Mingbin, L. Zhenyu, F. Xiujun, S. Zonghai, G. Ping, C. Ze, Z. Baozhen, N. Dapeng, M. Yifan, C. Lintao, Adv. Healthc. Mater. 5 (2016) 2161–2167.
[281] L.H. Liu, Y.H. Zhang, W.X. Qiu, L. Zhang, F. Gao, B. Li, L. Xu, J.X. Fan, Z.H. Li, X.Z. Zhang, Small 13 (2017).
[282] A.M. Shannon, D.J. Bouchier-Hayes, C.M. Condron, D. Toomey, Cancer Treat. Rev. 29 (2003) 297–307.
[283] J. Jiang, C. Auchinvole, K. Fisher, C.J. Campbell, Nanoscale 6 (2014) 12104–12110.
[284] L.-H. Liu, W.-X. Qiu, Y.-H. Zhang, B. Li, C. Zhang, F. Gao, L. Zhang, X.-Z. Zhang, Adv. Funct. Mater. (2017) 1700220.
[285] C.C. Huang, W.T. Chia, M.F. Chung, K.J. Lin, C.W. Hsiao, C. Jin, W.H. Lim, C.C. Chen, H.W. Sung, J. Am. Chem. Soc. 138 (2016) 5222–5225.
[286] W. Fan, W. Bu, B. Shen, Q. He, Z. Cui, Y. Liu, X. Zheng, K. Zhao, J. Shi, Adv. Mater. 27 (2015) 4155–4161.
[287] T. Thambi, V.G. Deepagan, H.Y. Yoon, H.S. Han, S.H. Kim, S. Son, D.G. Jo, C.H. Ahn, Y.D. Suh, K. Kim, I.C. Kwon, D.S. Lee, J.H. Park, Biomaterials 35 (2014) 1735–1743.
[288] Q. Lin, C. Bao, Y. Yang, Q. Liang, D. Zhang, S. Cheng, L. Zhu, Adv. Mater. 25 (2013) 1981–1986.
[289] H. Liu, Y. Xie, Y. Zhang, Y. Cai, B. Li, H. Mao, R. Yu, RSC Adv. 6 (2016) 113933–113939.
[290] B.W. Henderson, V.H. Fingar, Cancer Res. 47 (1987) 3110–3114.
[291] C. Qian, J. Yu, Y. Chen, Q. Hu, X. Xiao, W. Sun, C. Wang, P. Feng, Q.D. Shen, Z. Gu, Adv. Mater. 28 (2016) 3313–3320.
[292] C. Zhang, K. Zhao, W. Bu, D. Ni, Y. Liu, J. Feng, J. Shi, Angew. Chem. Int. Ed. 54 (2015) 1770–1774.
[293] Z.S. Wu, L. Chen, J. Liu, K. Parvez, H. Liang, J. Shu, H. Sachdev, R. Graf, X. Feng, K. Mullen, Adv. Mater. 26 (2014) 1450–1455.
[294] H. Tian, Z. Luo, L. Liu, M. Zheng, Z. Chen, A. Ma, R. Liang, Z. Han, C. Lu, L. Cai, Adv. Funct. Mater. 27 (2017) 1703197.
[295] H. Wu, Z. Ding, D. Hu, F. Sun, C. Dai, J. Xie, X. Hu, J. Pathol. 227 (2012) 189–199.
[296] R.J. DeBerardinis, A. Mancuso, E. Daikhin, I. Nissim, M. Yudkoff, S. Wehrli, C.B. Thompson, Proc. Natl. Acad. Sci. USA 104 (2007) 19345–19350.
[297] J. Chiche, M.C. Brahimi-Horn, J. Pouyssegur, J. Cell. Mol. Med. 14 (2010) 771–794.
[298] P. Swietach, A. Hulikova, R.D. Vaughan-Jones, A.L. Harris, Oncogene 29 (2010) 6509–6521.
[299] A.P. Halestrap, M.C. Wilson, IUBMB Life 64 (2012) 109–119.
[300] F.A. Gallagher, M.I. Kettunen, S.E. Day, D.E. Hu, J.H. Ardenkjaer-Larsen, R. Zandt, P.R. Jensen, M. Karlsson, K. Golman, M.H. Lerche, K.M. Brindle, Nature 453 (2008) 940–943.
[301] G. Xihui, Y. Qi, L. Zining, K. Mengjing, Z. Xingyu, L. Sihan, Z. Jianping, Z. Ren, C. Liang, M. Ying, L. Cong, Adv. Mater. 29 (2017) 1603917.
[302] Y. Chen, D. Ye, M. Wu, H. Chen, L. Zhang, J. Shi, L. Wang, Adv. Mater. 26 (2014) 7019–7026.
[303] A. Gulzar, J. Xu, L. Xu, P. Yang, F. He, D. Yang, G. An, M.B. Ansari, Dalton Trans. 47 (2018) 3921–3930.
[304] C. Zhang, W. Bu, D. Ni, C. Zuo, C. Cheng, Q. Li, L. Zhang, Z. Wang, J. Shi, J. Am. Chem. Soc. 138 (2016) 8156–8164.
[305] T.E. Barnhart.
[306] C. Lotz, D.K. Kelleher, B. Gassner, M. Gekle, P. Vaupel, O. Thews, Oncol. Rep. 17 (2007) 239–244.
[307] E.K. Rofstad, B. Mathiesen, K. Kindem, K. Galappathi, Cancer Res. 66 (2006) 6699–6707.
[308] A. Som, R. Raliya, L. Tian, W. Akers, J.E. Ippolito, S. Singamaneni, P. Biswas, S. Achilefu, Nanoscale 8 (2016) 12639–12647.
[309] F. Pittella, K. Miyata, Y. Maeda, T. Suma, S. Watanabe, Q. Chen, R.J. Christie, K. Osada, N. Nishiyama, K. Kataoka, J. Control. Release 161 (2012) 868–874.
[310] J. Li, Y.C. Chen, Y.C. Tseng, S. Mozumdar, L. Huang, J. Control. Release 142 (2010) 416–421.
[311] S. Chun-Yang, L. Yang, D. Jin-Zhi, C. Zhi-Ting, X. Cong-Fei, W. Jun, Angew. Chem. Int. Ed. 55 (2016) 1010–1014.
[312] H.J. Li, J.Z. Du, X.J. Du, C.F. Xu, C.Y. Sun, H.X. Wang, Z.T. Cao, X.Z. Yang, Y.H. Zhu, S. Nie, J. Wang, Proc. Natl. Acad. Sci. USA 113 (2016) 4164–4169.
[313] T. Mizuhara, K. Saha, D.F. Moyano, C.S. Kim, B. Yan, Y.K. Kim, V.M. Rotello, Angew. Chem. Int. Ed. 54 (2015) 6567–6570.
[314] H.S. Sundaram, J.-R. Ella-Menye, N.D. Brault, Q. Shao, S. Jiang, Chem. Sci. 5 (2014) 200–205.
[315] Q. Jin, J.-P. Xu, J. Ji, J.-C. Shen, Chem. Commun. (2008) 3058–3060.
[316] E.S. Lee, H.J. Shin, K. Na, Y.H. Bae, J. Control. Release 90 (2003) 363–374.
[317] K. Zhou, Y. Wang, X. Huang, K. Luby-Phelps, B.D. Sumer, J. Gao, Angew. Chem. Int. Ed. 50 (2011) 6109–6114.
[318] R.A. Cairns, I.S. Harris, T.W. Mak, Nat. Rev. Cancer 11 (2011) 85–95.
[319] C. Gorrini, I.S. Harris, T.W. Mak, Nat. Rev. Drug Discov. 12 (2013) 931–947.
[320] M. Lopez-Lazaro, Cancer Lett. 252 (2007) 1–8.
[321] J.A. Cook, D. Gius, D.A. Wink, M.C. Krishna, A. Russo, J.B. Mitchell, Semin. Radiat. Oncol. 14 (2004) 259–266.
[322] P.D. Ray, B.W. Huang, Y. Tsuji, Cell. Signal 24 (2012) 981–990.
[323] L.B. Sullivan, N.S. Chandel, Cancer Metab. 2 (2014) 17.
[324] F. Muhammad, A. Wang, L. Miao, P. Wang, Q. Li, J. Liu, J. Du, G. Zhu, Langmuir 31 (2015) 514–521.
[325] X. Ma, A.C. Hortelao, T. Patino, S. Sanchez, ACS Nano 10 (2016) 9111–9122.
[326] H. Chen, J. Tian, W. He, Z. Guo, J. Am. Chem. Soc. 137 (2015) 1539–1547.
[327] Z. Jin, Y. Wen, L. Xiong, T. Yang, P. Zhao, L. Tan, T. Wang, Z. Qian, B.-L. Su, Q. He, Chem. Commun. 53 (2017) 5557–5560.
[328] F.Q. Schafer, G.R. Buettner, Free. Radic. Biol. Med. 30 (2001) 1191–1212.
[329] H.J. Kim, A. Kim, K. Miyata, K. Kataoka, Adv. Drug. Deliv. Rev. 104 (2016) 61–77.
[330] L. Yu, Y. Chen, H. Lin, W. Du, H. Chen, J. Shi, Biomaterials 161 (2018) 292–305.
[331] P. Huang, Y. Chen, H. Lin, L. Yu, L. Zhang, L. Wang, Y. Zhu, J. Shi, Biomaterials 125 (2017) 23–37.
[332] A. Naba, K.R. Clauser, S. Hoersch, H. Liu, S.A. Carr, R.O. Hynes, Mol. Cell. Proteomics 11 (2012), M111.014647.
[333] C. Ricciardelli, R.J. Rodgers, Semin Reprod. Med. 24 (2006) 270–282.
[334] S. Barua, S. Mitragotri, Nano Today 9 (2014) 223–243.
[335] H. Gong, Y. Chao, J. Xiang, X. Han, G. Song, L. Feng, J. Liu, G. Yang, Q. Chen, Z. Liu, Nano Lett. 16 (2016) 2512–2521.
[336] H. Zhou, Z. Fan, J. Deng, P.K. Lemons, D.C. Arhontoulis, W.B. Bowne, H. Cheng, Nano Lett. 16 (2016) 3268–3277.
[337] K.P. Olive, M.A. Jacobetz, C.J. Davidson, A. Gopinathan, D. McIntyre, D. Honess, B. Madhu, M.A. Goldgraben, M.E. Caldwell, D. Allard, K.K. Frese, G. Denicola, C. Feig, C. Combs, S.P. Winter, H. Ireland-Zecchini, S. Reichelt, W.J. Howat, A. Chang, M. Dhara, L. Wang, F. Ruckert, R. Grutzmann, C. Pilarsky, K. Izeradjene, S.R. Hingorani, P. Huang, S.E. Davies, W. Plunkett, M. Egorin, R.H. Hruban, N. Whitebread, K. McGovern, J. Adams, C. Iacobuzio-Donahue, J. Griffiths, D.A. Tuveson, Science 324 (2009) 1457–1461.
[338] M.G. Slomiany, L. Dai, P.A. Bomar, T.J. Knackstedt, D.A. Kranc, L. Tolliver, B.L. Maria, B.P. Toole, Cancer Res. 69 (2009) 4992–4998.

[339] C. Yang, Y. Liu, Y. He, Y. Du, W. Wang, X. Shi, F. Gao, Biomaterials 34 (2013) 6829–6838.
[340] K.L. Lee, K.L. Albee, R.J. Bernasconi, T. Edmunds, Biochem. J. 327 (Pt 1) (1997) 199–202.
[341] A. Parodi, S.G. Haddix, N. Taghipour, S. Scaria, F. Taraballi, A. Cevenini, I.K. Yazdi, C. Corbo, R. Palomba, S.Z. Khaled, J.O. Martinez, B.S. Brown, L. Isenhart, E. Tasciotti, ACS Nano 8 (2014) 9874–9883.
[342] T.D. McKee, P. Grandi, W. Mok, G. Alexandrakis, N. Insin, J.P. Zimmer, M.G. Bawendi, Y. Boucher, X.O. Breakefield, R.K. Jain, Cancer Res. 66 (2006) 2509–2513.
[343] T.T. Goodman, P.L. Olive, S.H. Pun, Int. J. Nanomed. 2 (2007) 265–274.
[344] S.J. Kuhn, S.K. Finch, D.E. Hallahan, T.D. Giorgio, Nano Lett. 6 (2006) 306–312.
[345] M.R. Villegas, A. Baeza, M. Vallet-Regi, ACS Appl. Mater. Interfaces 7 (2015) 24075–24081.
[346] L.M. Coussens, B. Fingleton, L.M. Matrisian, Science 295 (2002) 2387–2392.
[347] S. Kummar, M. Raffeld, L. Juwara, Y. Horneffer, A. Strassberger, D. Allen, S.M. Steinberg, A. Rapisarda, S.D. Spencer, W.D. Figg, X. Chen, I.B. Turkbey, P. Choyke, A.J. Murgo, J.H. Doroshow, G. Melillo, Clin. Cancer Res. 17 (2011) 5123–5131.
[348] J. Mateo, J. Berlin, J.S. de Bono, R.B. Cohen, V. Keedy, G. Mugundu, L. Zhang, A. Abbattista, C. Davis, C. Gallo Stampino, H. Borghaei, Cancer Chemother. Pharmacol. 74 (2014) 1039–1046.
[349] B. Besse, L.C. Tsao, D.T. Chao, Y. Fang, J.C. Soria, S. Almokadem, C.P. Belani, Ann. Oncol. 24 (2013) 90–96.
[350] J. Couzin-Frankel, Science 342 (2013) 1432–1433.
[351] H. Tang, J. Qiao, Y.X. Fu, Cancer Lett. 370 (2016) 85–90.
[352] K. Shao, S. Singha, X. Clemente-Casares, S. Tsai, Y. Yang, P. Santamaria, ACS Nano 9 (2015) 16–30.
[353] M.F. Bachmann, G.T. Jennings, Nat. Rev. Immunol. 10 (2010) 787–796.
[354] H.A.E, I.L, D.S.S, Biopharm. Drug Dispos. 19 (1998) 193–197.
[355] Y. Qian, H. Jin, S. Qiao, Y. Dai, C. Huang, L. Lu, Q. Luo, Z. Zhang, Biomaterials 98 (2016) 171–183.
[356] J. Park, S.H. Wrzesinski, E. Stern, M. Look, J. Criscione, R. Ragheb, S.M. Jay, S.L. Demento, A. Agawu, P. Licona Limon, A.F. Ferrandino, D. Gonzalez, A. Habermann, R.A. Flavell, T.M. Fahmy, Nat. Mater. 11 (2012) 895–905.
[357] Z. Xu, Y. Wang, L. Zhang, L. Huang, ACS Nano 8 (2014) 3636–3645.
[358] P.P. Hsu, D.M. Sabatini, Cell 134 (2008) 703–707.
[359] Y.H. Ko, B.L. Smith, Y. Wang, M.G. Pomper, D.A. Rini, M.S. Torbenson, J. Hullihen, P.L. Pedersen, Biochem. Biophys. Res. Commun. 324 (2004) 269–275.
[360] A.V. Kabanov, E.V. Batrakova, V.Y. Alakhov, J. Control. Release 91 (2003) 75–83.
[361] O. Warburg, Science 123 (1956) 309–314.
[362] H. Ying, A.C. Kimmelman, C.A. Lyssiotis, S. Hua, G.C. Chu, E. Fletcher-Sananikone, J.W. Locasale, J. Son, H. Zhang, J.L. Coloff, H. Yan, W. Wang, S. Chen, A. Viale, H. Zheng, J.H. Paik, C. Lim, A.R. Guimaraes, E.S. Martin, J. Chang, A.F. Hezel, S.R. Perry, J. Hu, B. Gan, Y. Xiao, J.M. Asara, R. Weissleder, Y.A. Wang, L. Chin, L.C. Cantley, R.A. DePinho, Cell 149 (2012) 656–670.
[363] M.G. Vander Heiden, L.C. Cantley, C.B. Thompson, Science 324 (2009) 1029–1033.
[364] S.Y. Li, H. Cheng, B.R. Xie, W.X. Qiu, J.Y. Zeng, C.X. Li, S.S. Wan, L. Zhang, W.L. Liu, X.Z. Zhang, ACS Nano 11 (2017) 7006–7018.
[365] W. Fan, N. Lu, P. Huang, Y. Liu, Z. Yang, S. Wang, G. Yu, Y. Liu, J. Hu, Q. He, J. Qu, T. Wang, X. Chen, Angew. Chem. Int. Ed. 56 (2017) 1229–1233.
[366] M. Huo, L. Wang, Y. Chen, J. Shi, Nat. Commun. 8 (2017) 357.
[367] H. Chen, W. He, Z. Guo, Chem. Commun. (Camb. Engl.) 50 (2014) 9714–9717.
[368] P. Vaupel, F. Kallinowski, P. Okunieff, Cancer Res. 49 (1989) 6449–6465.
[369] D. Peer, J.M. Karp, S. Hong, O.C. Farokhzad, R. Margalit, R. Langer, Nat. Nanotechnol. 2 (2007) 751–760.
[370] H. Maeda, Cancer Sci. 104 (2013) 779–789.
[371] N. Kamaly, B. Yameen, J. Wu, O.C. Farokhzad, Chem. Rev. 116 (2016) 2602–2663.
[372] H.S. Choi, W. Liu, P. Misra, E. Tanaka, J.P. Zimmer, B. Itty Ipe, M.G. Bawendi, J.V. Frangioni, Nat. Biotechnol. 25 (2007) 1165–1170.
[373] P. Kumari, B. Ghosh, S. Biswas, J. Drug. Target 24 (2016) 179–191.
[374] R. Toy, P.M. Peiris, K.B. Ghaghada, E. Karathanasis, Nanomedicine (London, England) 9 (2014) 121–134.
[375] Y. Geng, P. Dalhaimer, S. Cai, R. Tsai, M. Tewari, T. Minko, D.E. Discher, Nat. Nanotechnol. 2 (2007) 249–255.
[376] K. Yang, Y.Q. Ma, Nat. Nanotechnol. 5 (2010) 579–583.

**Arif Gulzar** obtained his doctorate degree in material Science and Chemical Engineering from Harbin Engineering University under the supervision of Prof. Piaoping Yang. He is currently working as post doctorate research scholar in Prof. Piaoping's lab and his research interests include biomedical applications of graphene oxide constructed nanomaterial and rare earth based luminescent upconversion nanomaterials for cancer theranostic.

**Jiating Xu** was born in Anhui, China, in 1990. He received his Bachelor of Science degree at Northeast Forestry University (Harbin, China) in 2014. He is currently a doctorate research student at Harbin Engineering University under the supervision of Prof. Piaoping Yang. His research mainly focuses on lanthanide-doped luminescent nanomaterials and their application in cancer theranostic.

**Chen Wang** was born in Liaoning, China, in 1988. He received his BS (2010) and MS (2013) degrees in materials science and engineering from Shenyang University of Technology. He is currently pursuing his PHD under the guidance of Prof. Piaoping Yang at Harbin Engineering University. His current research focuses on the synthesis, optical spectroscopy, and bio applications of lanthanide-based luminescent nanomaterials.

**Fei He** was born in Inner Mongolia, China, in 1985. He received his B.S. and Ph.D. degrees from Harbin Engineering University (Harbin, China) in 2009 and 2013, respectively. His current research interests include the design and fabrication of the rare earth based multifunctional nano-composite materials with the enhanced physical/chemical properties and their applications in the biomedical field.

**Dan Yang** was born in Jilin, China, in 1988. She received her Bachelor of Science degree at Beihua University (Jilin, China) in 2012. She is currently a doctorate research student at Harbin Engineering University under the supervision of Prof. Piaoping Yang. Her research mainly focuses on rare-earth based luminescent nanomaterials and their application in cancer theranostic.

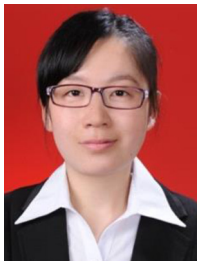

**Shili Gai** is currently an associate professor in Harbin Engineering University (Harbin, China). She received her B.S. and Ph.D. degrees from Harbin Engineering University in 2009 and 2013, respectively. Her research focuses on rare earth luminescence materials and multifunctional composite materials, including the study of the controllable synthesis, physical chemical properties, and biomedical applications.

**Piaoping Yang** is currently a Professor of Chemistry in the College of Material Science and Chemical Engineering at Harbin Engineering University (Harbin, China). He received his B.S. degree at Nankai University (Tianjin, China) and his Ph.D. degree at Jilin University (Changchun, China). After graduation, he joined Prof. Jun Lin's group for postdoctoral research. His research mainly focuses on the fabrication and biomedical applications of rare earth based functional materials.

**Jun Lin** is a professor at the Changchun Institute of Applied Chemistry (CIAC), Chinese Academy of Sciences (CAS). He received BSc and MSc degrees in inorganic chemistry from Jilin University, in 1989 and 1992, respectively, and a PhD degree (inorganic chemistry) from CIACCAS, in 1995. He has worked as a postdoctor for more than 4 years in CityU (HK, 1996), INM (Germany, 1997) and VCU/UNO (USA, 1998–1999). His research interests include luminescent materials and multifunctional composite materials together with their applications in display, lighting and biomedical fields. He has published more than 400 peer-reviewed journal articles in related fields.

**Dayong Jin** received a PhD degree (Photonics) from Macquarie University in 2007. At Macquarie, he has been promoted to Lecturer in 2010, Senior Lecturer in 2013, Associate Professor in 2014, and Professorial Fellow in 2015. He moved to the University of Technology Sydney (UTS) in 2015, and was promoted to Distinguished Professor in 2017. He directs the Australian Research Council IDEAL Research Hub and the Institute for Biomedical Materials & Devices (IBMD), at UTS. His research has been in the physical, engineering and interdisciplinary sciences. He is a technology developer with expertise covering optics, luminescent materials, sensing, automation devices, microscopy imaging, and analytical chemistry to enable rapid detection of cells and molecules and engineering of sensors and photonics devices.

**Bengang Xing** received his Ph.D. in Department of Chemistry, Nanjing University in 2000. Then he moved to the Hong Kong University of Science and Technology to work as research associate until early of 2003. After that, he held his Post-Doc. Fellow appointments at Crump Institute of Molecular Imaging at University of California, Los Angles and Molecular Imaging Programme at School of Medicine, Stanford University. In 2006, he was appointed as a faculty member at Division of Chemistry and Biological Chemistry (CBC), School of Physical and Mathematical Sciences (SPMS), Nanyang Technological University (NTU), Singapore, where he passed his tenure in 2011. His current research interests mainly focus on fluorescent imaging, chemical biology and nanomedicine.